ABSTRACT

Title of Document: THE ROLE OF ER STRESS IN SKELETAL MUSCLE ATROPHY IN AMYOTROPHIC LATERAL SCLEROSIS

Dapeng Chen, Doctor of Philosophy, 2015

Dissertation directed by: Assistant Professor Eva R. Chin, Kinesiology

Amyotrophic lateral sclerosis (ALS) is a devastating disease which affects both motor neurons and skeletal muscle. Skeletal muscle atrophy and weakness are two of the main features of ALS disease progression. We hypothesized that disruptions in the sarcoplasmic reticulum and endoplasmic reticulum (SR/ER) play an important role in skeletal muscle pathology in ALS. This dissertation is comprised of three studies investigating ER stress in skeletal muscle and its relationship to oxidative stress and SR Ca^{2+} regulation. Study#1 established that the ER stress markers PERK, IRE1α and Grp78/BiP as well as the ER-stress specific apoptotic marker CHOP are upregulated in skeletal muscle of ALS transgenic (ALS-Tg) mice and that these changes were greater in fast white vs. slow red muscles. Study #2 showed that skeletal muscle-specific overexpression of the SR Ca^{2+} ATPase SERCA1 improved motor function, delayed disease onset and attenuated the muscle atrophy in ALS-Tg mice but did not attenuate the ER stress markers. Study #3 investigated the potential molecular mechanisms of ER

stress in skeletal muscle pathology in ALS. This final dissertation study showed that the Grp78/BiP protein interacts with SERCA1 and various mitochondrial proteins including ATP synthase subunits in skeletal muscle of ALS-Tg but not wild-type mice. Disruption of the Grp78/BiP-SERCA1 protein-protein interaction by antibody sequestration of Grp78/BiP decreased SERCA ATPase activity, suggesting that Grp78/BiP preserves SERCA function. In C2C12 myocytes, oxidative stress induced by H_2O_2 dramatically decreased SERCA ATPase activity and catalase, which removes H_2O_2, could recover SERCA ATPase activity. Inhibition of ER stress by 4-PBA partially rescued H_2O_2-induced decreases in SERCA ATPase activity suggesting that this mechanisms can mitigate oxidative stress-induced SERCA impairment. Collectively, these studies provided insight into the cellular mechanisms underlying skeletal muscle dysfunction in ALS and suggest a role for ER stress chaperone proteins in minimizing Ca^{2+} overload damage in skeletal muscle. These data further suggest that the ER stress pathway could be a novel therapeutic strategy to treat skeletal muscle dysfunction in ALS.

THE ROLE OF ER STRESS IN SKELETAL MUSCLE ATROPHY IN AMYOTROPHIC LATERAL SCLEROSIS

By

Dapeng Chen

Dissertation submitted to the Faculty of the Graduate School of the
University of Maryland, College Park, in partial fulfillment
of the requirements for the degree of
Doctor of Philosophy
2015

Advisory Committee:
Assistant Professor Eva R. Chin, Chair
Associate Professor Espen E. Spangenburg
Professor Stephen M. Roth
Research Associate Yan Wang
Professor Catherine Fenselau, Dean's Representative

Acknowledgements

Firstly, I would like to thank my family. Without their support, I would not have been in the United States and finished my degree in the University of Maryland. I also would like to thank my academic adviser Eva Chin for her support on my Ph.D. study and research. Her patience, her motivation, and her immense knowledge always help me. Without her support, this dissertation would not have been possible.

Besides my family and my adviser, I would like to thank my thesis committee members: Dr. Fenselau, Dr. Roth, Dr. Spangenburg, and Dr. Wang. I thank them for their thoughtful comments on my research and their insightful questions which encourage me to think about my research from various novel perspectives. Specifically, I would like to thank Dr. Fenselau and Dr. Yan for guiding me into the protein mass spectrometry field. Thank Dr. Spangenburg for giving access to laboratory and research facilities. Thank Dr. Roth for being the best ever graduate student director in the department and always supporting our graduate student research.

I also would like to thank my fellow lab-mates: Davi Mazala, Alicia DeRusso, Harry Li and Samuel English. Thank you for being the coolest colleagues and friends. I would like to take this opportunity to say *thank you* to my friends and the exercise physiology group: Adam, Molly, cowboy, Rian, Fonzo, Jen$ … Without you guys, my graduate student life could not have been so awesome.

Tables of Contents

List of Tables

List of Figures

Chapter 1: Introduction and Specific Aims

Background

Amyotrophic lateral sclerosis (ALS) is a devastating disease which affects both motor neurons and skeletal muscle (1). It affects approximately 30,000 people in the USA and the prevalence is 3-5 people/100,000 each year (1). Therefore, ALS is defined as a rare disease. Most ALS cases are sporadic with no known family history. However, the familial type of ALS, which contributes to ~10% of all ALS cases, has led to the identification of genetic causes of ALS (1). Mutations in the superoxide dismutase 1 (SOD1) gene were first identified in 1993 as a genetic cause of ALS (2; 3). Shortly thereafter, a mouse model of the Glycine to Alanine at codon 93 (G93A*SOD1) SOD1 mutation was generated and found to reproduce the ALS phenotypes (4) and this has been used as a valuable tool to understand the pathobiology of ALS.

ALS was traditionally viewed as a neurodegenerative disease, in which neuron degeneration causes muscle weakness (1). However, accumulating evidence indicated that skeletal muscle atrophy was temporally independent of motor neuron death, suggesting that muscle-specific pathological events could induce cell death in skeletal muscle of ALS (5). Indeed, skeletal muscle-specific overexpression of mutant SOD1 proteins was shown to induce skeletal muscle atrophy and ALS-like phenotype in mice (6). Moreover, when mutant SOD1 proteins were overexpressed in skeletal muscle, motor neuron cell death was observed, suggesting the important role of skeletal muscle in inducing ALS pathophysiology (6). Therefore, a better understanding of pathological mechanisms in skeletal muscle could be valuable and may lead to novel therapeutic methods to treat ALS.

Our previous study using the G93A*SOD1 mutant ALS mouse model showed that elevated resting intracellular calcium level was evident in the early pre-symptomatic stage, when the mice do not show any symptoms (7). Intracellular calcium level is tightly regulated and disruptions of calcium level are linked to the activation of various cellular stress signals, including endoplasmic reticulum stress (ER stress) (8). Activation of ER stress involves several ER stress markers including ER stress sensors protein kinase RNA-activated-like ER kinase (PERK), inositol-requiring kinase 1-alpha (IRE1α), activating transcription factor 6 (ATF6), ER chaperones chaperone immunoglobulin binding protein (Grp78/BiP), protein disulfide isomerase (PDI), and ER stress-specific cell death signals including C/EBP homologous protein (CHOP) and caspase-12 (9). In Study #1 we have shown that ER stress is induced in skeletal muscle of the G93A*SOD1 mouse model of ALS (10). Based on these findings, we hypothesized that ER stress activation contributes to muscle atrophy in ALS mice based on several lines of evidence: 1) ER stress-specific cell death signal CHOP was upregulated at early pre-symptomatic stage and was increased further when mice were in the late symptomatic stage, suggesting that CHOP expression is related to disease progression; 2) activation of ER stress is a skeletal muscle-specific event; and 3) ER stress activation was induced more in fast white than in slow red muscle fiber type, consistent with the preferential decline in fast motor units in this ALS mouse model (11).

SERCA1 is an ATP-dependent calcium pump located on the ER membrane and responsible for taking up intracellular calcium into SR/ER lumen during skeletal muscle contraction (12). As the most abundant protein in the SR/ER, SERCA1 is essential to preserve calcium homeostasis and decreased SERCA1 function has been linked to

various muscle pathological conditions such as in muscular dystrophy and muscle atrophy (12; 13).

Based on our findings that elevations in skeletal muscle intracellular Ca^{2+} was associated with ER stress during symptom progression in the G93A*SOD1 mice, we tested the hypothesis that increasing intracellular Ca^{2+} clearance with increased overexpression of the SR Ca^{2+} ATPase pump (SERCA1) would attenuate the muscle atrophy and ER stress. In Study #2 (Chapter 4) muscle-specific SERCA1 overexpressing mice were crossed with the G93A*SOD1 mice to generate G93A*SOOD1/+SERCA1 mice. This mice had a reduction in muscle atrophy, improved grip function and a delay in disease progression in G93A*SOD1/+SERCA1 mice (Chen *et al.*. manuscript in review; Chapter 4). While this suggested a recovery of the pathophysiology of skeletal muscle with increased SERCA1 expression and increased intracellular Ca^{2+} clearance, there was not a decrease in Grp78/BiP or the ER stress apoptotic marker CHOP. Our results indicated that the rescue effects of SERCA1 overexpression on ALS mice could be independent of inhibition of the ER stress pathway. These data also indicate that skeletal muscle pathology involves various pathological mechanisms and that other mechanisms such as oxidative stress and mitochondrial dysfunction contribute to the disease pathology (14). Therefore, it is not surprising that SERCA1 overexpression improved skeletal muscle function via modulating some other pathological factors. However, considering that SERCA1 proteins are the most abundant proteins in skeletal muscle, we cannot rule out the possibility that overexpression of SERCA1 proteins leads to ER protein overload and thus induced the activation of ER stress. Indeed, in our study, SERCA1 overexpression was shown to induce upregulate ER stress markers even in

skeletal muscle of wild type mice (Chapter 4). Nevertheless, our SERCA1 overexpression in ALS mice study clearly showed that SERCA1 protein is critical to preserve skeletal muscle function in ALS mice. Moreover, improved skeletal muscle function is consistent with a delayed disease progression, suggesting that skeletal muscle pathology plays a very important role in inducing whole body pathogenesis in ALS.

A separate *in vivo* drug treatment study also supports our notion that SERCA1 function is critical to preserve skeletal muscle function and an improved phenotype in ALS-Tg mice. When G93A*SOD1 mice were treated *in vivo* with 6-gingerol, a compound previously shown to increase SERCA1 activity *in vitro*, there were improvements in muscle grip function and an attenuation of ER stress markers Grp78/BiP and CHOP ((15); manuscript in preparation). Since 6-gingerol has also been shown to have anti-oxidant properties (16), we hypothesized that the efficacy of this compound in reducing ER stress may be due, at least in part, to the anti-oxidant properties of 6-gingerol. This would also explain why SERCA1 overexpression in itself had different effects from 6-gingerol.

Mutant SOD1 proteins are thought to induce the ALS phenotype via a "gain-of-function" effect (17). SOD1 proteins are responsible for catalyzing superoxide free radicals to hydrogen peroxide (H_2O_2), which is then degraded to O_2 and H_2O by catalase. However, hyper-activity of mutant SOD1 proteins induces oxidative stress by over producing H_2O_2. Therefore, oxidative stress, particularly excess H_2O_2 is suggested to be the main contributor to inducing skeletal muscle pathology in ALS. Collectively, our results revealed that: i) intracellular Ca^{2+} regulation is altered and ER stress activated in skeletal muscle of ALS mice; and ii) ER stress was not rescued by SERCA1

overexpression but was attenuated by a compound with anti-oxidant properties. Thus, we further hypothesized that the oxidative stress along with altered Ca^{2+} regulation could be causally linked to the skeletal muscle ALS pathobiology in the G93A*SOD1 mice.

The purpose of Study #3 (Chapter 5) was to investigate the role of oxidative stress and ER stress in the skeletal muscle pathobiology in ALS. Based on our previous studies showing that Grp78/BiP was dramatically upregulated in skeletal muscle of G93A*SOD1 mice (10) and was attenuated by the *in vivo* treatment of these mice with 6-gingerol (15), this project specifically focused on oxidative stress and Grp78/BiP protein. Grp78/BiP is a member of 70 kDa heat shock proteins (hsp70) family and has been shown to be upregulated under ER stress conditions and thus used widely as a classical marker for ER stress activation (18). Moreover, Grp78/BiP is an ER chaperone and required to maintain ER function. Previous studies established the role of protein-protein interactions of Grp78/BiP with other proteins in preserving ER function and cellular homeostasis by binding to unfolded/misfolded proteins and directing their intracellular folding and translocation (18). The biological significance of Grp78/BiP is demonstrated by studies showing that Grp78/BiP is important in protein quality control pathways such as ER-associated protein degradation (ERAD) and ER stress-induced autophagy (9). In light of these facts, a better understanding of Grp78/BiP protein interacting patterns in skeletal muscle is essential to elucidating the mechanisms of the protective role of Grp78/BiP in preserving ER function and cellular homeostasis. Preliminary data revealed that one of the Grp78/BiP binding partners was SERCA1, further prompting investigation into the protein-protein interaction and functional relationship between Grp78/BiP and SERCA1 in maintaining intracellular Ca^{2+} homeostasis and attenuating ER stress in skeletal muscle.

Specific Aims

Specific Aim 1*:* To investigate Grp78/BiP protein-protein interactions in skeletal muscle of wild type and ALS mice using Grp78/BiP co-immunoprecipitation (Co-IP) and MS/MS-based proteomics techniques.

Hypothesis: analysis of Grp78/BiP Co-IP products using MS/MS will identify novel binding proteins in skeletal muscle and these will differ between skeletal muscle of wild type and ALS animals, both in proteins identified and protein abundance.

As previous mentioned, Grp78/BiP conducts its protective role in maintaining ER function via binding to unfolded/misfolded proteins (19). Studies also indicated that the interaction of Hsp70s and their targeting proteins is a beneficial event under several cellular stress events via enhancing SERCA1 function (20). Our preliminary data showed that SERCA1, a key calcium pump located in ER membrane in skeletal muscle, was identified in the Grp78/BiP co-IP products.

Specific Aim 2: To investigate the effects of Grp78/BiP and SERCA1 interaction on SERCA function.

Hypothesis: SR Ca^{2+} ATPase activity in SR vesicles isolated from skeletal muscle of mice will decrease when incubated with Grp78/BiP antibody compared with no antibody or control IgG antibody incubation.

Oxidative stress has been associated with disease pathology including skeletal muscle pathology in ALS and its role in initiating cell death has been documented (21). Moreover, other studies report that oxidative stress could activate ER stress and its biological consequences need to be further evaluated (22; 23). In the light of these facts,

we hypothesized that oxidative stress contributes to decreased SERCA1 ATPase activity and elevated intracellular calcium level (7).

Specific Aim 3*:* To investigate the role of oxidative stress in inducing ER stress response and regulating SERCA function in a C2C12 cell culture model.

Hypothesis #1: In C2C12 myotubes, hydrogen peroxide (H_2O_2) treatment will activate ER stress and decrease SR Ca^{2+} ATPase activity.

Hypothesis 2: Catalase and the chemical chaperone 4-phenyl butyric acid (4-PBA) will prevent the decrease in SR Ca^{2+} ATPase activity induced by H_2O_2.

Chapter 2: Review of Literature

Amyotrophic lateral sclerosis

Amyotrophic lateral sclerosis (ALS), also termed Lou Gehrig's disease in the United States, was first reported in 1869 by Jean Martin Charcot, a French neurologist and anatomical pathology professor (1). Based on his observations, the characterization of ALS was described as "*a progressive death of upper and lower motor neurons*". Subsequent research confirmed that degeneration of upper motor neurons was found in the motor cortex of the brain, which contributed to ALS syndrome by causing excessive muscle contraction from neuron hyper-excitability (1). The degeneration of lower motor neurons was found in the brain stem, which, it suggested, contributed to muscle atrophy and muscle weakness (1).

ALS is a devastating neurodegenerative disease without expeditious diagnosis and effective treatment (24). It affects three out of 100,000 people a year in the United States (1; 25; 26). Most people are diagnosed with ALS between 45-55 years of age, and disease cases decrease dramatically after 80 years of age (27-29). ALS has been characterized as two types: familial and sporadic. Familial ALS, which occurs in a family lineage and accounts for ~5 to 10% of all ALS cases, has been shown to be associated with several gene mutations such as superoxide dismutase 1 (copper/zinc, SOD1), Tat DNA binding protein (TDP-43), and chromosome 9 open reading frame 72 (C9ORF72) (29-31). Mutations in SOD1 protein contribute to around 20% of total familial ALS cases (Figure 2.1) (29). This finding prompted the development of the SOD1 G93A transgenic mouse model by Gurney *et al*. (4; 32). SOD1 G93A transgenic mice replicate many of the ALS hallmarks seen in ALS patients, including loss of motor

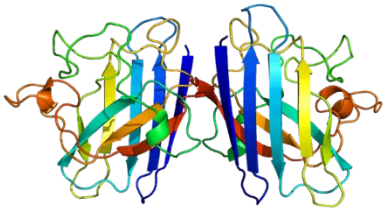

$$2O_2^- + 2H^+ \rightarrow H_2O_2 + O_2$$

Figure 2.1. Superoxide dismutase (Cu-Zn) SOD1 protein. SOD1 binds to copper and zinc ions and is responsible for removal of free superoxide radicals in cells by the chemical reaction converting superoxide to oxygen and hydrogen peroxide, which is then neutralized by catalase enzymes.

neurons and development of progressive muscle paralysis. Therefore, this mouse model has been widely used to study pathophysiological mechanisms of this disease (4; 32). Most ALS cases (~90%) are sporadic with unknown causative factors (1). Several environmental conditions have been proposed to be linked with sporadic ALS pathogenesis, including Guamanian ALS, and a higher incidence of disease in US Air Force and professional leagues soccer players (1). However, epidemiological studies failed to distinguish any specific factors contributing to development of those ALS phenotypes. Although the causes of sporadic ALS are still uncertain, it is suggested that those two forms of ALS share similar pathophysiological mechanisms (33; 34).

ALS has long been recognized as a typical neurodegenerative disease, in which motor neuron degeneration is mediated by the excessive activation of various postsynaptic receptors (35). According to this hypothesis, ALS pathology originates from motor neuron disorder, and skeletal muscle dysfunction is recognized as a secondary event resulting from degeneration of the motor system (36). Glutamate-induced cellular toxicity has been suggested to initiate the “dying-forward” process in the

neurodegeneration in ALS. Glutamate is a neurotransmitter in the nervous system. Immoderate releasing of glutamate, which is termed as glutamate-induced excitotoxicity, was suggested to trigger neurodegeneration via a calcium-dependent cell death signal pathway (37-39). Several lines of evidence collected by Baker *et al.* support the "dying-forward" model as clinical studies showed that over-excitability of the cortical area occurred early in sporadic ALS patients and came before onset of the disease in familial ALS patients (5). The "dying-forward" hypothesis is further supported by the fact that a clinical drug, *Riluzole*, which is an inhibitor of glutamate releasing, has been shown to improve the survival of ALS patients by repressing cortical hyper-excitability (37; 38). Besides glutamate-induced pathogenesis of ALS, other mechanisms proposed to explain ALS include mitochondrial dysfunction, increased oxidative stress, and protein aggregates-induced ER stress (Figure 2.2) (24).

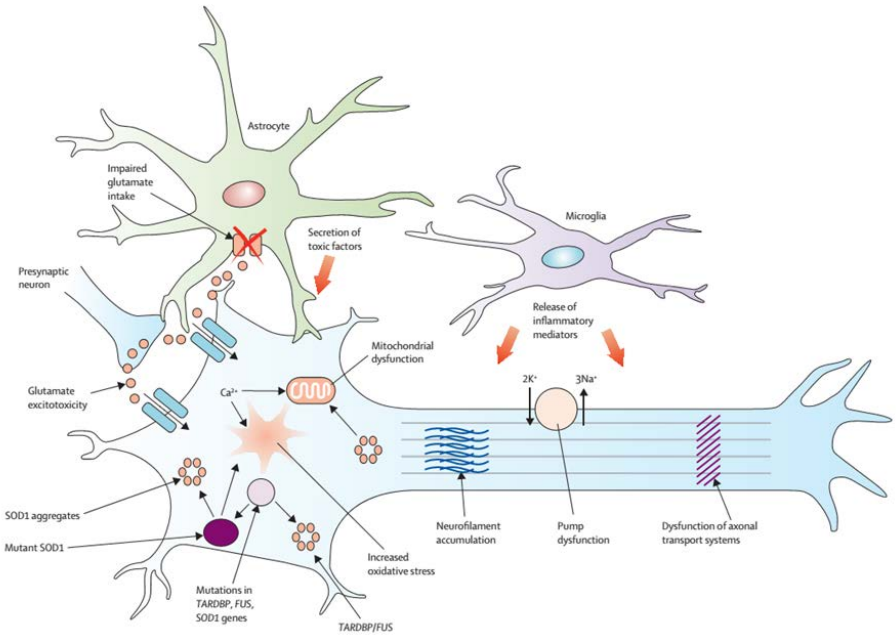

Figure 2.2. Mutant SOD1 induced cellular toxicity in motor neurons of ALS. Motor neuron degeneration in ALS has been shown to involve in various pathological events such as glutamate excitotoxicity, mitochondrial dysfunction, oxidative stress, and protein aggregates. Adapted from figure 2 from Kiernan, et al, 2011.

Mitochondrial dysfunction - Mitochondria damage and dysfunction is involved in a range of human diseases because of its primary role in cell energetics, preserving cellular homeostasis, buffering intracellular calcium levels, and initiating mitochondrion-dependent cell death signals (40). Consequently, mitochondrial dysfunction has been emerging as a main contributor to the pathogenesis of various neurodegenerative diseases including Alzheimer's disease, Parkinson's disease, and ALS (Figure 2.3) (41).

In ALS, mitochondrial dysfunction is suggested as an important factor inducing ALS pathogenesis. Autopsy analysis of sporadic ALS cases conducted by Wong *et al.* showed that aberrant mitochondria were present in various pathological tissues including

proximal axons, anterior horns, and skeletal muscle (41). Moreover, previous studies suggested that the morphological and ultrastructural alterations in mitochondria were linked to the decrease in their function (42; 43). Indeed, it has been shown that mitochondrial function in ALS patients was consistently impaired, as indicated by decreased mitochondrial electron transfer chain activity, mitochondrial DNA damage, resulting decreased respiratory function, over-production of free radicals, and dysregulation of calcium signals in motor neurons (35; 44; 45). Despite the presence of mitochondrial dysfunction in ALS, questions remain over whether mitochondrial disorder is a primary cause of ALS pathogenesis or simply a pathological consequence of motor neuron degeneration.

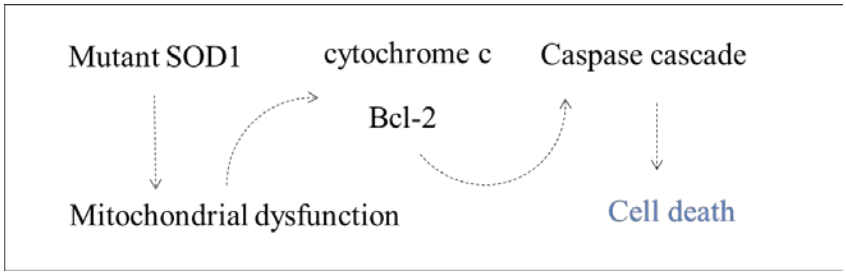

Figure 2.3. Mutant SOD1 induced mitochondrial dysfunction in ALS. Mutant SOD1 has been reported to translocate to mitochondria and interact with mitochondrial proteins such as Bcl-2 and translocation machinery proteins, resulting in release of cytochrome C and induce mitochondria-dependent apoptosis pathway.

The use of animal models of ALS has provided a better understanding of the role of mitochondrial dysfunction in ALS pathogenesis. Histological examinations of motor neurons in ALS mice showed the presence of abnormal membrane-bound organelles, which were suspected to be the product of mitochondrial degradation (4). Furthermore,

those abnormal membrane-bound organelles were suggested as a primary factor inducing cellular pathological change. A systematic study conducted by Palomo *et al.* (46) using SOD1*G93A mice showed that the excessive emerging of those organelles in spinal cords were related with the onset of ALS disease, which is defined by a sudden decreased muscle strength and function without massive motor neuron death. This indicated that mitochondrial disorder might be a cellular event triggering early onset of the disease, not merely a consequence of motor neuron degeneration.

Mutant SOD1 proteins-induced cell toxicity was indicated to cause pathological changes of mitochondria and decreased mitochondrial function in ALS, as one study conducted by Nguyen *et al.* (47) showed mitochondrial depolarization, a biomarker indicating respiratory chain dysfunction, when neuroblastoma cells were transfected with mutant SOD1. Besides the decrease in mitochondrial function, a higher intracellular calcium level was also seen in this study, indicating impaired mitochondrial calcium buffering capacity (47). The use of SOD1*G93A ALS mice study further supported this notion. Yi *et al.* (48) showed dysregulation of mitochondrial respiratory chain enzymes and increased cytoplasmic calcium level were observed in isolated primary motor neurons of ALS mice.

Decreased mitochondrial function and impaired calcium buffering capacity induced by mutant SOD1 proteins could also contribute to the motor neuron degeneration seen in ALS (12; 23; 49). Decreased mitochondrial calcium buffering capacity is speculated to be involved in glutamate-induced excitotoxicity in motor neurons. This notion is supported by finding that moto neuron overexpression of GLUR2, which is a calcium-permeable AMPA receptor, attenuated disease progression in SOD1 G93A ALS

mice (50; 51). Second, an increase in intracellular calcium level is associated with the elevated production of free radicals from mitochondria, which is suggested to induce cell death (35; 52; 53). This notion is partly supported by the studies conducted by An *et al.* (54) showed that treatment of antioxidant chemicals had beneficial effects on mutant SOD1 ALS mice. Upon the existence of mitochondrial dysfunction, cells could initiate mitochondria-dependent apoptotic cell death pathways via releasing pro-apoptotic factors such as cytochrome c, Bad, Bid, and Bim (55-57). Mitochondria-dependent apoptotic cell death pathway are involved in motor neuron degeneration in ALS and cytochrome c has been shown to be released and lead to activation of caspase-9 in the motor neurons of SOD1*G93A ALS mice (58). Therefore, inhibition of mitochondria-dependent apoptotic cell death pathway is considered a therapeutic strategy to treating ALS. It has been shown that overexpression of Bcl-2, which is an anti-apoptotic factor, attenuated motor neurons loss and disease progression in mutant SOD1 ALS mice (59). Besides the use of transgenetic methods, pharmacological intervention suppressing the releasing of pro-apoptotic factors was shown to have beneficial effects. Minocycline treatment, a chemical inhibiting cytochrome c release, was shown to delayed disease progression in transgenic ALS mice (60-62).

Oxidative stress - It is still debatable that whether oxidative damage in ALS is a secondary event as a consequence of disease or a predominant factor causing ALS pathogenesis (14; 63; 64). Genetic SOD1 mutations, which play an important role in regulating cellular oxidative/redox status, contribute to around 15% of all familial ALS cases (65). Based on these observations, mutant SOD1 proteins were speculated as a primary factor inducing ALS pathology. Several hypotheses were proposed to interpret

mutant SOD1 induced toxicity: 1) “loss of function” of mutant SOD1 proteins leads to generation of high level of superoxide and peroxynitrite; 2) “dominant-negative” mechanism is induced by mutant SOD1, in which mutant SOD1 proteins are proposed to lose the activity as well as repress normal SOD1 proteins; 3) “gain-of-function” of mutant SOD1 results in over-production of reactive oxygen radicals (4; 17). “Loss-of-function” and “dominant-negative” mechanisms of mutant SOD1 have now been dismissed since SOD1 knockout mice do not show ALS phenotypes, suggesting that mutant SOD1 proteins acquire toxicity in a “gain-of-function” manner (4; 66; 67).

The oxidative stress-induced cellular toxicity in ALS was proposed based on the “gain-of-function” principle of mutant SOD1 proteins (4). SOD1 proteins are involved in catalyzing super oxygen into hydrogen peroxide (Figure 2.1). Mutant SOD1 proteins prompt the over-production of reactive hydroxyl radicals such as hydrogen peroxide, resulting in a succession of reactions that trigger oxidative damage. Animal studies further confirmed this notion. Previous studies conducted by Cookson *et al.* showed that the disease progression in SOD1 G93A mice was consistent with the oxidized products (17; 68). Besides reactive hydroxyl radicals, peroxynitrite was suggested to be another candidate contributing to oxidative damages mediated by mutant SOD1 proteins (14). This notion was based on the fact that elevated levels of 3-nitrotyrosine, which is used as a marker to evaluate oxidative damage induced by peroxynitrite, were seen in both mutant SOD1 transgenic ALS mice and ALS patients (69).

Considering its important role in inducing ALS pathology, oxidative stress has long been recognized as an attractive mechanism for developing therapeutic treatment for ALS (70-72). Many clinical trials have been carried out evaluating anti-oxidant

treatments but efficacy was surprisingly disappointing (73; 74). For example, Vitamin E, which is a fat-soluble antioxidant stopping production of reactive oxygen species, has been tested in several well controlled double-blind studies (73). In one study, 289 patients diagnosed with ALS less than five years before being enrolled were treated with a 500mg Vitamin E twice a day for 12 months. Although it was stated that ALS patients in the vitamin E treatment group had less chance to develop into a more aggressive state of ALS, the treatment had no significant effect on some other key outcome measures as well as no effects on the survival rate (74). To rule out the possibility of using a sub-optimal dose, another study (83) used a higher dose of Vitamin E (5000 mg) treatment in 160 ALS patients for 18 months. Consistent with the previous study, no significant treatment effect was seen in this study and there was no evidence showing improvement in disease endpoint tests such as assisted ventilation and time to death rate (73; 74). Based on these observations, doubts were raised about whether oxidative stress plays a primary role in modulating ALS disease progression. Consequently, to better understand the lack of efficacy of the Vitamin E treatment, other factors, such as drug pharmacokinetics, needed to be considered. Vitamin E would need to be delivered into the right tissues and cells (i.e. to motoneurons) to perform its anti-oxidation effect. A dose-response study investigating vitamin E levels in fluids of different parts of the body indicated that vitamin E was not delivered readily to the central neuron system, which partly explained why both moderate and high amount dosage of vitamin E had no significant effect on ALS disease progression (73; 74). In light of this finding, other anti-oxidants with improved SNS penetrance would need to be developed and tested.

Mitochondria are considered as the main site producing reactive oxygen species and a great quantity of evidence showing that mitochondrial dysfunction is a major contributor to ALS pathology (64; 75). As mentioned previously, mitochondria morphological alterations and dysfunction have been observed in motor neurons and skeletal muscle of both ALS patients and ALS animal models (66; 76; 77). In light of those facts, therapeutic strategies targeting both oxidative damage and mitochondrial dysfunction would be more favorable (Figure 2.4).

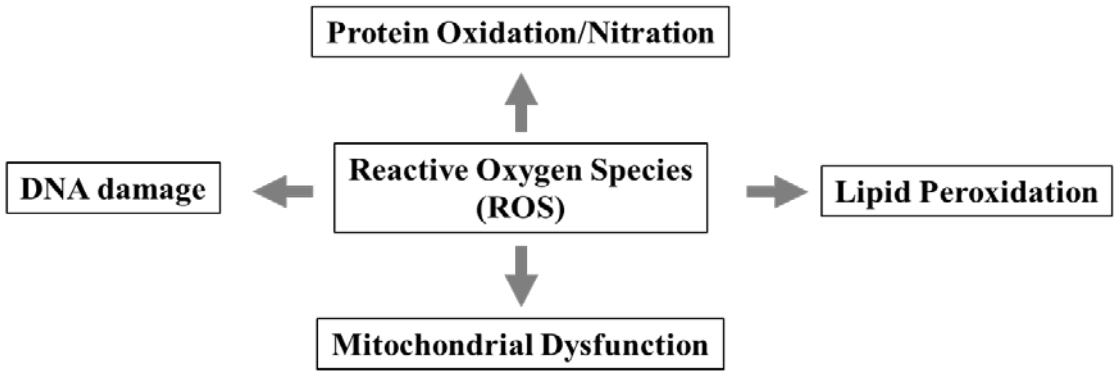

Figure 2.4. Mutant SOD1-mediated activation of oxidative stress. Oxidative stress is induced in pathological tissues of ALS via "gain-of-function" mechanism and associated with various cellular toxicity events including DNA damage, mitochondrial dysfunction, lipid peroxidation, and irreversible protein oxidation/nitration.

Protein Aggregates - Neurodegenerative diseases are commonly characterized by intracellular aberrant protein aggregates but it is still questionable whether protein aggregates are involved in disease pathogenesis or are simply an inoffensive cellular defense event eliminating harmful mutant proteins (78-81). The early formation of

SOD1-enrich protein aggregates was found in pathological tissues of both ALS patients and animal models, as well as in cells with expression of mutant SOD1, indicating it as a typical pathological event in ALS (82; 83). The formation of mutant SOD1-enriched protein aggregates was thought to be due to defects in mutant SOD1 protein metal binding region. In the normal condition, the SOD1 protein structure is maintained by the metal ions; however, mutant SOD1 proteins, such as in G85R form, are more likely to form protein aggregates due to the weaker metal ion binding capacity, resulting in decreased thermal stability and high susceptibility of forming aggregates (84). Studies conducted by several groups showed that SOD1-enriched protein aggregates existed prior to the manifestation of ALS symptoms and were concomitant with disease progression, suggesting that it is likely an early event involved in ALS pathogenesis (82; 85-87). Several mechanisms have been proposed to interpret mutant SOD1-induced toxic properties including mutant SOD1-mediated coaggregation of essential components, low efficiency of ubiquitin-mediated removal of mutant SOD1 proteins, and impaired chaperone capacity to properly fold proteins in the ER lumen (86; 88; 89).

Previous studies indicated that there was a tight link between mutant SOD1-enriched protein aggregates, mitochondrial dysfunction, and oxidative stress (33). Normal SOD1 proteins are mainly located in cytoplasm. However, mutant SOD1 proteins were found to be ectopically translocated to other organelles such as within mitochondria and the intermembrane spaces, indicating their pathological role in initiating mitochondrial pathological changes such as impaired respiratory activity, overproduction of reactive oxygen species, and activation of mitochondrial-dependent cell death signals (4; 26; 40; 90). Removal of mutant SOD1-enriched protein aggregates has also been

shown to be an effective therapeutic method to slow down ALS disease progression (91-93). For example, selective degradation of protein aggregates by overexpressing Dorfin, which is a RING finger-type E3 ubiquitin ligase, was found to alleviate mutant SOD1-induced toxicity and protect neuron cells from different lines of SOD1 mutations (93). Furthermore, transgenic overexpression of 70 kDa heat shock protein in a mouse model of ALS was shown to reduce the formation of protein aggregates, preserve motor neuron survival, and increase the viability rate (94).

Unfolded Protein Response & ER Stress

In Eukaryotic cells, the endoplasmic reticulum (ER) is a highly developed organelle which is essential to conduct various cellular processes such as preserving intracellular calcium homeostasis and protein synthesis (9; 18; 21; 95; 96). The newly synthesized polypeptides are translated into the ER lumen, where proteins are continuously translated with the assistance of ER chaperones and get properly folded. Before being transported to the Golgi compartment, newly synthesized proteins experience a cellular "quality control" event, in which misfolded or unfolded proteins are either conserved in the ER lumen for further modifications or guided to a protein degradation pathway called ER-associated degradation (ERAD) (9; 18).

Numerous pathological events such as calcium depletion and changes of oxidative/redox status in the ER lumen, could result in accumulation of a large quantity of misfolded and unfolded proteins in the ER, which is known to activate a cellular stress response named unfolded protein response (UPR) or ER stress (Figure 2.5) (8; 97). Short term ER stress activation is manageable with the primary goal to preserve normal ER function and cellular homeostasis by upregulating proteins involved in ER folding

capacity and protein degradation. However, prolonged or severe ER stress is harmful and has been showed to induce apoptosis via activation of the ER stress-specific cell death pathway (9).

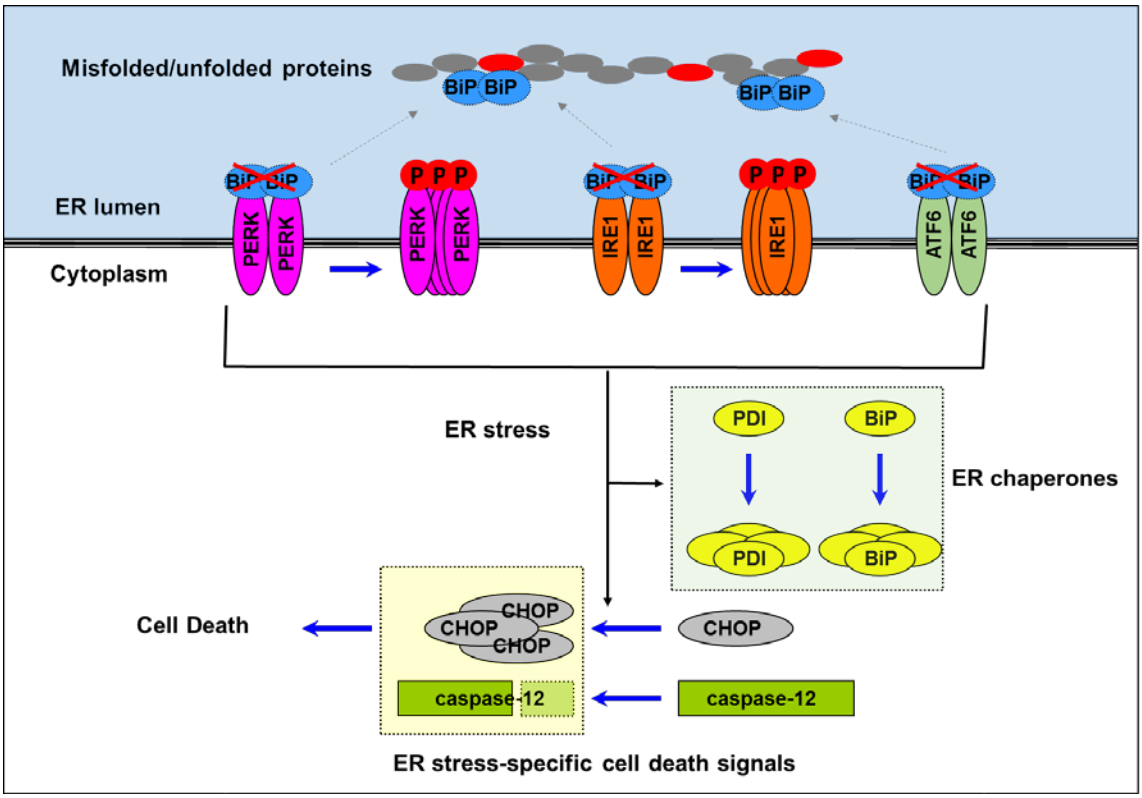

Figure 2.5. Unfolded Protein Response (UPR) and ER stress pathway. Under normal condition, ER stress sensors PERK, IRE1, and ATF6 bind to Grp78/BiP (BiP) and are inhibited. Upon accumulation of misfolded and unfolded proteins, BiP is preferable to bind to those proteins and then ER stress are activated. The consequence of activation of ER stress is to upregulate ER chaperones, which are essential for proper protein folding; if fails to handle the stress, ER stress-specific cell death pathway will be induced via upregulation of CHOP and cleavage of caspase-12.

Under normal conditions, three specific ER stress sensors, inositol-requiring kinase 1 (IRE1α), protein kinase RNA-like endoplasmic reticulum kinase (PERK), and activating transcription factor 6 (ATF6), are retained and inhibited by an ER membrane protein Grp78/BiP (78 kDa - glucose regulated protein) (9; 98). Upon the accumulation of misfolded and unfolded proteins in the ER lumen, Grp78/BiP binds to those abnormal proteins and moves away from ER stress sensors IRE1α, PERK, and ATF6 (9; 99). Consequently, ER stress sensors are aggregated and activated, resulting in a succession of events that attenuate the production of misfolded and unfolded proteins in the ER lumen by upregulating ER chaperones, repressing mRNA translation, and directing misfolded and unfolded proteins to proteasome for protein degradation (9). If the ER stress response is not able to reduce the accumulation of misfolded and unfolded proteins, the ER stress-specific cell death pathway is induced, including upregulation of the pro-apoptotic transcription factor C/EBP homologous protein (CHOP) and caspase-12 (Figure 2.5) (9; 100; 101).

IRE1α – IRE1α belongs to the type I transmembrane protein that is located on the ER membrane with two functional sequences: a serine/threonine protein kinase domain and a ribonuclease endonuclease domain (102). Under normal conditions, IRE1α interacts with Grp78/BiP and thus retains its nonfunctioning form. Accumulation of misfolded and unfolded proteins results in departure of Grp78/BiP and the formation of IRE1α homodimers, and initiation its endonuclease activity by autophosphorylation (103). The comprehensive effect of IRE1α phosphorylation is to regulate gene expression and to induce posttranslational modifications of mRNAs encoding secreted proteins participating in ER stress and ERAD pathways. Consequently, activation of IRE1α

results in repression of protein synthesis and release of protein overload in the ER lumen (104; 105). Specifically, one primary target of IRE1α endonuclease activity is X-box binding protein (Xbp-1). Activation of IRE1α yields a spliced and active form of Xbp-1, which is known as a transcriptional factor and regulates various gene expressions involved in ER stress and ERAD pathways (96; 102). Cells with either IRE1α or Xbp-1 knockout fail to initiate ER-induced protein degradation, indicating their importance in protein homeostasis (9).

The IRE1α – Xbp-1 pathway has also been shown to play an essential role in a mammalian survival and tissue development (96; 106; 107). Knockout of either IRE1α or Xbp-1 results in embryonic lethality in mice (96; 102). Furthermore, although heterozygous Xbp-1 knockout mice show a normal phenotype, these mice develop insulin resistance under a high-fat diet challenge (108). In addition, the ER stress signaling pathway-mediated IRE1α activation and Xbp-1 splicing has been shown to play an essential role in mediating beta cell differentiation as one study showed that cells with IRE1α deficiency had the ability to product pro-beta cells but not mature beta cells (109; 110). IRE1α – Xbp-1 was required to produce beta cell receptors and to allow the translocation of mature beta cells into antibody-secreting plasma cells, indicating the importance of IRE1α – Xbp-1 in each stage of beta lymphopoiesis (109; 110). IRE1α also has been reported to be involved in cell death mechanisms as it has been shown to interact with various pro-apoptotic and anti-apoptotic cell death factors including B-cell leukemia/lymphoma 2 (Bcl-2) family protiens, Bcl-2 killer (BAK), and Bcl-2 associated X protein (Bax) (111). The IRE1α-mediated activation of apoptosis signal-regulating kinase (ASK1) and Jun N-terminal kinase (JNK) has been reported to prompt cell death

mechanism via activation pro-apoptotic factor BIM, which belongs to the Bcl-2 family (112; 113). Besides modulating various cell death pathways, IRE1α was also known to activate a list of cysteine proteases such as caspase-12 (mouse) and caspase-4 (human) proteins (100; 114). Caspase-4 has been recognized as an ER stress-specific cell death factor as previous studies showed that cells with caspase-4 deficiency were resistant to ER stress-induced cell death but not to mitochondrial dysfunction-induced cell death signals induced such as in UV exposure and DNA toxins conditions (115-117).

PERK – upon activation of ER stress, the cellular response is expected to reduce protein synthesis and secretion through the ER lumen, thus ER homeostasis can be preserved. The ER stress-mediated activation of PERK phosphorylation has been shown to contribute to this process by activating various downstream signaling factors, such as phosphorylation of eukaryotic translation initiation factor 2 alpha (eIF2α) (118). PERK is a transmembrane protein kinase located on the ER membrane and interacts with Grp78/BiP in its inactive form (104). Upon activation of ER stress, Grp78/BiP preferentially interacts with misfolded and unfolded proteins in the ER lumen, resulting in oligomerization and autophosphorylation of PERK. PERK-mediated phosphorylation of its downstream signal eIF2α has been shown to slow down mRNA translation events and thus relief ER protein overload. On the other hand, phospho-PERK activates selective mRNA translation such as activating transcription factor 4 (ATF4), which modulates various gene promoters encoding several genes involved in ER stress, ER chaperones, and protein metabolism (18; 104; 119). The essential role of the PERK pathway was confirmed by cell knockout studies, in which they showed that PERK deficienct cells could not activate eIF2α phosphorylation and were more sensitive to cell

death signals induced by ER stress, suggesting this pathway is important to preserve cellular homeostasis and ER function (9; 18).

Besides phosphorylating eIF2α, PERK has also been shown to mediate other transcription factors such as nuclear respiratory factor 2 (NRF2), which is suggested to regulate protein expression involved in the oxidative stress response (120). This notion is supported by the fact that PERK phosphorylation caused the translocation of NRF2 from cytoplasm to nucleus and that cells lacking NRF2 were more resistant to ER stress-induced cell death signals, indicating that the PERK phosphorylation-mediated pathway protected cells from ER stress (121). Although PERK autophosphorylation has a protective role during activation of ER stress, it has also been suggested to contribute to cell death. Based on the observation that eIF2α phosphorylation can activate the pro-inflammatory signaling protein nuclear factor kappa B (NFκB), which is a transcriptional factor linked to various pathological conditions such as in cancer, tissue atrophy, and autoimmune diseases, PERK activation of eIF2α may also be pro-apoptotic (9; 122-124). For example, our previous study (Chapter 3) showed that PERK was phosphorylated in skeletal muscle of a mouse model of ALS and one of its downstream signals CAAT/enhance binding protein (C/EBP) homolgous protein (CHOP) was upregulated accordingly, suggesting that ER stress-mediated activation of PERK may contribute to cell death in skeletal muscle (10; 125).

ATF6 – Activating transcriptional factors (ATF6) alpha and beta have been identified as additional important ER stress sensors besides PERK and IRE1α (104). Instead of experiencing autophosphorylation after separating from Grp78/BiP, ATF6 is shown to translocate from ER membrane to the Golgi, where ATF6 is cleaved by certain

protease (104). Consequently, as a transcriptional factor, the spiced form of ATF6 is released into the cytoplasm and then relocates to the nucleus to modulate gene expression (106). Genes regulated by ATF6 include a list of targets that contribute to cell survival mechanisms including those that have chaperone activity and those that remove misfolded and unfolded proteins in the ER lumen, such as Xbp-1, Grp78/BiP, and ER degradation enhancing alpha-mannosidase like protein 1 (EDEM) (106).

Grp78/BiP – The ER is considered to be one of the most dynamic cell organelles based on its interaction with other cellular components such as mitochondria and nuclei (18; 104; 119). The ER is the main site for protein synthesis and calcium storage, and has been shown to play an important role in conducting cell signaling processes, modulating cellular stress, and maintaining cellular homeostasis (18; 119). This notion is further supported by that fact that in eukaryotic cells the ER encompasses nearly 50% of its cellular membrane system. As one of the most important ER chaperones, Grp78/BiP has been recognized as the predominant factor regulating ER function. A large number of studies show that Grp78/BiP participated in various cellular processes including maintaining ER membrane integrity, managing protein folding, regulating ER-associated misfolded protein degradation, preserving ER calcium homeostasis and modulating ER stress pathway (Figure 2.6) (18; 104; 119).

Grp78/BiP is one of the Hsp70 family members with ATP binding sequences interacting with unfolded proteins (18). Newly synthesis polypeptides are translocated into the ER lumen, where they experience further folding following post-translational modification with the assistance of a list of ER chaperones such as Grp78/BiP and PDI (18). In most cases, the newly synthesized proteins are folded correctly; however, some

proteins or regions of a protein are not correctly modified and folded (18). In this case, Grp78/BiP, with the assistance of its cofactors, recruit and bind to the unfolded regions of the proteins in an ATP-dependent manner (18). After a cycle of protein folding events, the proteins are released from the ER to their home-components if folded properly, or experience another cycle of ATP-dependent folding and ultimately, directed to protein degradation process if the unfolded protein events are irreversible (18).

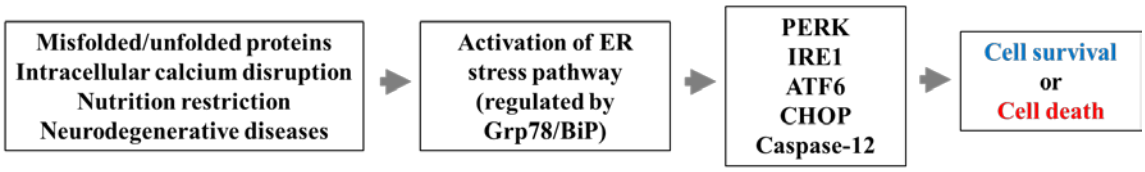

Figure 2.6. The primary role of Grp78/BiP in determining cell destiny under various cellular stress conditions. Various cellular stress processes are known to activate ER stress pathway such as intracellular calcium disruption. Grp78/BiP is suggested to play a central role in modulating different ER stress components to determine the cell destiny.

Free intracellular calcium is recognized as a secondary messenger modulating various key cell processes (126). The ER plays an essential role in controlling intracellular calcium level through regulation of several calcium transporters, channels, pumps, and buffering-proteins located on the ER membrane such as ryanodine receptor (RyR), inositol trisphosphate receptor, SERCAs, and Grp78/BiP (127). The role of Grp78/BiP in handling intracellular calcium concentration has been established in studies. Cells with Grp78/BiP overexpression had a significant better capacity to bind intracellular calcium (128; 129).

Recent evidence indicated that activation of autophagy is associated with the ER stress signaling pathway and that Grp78/BiP is essential for ER stress-induced autophagy activation (19). This notion is based on the observation that cells with Grp78/BiP knockdown showed nutrition restriction-induced ER stress activation and LC3 conversion, a hallmark of autophagy, but were deficient in forming double-membrane autophagosomes (19). Furthermore, disruptions in ER integrity such as increased numbers of ER structures and ER lumen expansion were observed in cells with Grp78/BiP knockdown, suggesting that activation of autophagy was tightly associated with ER homeostasis and that Grp78/BiP played an essential role in initiating these cell processes (18; 119).

Grp78/BiP protein has long been established as an ER-located chaperone as it contains an ER-residence sequence KDEL on the C-terminus (18). However, the large-scale study of cancer cell membrane proteins showed that Grp78/BiP was located on the cell surface, suggesting that activation of ER stress could lead to Grp78/BiP translocation from ER lumen to cell surface (129). Grp78/BiP has also been reported to be present unusually in mitochondria and nuclei. The role of ER stress and uncommon expression of Grp78/BiP in deteriorating mitochondrial function was investigated (130; 131). In those studies, it was reported that activation of ER stress could induce translocation of Grp78/BiP from the ER lumen to the plasma membrane, where Grp78/BiP was acting as a component of a receptor to initiate the translocation of a cell death signal protein ISM-1 (130; 131). After translocation to the cytoplasm, ISM-1 was shown to interact with a mitochondrial inner membrane protein ATP/ADP carrier. This protein-protein interaction would impair the function of ATP/ADP carrier and thus disrupt its ability to

transport ATP and ADP, ultimately resulting in depletion of cytoplasmic ATP levels (130; 131). Although this study did not test the biological consequence of the depleted cytoplasmic ATP level directly, it is largely known that ATP depletion is one of the causes of mitochondrial-dependent cell death (130; 131).

ER stress-induced cell death - Early activation of ER stress is an essential cellular event that aims to respond to various physiological/pathological challenges via upregulation of ER chaperones, repression of protein synthesis, and removal of unfolded/misfolded proteins (9). However, chronic and persistent activation of ER stress can be irreversible and eventually leads to cell death (9). ER stress-induced cell death has been linked to several deleterious conditions such as beta cell dysfunction in diabetes, development of neurodegenerative diseases, and cardiac muscle cell death (114; 116; 132). Having a better understanding of ER stress-induced cell death mechanisms and its related signals is essential to future development of therapeutic inventions to treat these diseases. On the one hand, ER stress is a necessary cell biological event contributing to the preservation of normal cellular function; on the other hand, as mentioned previously, severe and prolonged ER stress can trigger cell death via activation of several downstream signals. Therefore, it is biologically more beneficial and reasonable to prevent ER stress-induced cell death at the level of the cell death-related signals. Indeed, several studies have shown deletion of specific ER stress-induced cell death signals is an attractive strategy to prevent cellular dysfunction induced by ER stress (Figure 2.7).

Several cellular disturbances have been shown to trigger ER stress and cell death such as massive accumulation of unfolded proteins, cytoplasmic calcium dysfunction, redox/oxidative stress, and viral infection (9). Cellular pathways triggering cell death

under ER stress conditions have been investigated extensively and several mechanisms have been proposed, including apoptosis and aggressive autophagy (9). Caspase-12 and CHOP are two cell death signals specifically induced by ER stress (9). Caspase-12 has been shown to be located in the ER lumen and activated by ER stress induced signals but not by other signals such as mitochondrial-dependent apoptosis (9). The role of capase-12 in modulating cell death due to ER stress has been elucidated in both caspase-12 deficient and overexpression models as deficiency in caspase-12 resulted in cell death resistance in response to ER stress and caspase-12 overexpression sensitized cells to ER stress induced cell death (9; 114). Caspase-12 deletion has been used as a therapeutic approach to treat ER stress related cellular function as one study showed that knockout of caspase-12 attenuated ER stress-induced muscle pathology a mouse model of Duchenne Muscular Dystrophy (100).

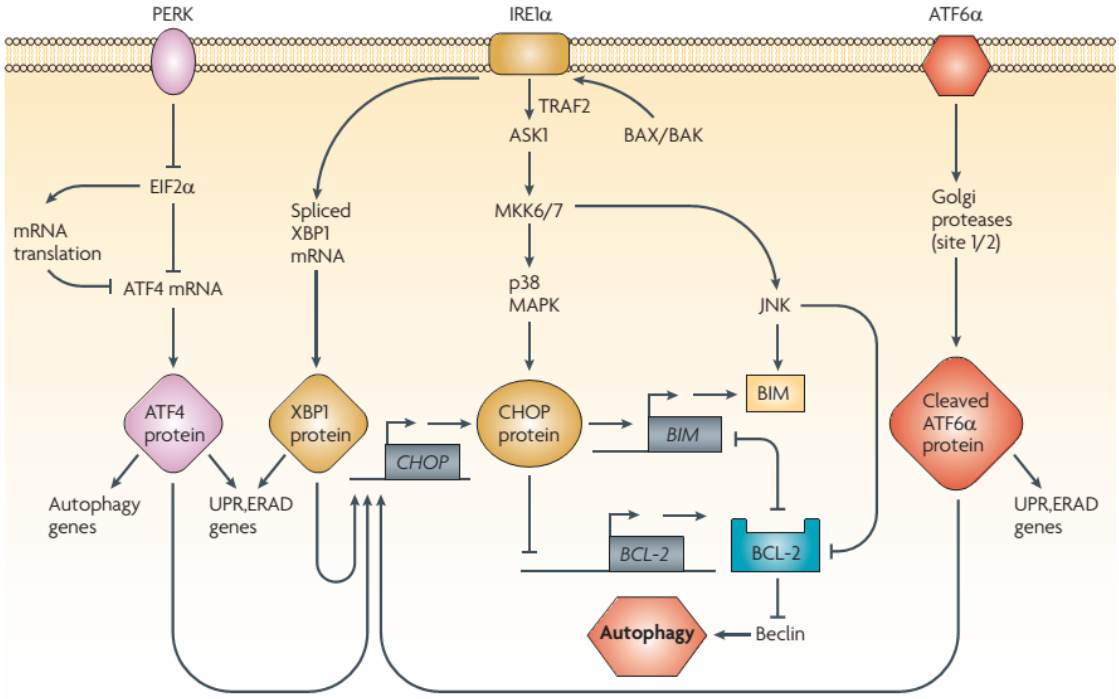

Figure 2.7. CHOP is a specific ER stress-induced cell death signal. Long term activation of ER stress pathway is known to trigger cell death signals and CHOP is found to be one of the specific cell death signals induced by fatal activation of ER stress. Several pathways are suggested to contribute to the upregulation of CHOP such as ASK1- p38/MAPK and JNK. As a transcriptional factor, CHOP is indicated to regulate gene expression involved in cell death such as Bcl-2 family proteins.

CHOP is one of the C/EBP family members and can be induced by several ER stress signals such as IRE1α and ATF6 (9). The role of CHOP in contributing to ER stress-induced cell death has been studied extensively and it appears likely that CHOP is a more attractive target to development therapeutic inventions for diseases in which severe ER stress is an underlying cause. A previous study showed that CHOP deficiency contributed to an attenuation of an oxidative stress response, improvement of beta cell

function, and beta cell survival in various animal models of diabetes (133). Besides being an important factor in modulating beta cell function in diabetes, CHOP has also has been shown to play an important role in other ER stress involved diseases such as kidney disease and brain damage (134). CHOP expression is induced in the early stage of ER stress activation and thus can be used as a specific marker to demonstrate activation of ER stress. However, extensive upregulation of CHOP requires cross-talk between different branches of the ER stress pathway and requires increased CHOP expression at the transcriptional level. CHOP protein post-translational modification has also been observed in previous studies, with phosphorylation of CHOP being induced by IRE1α – ASK1- p38 MAPK signals (135). The apoptotic role of CHOP was investigated and it has been shown that upregulation of CHOP could increase expression of Bim protein, which is a pro-apoptotic factor in the Bcl-2 family, and thus induces apoptosis under activation of ER stress (133; 136).

Besides introduction of protease- mitochondria-dependent cell death pathways, aggressive autophagy has been shown recently to be another way of inducing cell death under activation of ER stress (137). Autophagy is a necessary cell survival response devoted to protein degradation and removal of damaged cellular organelles under certain conditions such as starvation or accumulation of protein aggregates (138). A functional autophagy is initiated by the formation of a double layer membrane structure called an autophagosome, where targeted proteins or cell organelles are included and digested by certain lysosomal enzymes (19; 139). As mentioned previously, autophagy is an essential cellular process modulating cellular homeostasis; however, abnormal or aggressive autophagy could cause loss of cellular components under certain pathological conditions

such as neurodegenerative diseases and metabolic diseases. Autophagy-induced cell death is not necessarily involved in activation of apoptotic elements and is distinguished morphologically from traditional cell death pathways such as apoptosis and necrosis. Thus, autophagy is defined as a new pathway inducing cell death and may decide the cell destiny by interacting coordinately with these two traditional pathways. The rationale linking ER stress with autophagy is that accumulated unfolded/misfolded proteins need to be eliminated thus autophagy is one of the best candidates besides ERAD to conduct this task (138). Indeed, several studies showed that ER stress could trigger the formation of the autophagosome and inhibition/deletion of key ER stress elements could impair the effects of autophagy (19; 140). For example, two ER stress chemical inducers, DTT and tunicamycin, were shown to upregulate Atg8, which is a conserved marker for the formation of autophagosomes (19; 137; 140). Moreover, deletion of key ER stress elements IRE1α and Hac1 proteins resulted in an inhibition of autophagy, indicating that ER stress is upstream of autophagy (141). The important role of ER stress in inducing autophagy was investigated with a dominant-negative PERK, the dnPERK could inhibit the formation of the autophagosome, thus indicating that the PERK/eIF2α branch of ER stress is involved in activation of autophagy (141). ER stress has been shown to be a new pathway to induce autophagy in several studies but the delicate correlation between those two pathways still needs to be further investigated. Nevertheless, a better understanding of those pathways could prompt the development of therapeutic inventions treating pathological conditions induced by severe ER stress and aggressive autophagy.

ER stress & skeletal muscle

The role of the Sarcoplasmic/Endoplasmic Reticulum (SR/ER) in ER stress and ER-stress induced apoptosis in striated muscle is not well understood. This is an important new area of research within the fields of cardiac and neuromuscular diseases (142). Since, SR/ER is one of the largest organelles in muscle with the SR/ER covering as much as 50% of the volume of a muscle fiber, it could play a critical role in cellular pathology as well as in contraction-relation cycling. Double layers of SR/ER membrane are highly presentative and, similar to other cell organelles or structures, it has been shown that these membranes can be the donor of mitochondria during turnover and the formation of some key components such as the autophagosome (138). This notion has been further confirmed by the fact that abnormal changes in SR/ER morphology could be linked to skeletal muscle tissue pathology such as in DM1 (122-124).

SR/ER is the main site for preserving skeletal muscle intracellular calcium levels via the precise function of various calcium binding/buffer proteins in the ER lumen such as parvalbumin and calreticulin (97). ER membranes are not permeable to free calcium and the transportation of this ion is highly regulated by several ion channels and specific ATP-dependent calcium pumps located in the ER membrane such as SERCA1 and SERCA2 (8). Distribution of the intracellular calcium level due to disruption of those calcium buffering proteins, calcium channels, and calcium pumps could lead to severe cell dysfunction and eventually result in cell death (8). Simultaneously, a higher calcium level in the ER lumen and a lower calcium level in cytoplasm are essential to maintaining cellular redox/oxidative status as the ER lumen is the main site for protein synthesis and protein posttranslational modifications. The oxidative status in the ER lumen must be

maintained to enable formation of disulfide bonds. in addition, it has been shown that there is a tight dynamic interaction between ER and mitochondria as specific channels are involved in this interaction (23). The link between ER and mitochondria is critical as ER is buffering calcium levels in mitochondria, which is beneficial to keep mitochondrial homeostasis (143). Preliminary data from our proteomics study indicated that there could be more protein-protein interactions (PPIs) between proteins in ER and those in mitochondria (Chapter 5). Although the biological meaning of those PPIs has not been investigated in this dissertation, this finding is very interesting and is worthy of further evaluation based on the dynamic communication between and significance of ER-mitochondrial interactions.

ER stress has been linked to metabolic diseases as ER stress has been shown to be activated in the skeletal muscle under high fat diet treatment (144). ER stress has also been shown to be a beneficial event for muscle development as it is responsible for removal of vulnerable myoblasts via inducing apoptosis in those cells (145; 146). Inhibition of ER stress resulted in impaired muscle fiber function, indicating that moderate ER stress activation is essential to maintaining cellular quality control by eliminating underdeveloped cell types (145; 146). Another study showed that one branch of the ER stress pathway, via ATF6, was involved in the exercise-induced metabolic adaptation of skeletal muscle physiology by interacting with PGC1α (147). In this study, exercise challenge activated ER stress and knockout of ATF6 resulted in impaired recovery of skeletal muscle damage after exercise (147). Moreover, this study showed that in a mouse model of CHOP deletion, there was a similar phenotype to the PGC1α

knockout mouse model with an exercise intolerance phenotype, indicating the important role of ER stress in regulating skeletal muscle metabolic flexibility (147).

ER stress is also associated with skeletal muscle pathology as several studies detected the activation of ER stress under various pathological conditions such as in muscle dystrophy, muscle wasting, neurodegenerative diseases, and myotonic dystrophy 1 disease (22; 122-125; 148). A study using an animal model of DMD has further confirmed this notion. ER stress was activated in skeletal muscle of muscular dystrophy such as upregulation of CHOP and cleavage of caspase-12 (149). (149). Moreover, deletion of caspase-12 in one mouse model of DMD was shown to attenuate disease phenotypes including impaired muscle function and muscle fiber degeneration (149). This study suggested that ER stress activation plays a critical role in the muscle pathology in DMD and that deletion of key ER stress elements could be a novel way to improve muscle function in DMD. In another study, muscle biopsies from myotonic dystrophy 1 disease (DM1) patients were analyzed and ER stress was shown to be induced in skeletal muscle represented by upregulation of Grp78/BiP on both transcriptional and translational levels (124). ER stress has been a hot topic in the field of skeletal muscle related to metabolism and pathology since it plays an important role in regulating key cellular events such as protein quality control, mitochondrial turnover, intracellular calcium homeostasis, and cell death.

ER stress & ALS

Investigations into ER stress in ALS is possible due to the generation of a transgenic mouse model of ALS: the mutant G93A SOD1 mouse model (4). As mentioned previously, mutant SOD1 has normal dismutase enzymatic activity and the

"gain-of-function" is proposed as a working model for studying pathogenesis in ALS. SOD1 protein is located mostly in the cytoplasm but mutant SOD1 aggregates were shown to accumulate in other sites of the cells. Therefore, it was expected that protein aggregates could induce several cellular stress response pathways.

ER stress was investigated in both ALS patients and animal models of ALS (10; 21; 23; 95; 100; 140; 150-156). As expected, several lines of evidence suggest that ER stress was induced in motor neurons of human sporadic ALS, human familial ALS, and in animal models of ALS (151; 154). In a recent study, protein expression profiles were analyzed in spinal cords of human ALS patients and three ER stress sensors PERK, IRE1α, and ATF6 were shown to be significantly upregulated (153). Also, several ER stress-induced chaperones Grp78/BiP, PDI, and Erp57 were shown to be increased in spinal cords of ALS patients (153). The ER stress-induced cell death signals were also evaluated in the same study and the results showed the introduction of ER stress-induced cell death, including upregulation of CHOP, caspase-4, and p38 (Figure 2.7) (150).

The comprehensive analysis of the ER stress pathway, including ER stress sensors, ER chaperones, and apoptotic factors, fully supported the notion that ER stress was activated in spinal cords of ALS patients and upregulation of caspase-4 in ALS patients indicated that activation of ER stress may contribute, not only an early survival stage, but also late in disease to tissue pathology (140; 150; 152; 153). To further investigate this notion, animal models of ALS were used and it was shown that activation of ER stress and upregulation of CHOP occurred prior to disease onset (10). The evidence for ER stress participating in ALS pathology was also evaluated using both gain-of-function and loss-of-function transgenic animal models. Nervous system-specific deletion of Xbp-1,

which is a key ER stress induced protein and transcriptional factor, significantly extended the life span of ALS mice (140). Also, deletion of another ER stress element PUMA, which is a BH-3 only protein and induced by ER stress, was shown to increase motor neuron survival, delay disease progression, and preserve motor-neuron function (152). Collectively, those studies suggest that ER stress is induced in the nervous system of ALS and may contribute to motor neuron dysfunction and cell death.

ER stress activation in skeletal muscle of ALS has never been evaluated systematically and recent mass spectrometry-dependent high-through mapping of skeletal muscle in ALS indicated elevation of heat shock protein families including Grp78/BiP, suggesting ER stress could be present in skeletal muscle of ALS (10). Our lab determined the ER stress pathway in skeletal muscle of ALS mice and preliminary data showed that ER stress was present in skeletal muscle of ALS and may be linked to skeletal muscle pathology (10; 125). To rule out the possibilities of ubiquitous tissue activation of ER stress due to whole body mutant SOD1 overexpression, , we also assessed the ER stress pathway in tissues other than skeletal muscle and nerve. These other tissue (liver and cardiac muscle) did not show activation of ER stress, thus our results clearly showed that activation of ER stress is a specific event in skeletal muscle (10; 125).

Skeletal muscle & ALS

ALS has long been recognized as a motor neuron disease which firstly impairs upper and lower motor neurons and, as a consequence, causes progressive muscle atrophy (1). However, this point of view has been recently questioned by the observation that other cell types such as astrocytes and myocytes are involved in the ALS disease

phenotype. Thus, ALS is a disease affecting multiple cell types in which these cell types (i.e. muscle and nerve) interact coordinately to induce the ALS pathophysiology (5).

Skeletal muscle is one of the primary tissues affected in the muscle weakness phenotype of ALS. Mutant SOD1 proteins, linked to familial ALS, have been shown in skeletal muscle of both ALS patients and animal models of ALS, raising the question whether skeletal muscle contributes to ALS pathogenesis or not. In addition, a previous study using transgenic mice with skeletal muscle-specific expression of mutant SOD1 showed transgenic mice developed an ALS phenotype including progressive skeletal muscle atrophy, decreased muscle function, and other muscle pathology (157). Furthermore, another study employing the same strategy showed that mice with skeletal muscle restricted expression of mutant SOD1 developed muscle weakness and some neuronal deficits. More interestingly, besides presenting muscle abnormities, those transgenic mice developed impaired neuromuscular junction and loss of spinal motor neurons, suggesting that skeletal muscle vulnerability induced by mutant SOD1 toxicity is enough to prompt motor neuron degeneration in ALS (6).

Mitochondrial dysfunction in skeletal muscle of ALS – Mitochondrial dysfunction has been considered as the final pathological pathway involved in motor neuron degeneration in ALS due to its primary role in modulating key cellular processes such as ATP synthesis, calcium buffering, and cell death (66; 76; 77). It is suggested that mitochondrial dysfunction is a typical pathology in skeletal muscle of ALS as alterations in mitochondrial ultra-structure such as aggregates and giant size were reported in skeletal muscle of ALS patients and animal models of ALS (66; 76). Besides showing pathological changes of structure, mitochondrial function has also been determined and it

was shown that there was a decrease in mitochondrial function in skeletal muscle of ALS patients, including downregulation of NADH/CoQ oxidoreductase and complex IV (40; 158). Moreover, decreased ATP level and increased uncoupling protein 3 (UCP-3) have been reported in skeletal muscle of ALS mice and patients and it is suggested that upregulation of UCP-3 in skeletal muscle contributed to mitochondrial damage and muscle pathology in ALS (Figure 2.8) (158).

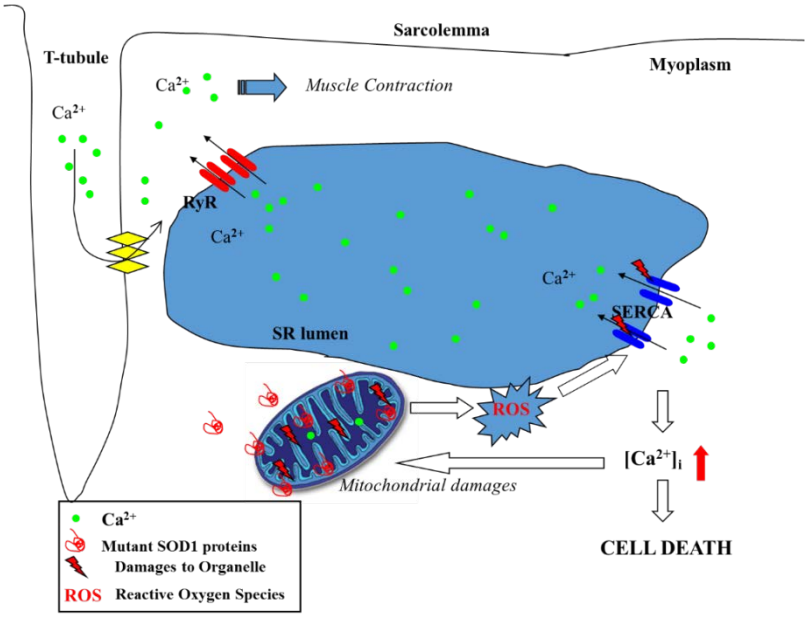

Figure 2.8. SR/ER system in skeletal muscle and proposed mechanisms contributing to skeletal muscle atrophy in ALS. SR/ER is the main site for calcium storage and intracellular calcium level is tightly regulated by ER-located proteins such as SERCAs and ryanodine receptors (RyR). Increased intramuscular calcium level has been reported and suspected to contribute to muscle atrophy in ALS via various cellular processes such as mitochondrial dysfunction and ROS generation.

Mutant SOD1 protein aggregates in skeletal muscle of ALS – Accumulation of unexpected protein aggregates in tissues including skeletal muscle is a hallmark feature of ALS pathology, although it is still debated whether these protein aggregates contribute to disease pathogenesis or are simply an adaptive protective mechanism (1). Previous studies showed two forms of protein aggregates were present in skeletal muscle of ALS mice: mutant SOD1-containing aggregates and non-SOD1 protein aggregates (82). However, their pathological role in inducing skeletal muscle dysfunction in ALS is still not clear. Mutant SOD1 protein aggregates are not suggested to be linked with disease progression based on the fact that higher protease activity was also observed, indicating an increased ability to remove mutant SOD1 in skeletal muscle (159). There is increasing evidence that non-SOD1 protein aggregates are involved in ALS disease progress and one study showed that there is a close correlation between non-SOD1 protein aggregates and over-production of reactive oxygen species in mitochondria of skeletal muscle (160). However, the role of different forms of protein aggregates in skeletal muscle needs further investigation.

Proteasome activity in skeletal muscle of ALS – As mentioned previously, the formation of protein aggregates in pathological tissues such as in motor neurons and skeletal muscle has been recognized as a hallmark of ALS (1). However, the clearance rate of protein aggregates conducted by the proteasome pathway between different tissues is divergent and it is suggested that skeletal muscle has better efficiency in removing mutant SOD1 proteins than motor neurons (161). The higher rate of removing mutant SOD1 proteins in skeletal muscle is thought to be due to of a higher concentration of the ubiquitin proteasome system and greater activation of autophagy in muscle cells (161;

162). Indeed, previous studies showed that the dysregulation of proteasome activity induced by mutant SOD1 was less impaired in C2C12 muscle cells as those cells demonstrated a higher chymotryptic proteasome activity, which is the main process of degradation misfolded and unfolded proteins (161). Moreover, autophagy has been shown extensively in muscle cells but not motor neuron cells, suggesting muscle cells have a better system to prevent the accumulation of protein aggregates (161). (161). Besides proteasome pathway and activation of autophagy, several muscle atrophy factors such as transcriptional factor forkhead box o3 (FOXO3) and NF-κB have been shown to be upregulated and contribute to the production of reactive oxygen species in skeletal muscle (157). It has been suggested that FOXO3 links oxidative stress to the autophagy pathway and it is suggested that moderate activation of autophagy could be an attractive therapeutic method to treat skeletal muscle dysfunction in ALS (157).

Chapter 3: Activation of the endoplasmic reticulum stress response in skeletal muscle of G93A*SOD1 Amyotrophic Lateral Sclerosis mice

The following article was published in the journal of Frontiers in Cellular Neuronscience (18 May 2015)

Activation of the endoplasmic reticulum stress response in skeletal muscle of G93A*SOD1 Amyotrophic Lateral Sclerosis mice

Dapeng Chen[1] Yan Wang[2] & Eva R. Chin[1,3]

School of Public Health, University of Maryland, College Park, MD

1. School of Public Health, University of Maryland, College Park, MD 20742.
2. College of Computer, Mathematics and Natural Sciences, University of Maryland, College Park, MD 20742.
3. Send correspondence: Dr. Eva R. Chin, School of Public Health, University of Maryland, College Park, MD 20742

Tel.: (301) 405-2478, Fax: (301) 405-5578
Email: erchin@umd.edu

Keywords: amyotrophic lateral sclerosis, skeletal muscle, endoplasmic reticulum stress, misfolded proteins, muscle atrophy, protein synthesis, unfolded protein response

Abstract

Mutations in Cu/Zn superoxide dismutase (SOD1) are one of the genetic causes of Amyotrophic Lateral Sclerosis (ALS). Although the primary symptom of ALS is muscle weakness, the link between SOD1 mutations, cellular dysfunction and muscle atrophy and weakness is not well understood. The purpose of this study was to characterize cellular markers of ER stress in skeletal muscle across the lifespan of G93A*SOD1 (ALS-Tg) mice. Muscles were obtained from ALS-Tg and age-matched wild type (WT) mice at 70d (pre-symptomatic), 90d and 120-140d (symptomatic) and analyzed for ER stress markers. In white gastrocnemius (WG) muscle, ER stress sensors PERK and IRE1α were upregulated ~2-fold at 70d and remained (PERK) or increased further (IRE1α) at 120-140d. Phospho-eIF2α, a downstream target of PERK and an inhibitor of protein translation, was increased by 70d and increased further to 12.9 –fold at 120-140d. IRE1α upregulation leads to increased splicing of X-box binding protein 1 (XBP-1) to the XBP-1s isoform. XBP-1s transcript was increased at 90d and 120-140d indicating activation of IRE1α signaling. The ER chaperone/heat shock protein Grp78/BiP was upregulated 2-fold at 70d and 90d and increased to 6.1-fold by 120-140d. The ER-stress-specific apoptotic signaling protein CHOP was upregulated 2-fold at 70d and 90d and increased to 13.3-fold at 120-140d indicating progressive activation of an apoptotic signal in muscle. There was a greater increase in Grp78/BiP and CHOP in WG vs. the more oxidative red gastrocnemius ALS-Tg at 120-140d indicating greater ER stress and apoptosis in fast glycolytic muscle. These data show that the ER stress response is activated in skeletal muscle of ALS-Tg mice by an early pre-symptomatic age and increases with disease progression. These data suggest a mechanism by which

myocellular ER stress leads to reduced protein translation and contributes to muscle atrophy and weakness in ALS.

Background

Amyotrophic Lateral Sclerosis (ALS) is a fatal motor neuron disease characterized by degeneration of motor neurons and progressive paralysis of skeletal muscle (1). ALS is inevitably fatal, with patients generally dying due to respiratory failure within 2-5 years of diagnosis (1). Although the majority of ALS cases are sporadic without family history, 5-10% of the total cases of ALS have a known genetic basis (1). Mutations in human Cu/Zn superoxide dismutase 1 (SOD1) account for ~20% of familial ALS (fALS) cases (1). Mice generated to express a human Cu/Zn SOD1 mutation found in fALS patients (Gly93 to Ala; G93A) develop a rapidly progressive and fatal motor neuron disease similar to the clinical phenotype of ALS (32). There is evidence that the SOD1 mutations exert their deleterious effects through a "gain-of-function" mechanism rather than through a loss of superoxide dismutase activity (4). The nature of this toxic "gain-of-function" is not known, although a number of putative mechanisms have been proposed, including oxidative stress, glutamate-mediated excitotoxicity, mitochondrial dysfunction, protein aggregation and endoplasmic reticulum (ER) stress (163).

Neurodegenerative diseases, including ALS, that result from unfolded/misfolded proteins have been linked to ER stress (164). Most newly synthesized proteins are folded properly in the ER, but unfolded and misfolded proteins accumulate in the ER lumen, causing cellular stress, activation of unfolded protein response (UPR) and an ER stress response (9). The ER stress response involves activation of three ER-resident stress

sensors: protein kinase RNA-activated-like ER kinase (PERK), inositol-requiring kinase 1-alpha (IRE1α), and activating transcription factor 6 (ATF6) (9). Normally, these ER stress sensors physically interact with the ER chaperone immunoglobulin binding protein (Grp78/BiP) which suppresses their activation (9). However, when unfolded/misfolded proteins accumulate, Grp78/BiP preferentially binds to unfolded/misfolded proteins, resulting in activation of the ER stress response, including an upregulation of genes encoding Grp78/BiP, protein disulfide isomerase (PDI) and down regulation of protein synthesis (104; 164). PERK activation induces the eukaryotic initiation factor 2 alpha subunit (eIF2α) kinase and phosphorylation of eIF2α resulting in inhibition of protein translation (9). Activation of IRE1α leads to the alternative splicing of the transcription factor X-box binding protein 1 (XBP1) to the spliced XBP1 form to induce genes that regulate protein quality control in the ER (9). Although ER stress is usually a short term homeostatic event essential for cell survival, prolonged and severe ER stress can trigger apoptosis by ER stress-specific cell death signals, including C/EBP homologous protein (CHOP) and caspase-12 (114; 165).

It has previously been shown that mutant SOD1 accumulates inside the ER, where it forms insoluble high molecular weight aggregates and interacts with Grp78/BiP in spinal cord microsomal fractions (151). Markers of ER stress activation have been shown in spinal cord sections of ALS patients and in mouse models of ALS (151; 153). Pathology studies show that ER stress is evident in spinal cords of ALS patients suggesting that ER stress-induced apoptosis may contribute to motor neuron death (21; 153). The ER stress response is also activated in mouse models of ALS, although the time course is controversial (21; 95; 150; 151; 153-155).

The targets of mutant SOD1-induced toxicity in ALS pathology are the motor neurons and the skeletal muscle that it innervates (166). While the primary focus has been on selective defects in the motor neuron causing muscle weakness and atrophy, it has been shown that muscle-restricted SOD1 mutations also recapitulate the hallmark signs of ALS, albeit at a slower rate of progression (6; 157). Thus, it has been proposed that defects in skeletal muscle, leading to muscle cell dysfunction, also contribute to the motor neuron pathology via a "dying-back" phenomenon. It has previously been shown that early markers of muscle adaptation in the G93A*SOD1 mouse (i.e. by 49d, prior to atrophy) include metabolic enzymes, particularly down regulation of enzymes of oxidative metabolism and upregulation of enzymes of glycolytic metabolism and increases in proteins involved in protein synthesis. (167). Putative markers of disease progression, which were altered at 98d when atrophy was evident, include glycolytic enzymes which decrease and cell stress markers (i.e. heat shock proteins) and transport proteins (i.e. albumin), which increase.

The intracellular mechanisms leading to altered gene/protein expression in skeletal muscle with disease-induced plasticity are not fully understood. However, there are reports of mitochondrial depolarization leading to reduced mitochondrial Ca^{2+} buffering and increased cytosolic Ca^{2+} which may trigger events in the muscle atrophy process (48; 168). Recently we reported impaired intracellular Ca^{2+} regulation in the sarcoplasmic reticulum (SR) in muscle fibres from G93A*SOD1 mice (7). The changes intracellular Ca^{2+} occurred prior to the decline in motor function (by 90d) and were associated with decreases in myocellular Ca^{2+} buffering proteins SERCA1, SERCA2 and parvalbumin. Based on the known association between SR/ER Ca^{2+} regulation and

protein folding (49; 142), and the putative contribution of skeletal muscle defects to the progression of ALS, we hypothesized that ER stress would be induced in skeletal muscle. Thus, the primary aim of this study was to investigate the ER stress signaling pathway in skeletal muscle at three different ages across the lifespan of the G93A*SOD1 mouse model of ALS. A secondary aim was to compare key markers of ER stress in skeletal muscles of varying fiber type composition and metabolic capacities as well as to non-muscle tissue. Our findings indicate that ER stress is activated in skeletal muscle of G93A*SOD1 mice as early as 70d, with ER stress pathways leading to inhibition of protein translation. Our data further suggest that defects in myocellular protein handling and activation of apoptosis may contribute to the muscle atrophy and weakness observed in ALS.

Methods

Ethics Statement

All procedures were conducted under a protocol approved by the Institutional Animal Care and Use Committee (IACUC) of the University of Maryland, College Park.

Animals

Control C57BL/6 SJL hybrid female and transgenic ALS B6SJL-Tg (SOD1-G93A) Gur/J (G93A*SOD1) male mice were obtained from The Jackson Laboratory. Wild-type control (WT) and transgenic G93A*SOD1 heterozygote (ALS-Tg) mice were bred to establish a colony at our animal care facility at the University of Maryland. Mice were weaned at postnatal day 21 and genotyped. Male and female ALS-Tg mice along with their wild-type littermates were investigated at a range of ages from the pre-

symptomatic to the symptomatic stages of the disease: i) early pre-symptomatic at postnatal day 70 (70d); ii) late pre-symptomatic at postnatal day 90 (90d); and iii) end stage at postnatal day 120-140 (120-140d) (see Table 1). Early signs of disease such as muscle tremors can be detected between 65 and 90d but overt muscle weakness and limitations in mobility do not occur until 100-120d (2). We chose the 70d and 90d time points based on differences observed in single muscle fiber resting intracellular Ca^{2+} concentration that we now have reported (7). The final time point (120-140d) was based on symptom progression, with the date of use determined by the inability of the mouse to right itself after 30s of being placed on its side as previously described by others (169).

At time of use, animals were euthanized by CO_2 inhalation followed by cervical dislocation. Skeletal muscles, cardiac muscle, and liver were harvested, quickly frozen in liquid nitrogen and stored at -80°C for subsequent analysis. Various skeletal muscles were harvested in order to assess differences in ER stress between muscles of varying fiber type and of different oxidative and glycolytic capacities. White gastrocnemius (WG) has primarily fast glycolytic fibers (97% type IIB, 1.5% IIX/B and 1.5% IIX), red gastrocnemius (RG) primarily fast oxidative glycolytic fibers (22% type IIB, 3% IIX/B, 20% IIX, 42% IIA and 8% and type I) (170) and diaphragm (DIA) has a mixed fiber type including both slow oxidative, fast oxidative and fast glycolytic fibres (39% type IIX, 23% type IIX/B, 23% IIA/X and 10% type I (171). Tibialis anterior (TA) has primarily fast glycolytic fibers (50% type IIB, 40% type IIX and 10% IIA), with reports of a fiber type shift to more oxidative (20% IIB, 10% IIX and 70% IIA) at 115d in the G93A*SOD1 mouse (169). In WT mouse muscle, glycolytic capacity is greatest in type IIB > IIB/X >IIX = type I > IIA/X > IIA (170) and thus expected to be highest in

WG>TA>DIA>RG. Conversely, in WT, oxidative capacity is greatest in type IIA > type I = type IIX > IIB and thus would be highest in RG>DIA>TA>WG.

Protein Extraction

The superficial (white) and deep (red) gastrocnemius, diaphragm, cardiac muscle, and liver tissues were used for assessment of protein levels using western blot technique. Tissue samples were homogenized on ice using a polytron at 50% maximal power for three 10 sec bursts, separated by 30 sec in ice cold lysis buffer (20 mM Hepes, pH= 7.5, 150 mM NaCl, 1.5 mM $MgCl_2$, 0.1% Triton X-100, 20% Glycerol) containing 1 mM DTT and protease inhibitor cocktail (cOmplete mini EDTA-free Protease Inhibitor Cocktail, Roche). After 20 min of incubation at 4^{o}C followed by centrifugation for 5 min at 20,000 × g, the supernatant was collected, quick frozen in liquid nitrogen and stored at -80oC until required.

Western Blot Analyses

Total protein concentration in the samples was determined using a BCA protein assay kit (Thermo Scientific). Samples were then prepared with loading buffer and denatured by incubating samples at 100^{o}C for 5 min. For western blot analyses, 30 μg total protein was loaded on bis-acrylamide gels and separated using polyacrylamide gel electrophoresis (PAGE). Samples were then transferred to PVDF membrane (Millipore) and blocked with 5% (w/v) non-fat dry milk in Tris-buffered saline (pH 8.0) for 1 hr. The appropriate primary antibodies were added (PERK, phospho-PERK (Thr 980), IRE1α, eIF2α, phospho-eIF2α (Ser51), Grp78/BiP, PDI, and CHOP; 1:1000, Cell Signaling Technology) and membranes were incubated at 4oC overnight, washed and

then and subsequently probed with HRP-linked anti-rabbit IgG or anti-mouse IgG antibodies (1:1000, Cell Signaling Technology) 1 hr at room temperature. Secondary antibodies were detected using HRP-linked chemiluminescence with SuperSignal West Dura Chemiluminescence Substrate (Thermo Scientific) and imaged using the chemiluminescence imaging system (GeneGnome, Syngene). The signal for the target protein of each sample was quantified using densitometry (Image J Software) and expressed in arbitrary unit (AU). GAPDH (1:2000, Thermo Scientific) or β-actin (1:1000, Cell Signaling Technology) was used to confirm equal protein loading across samples.

Mass Spectrometry based protein relative quantification

To confirm differential expression of ER stress proteins using a non-antibody based method, we completed in-gel digestion of proteins in the molecular weight range of the Grp78/BiP protein. We focused on the Grp78/BiP protein based on preliminary work with an antibody that gave us a divergent response (125) to the one we report here. Skeletal muscle total protein samples were prepared as described previously. For the purpose of protein separation, 30 μg of total protein was loaded onto 8% one-dimensional SDS-PAGE gel. After gel electrophoresis, protein bands were stained using a protein blue stain kit (Thermo Scientific). The targeted bands (~80 kDa) were carefully excised and in-gel tryptic digestion carried out following standard procedure. Briefly, proteins were reduced with 5 mM DTT, alkylated with 55 mM iodoacetamide, and digested with 20 ng/μL trypsin (Life TechnologiesTM) at 37°C overnight. All reagents were dissolved in 50 mM ammonium bicarbonate (pH 8.5).

After trypsin digestion, peptide products were collected and analyzed by nano LC-MS/MS analysis using LTQ Orbitrap mass spectrometer coupled to a Shimadzu 2D Nano HPLC system. Peptides were loaded with an autosampler into an Zorbax SB-C18 trap column (0.3×5.0 mm) (Agilent Technologies, Palo Alto, CA) at 10 µL/min with solvent A (97.5% water, 2.5% ACN, 0.1% formic acid) for 10 min, then eluted and separated at 300 nL/min with a gradient of 0-35% solvent B (2.5% water, 97.5% ACN, 0.1% formic acid) in 30 min using a Zorbax SB-C18 nano column (0.075×150 mm). The mass spectrometer was set to acquire a full scan at resolution 60,000 (m/z 400) followed by data dependent MSMS analysis of top 10 peaks with more than 1 charge in the linear ion trap at unit mass resolution. The resulting LC-MS/MS data were searched against a mouse protein database generated from uniprot and a common contaminant database using Mascot (v2.3) and Sequest search engines through Proteome Discoverer (v1.4). Carbomidomethylation at Cys was set as fixed modification. Methionine oxidation and asparagine and glutamine deamidation were set as variable modification. Spectral counting with normalized total spectra was carried out using Scaffold software, (Proteome Software, Inc). Protein probability >99% and at least one unique peptide with a probability score >95% were set to as minimum requirement for protein identification.

Gene Expression

In order to investigate transcriptional events involved in ER stress pathway, we isolated mRNA from tibialis anterior muscle (TA) and examined transcript levels of XBP-1, GRP78/BiP, and CHOP. Briefly, total RNA was isolated using TriPure Reagent (Roche) and RNA content was determined by using a NanoDrop spectrophotometer and mRNA was diluted to 5ng/µL. Reverse transcription from mRNA to cDNA was

conducted by using One-Step RT-PCR System (Life TechnologiesTM). Semi-quantitative PCR (sqPCR) was used to determine gene transcriptional levels and the primer information such as XBP-1, CHOP, and 18s was acquired from a previous study (2). The band intensity of PCR products were quantified using densitometry (Image J Software) and expressed in arbitrary unit (AU). For XBP-1, two variants of XBP1 mRNA are expressed in cells. Under normal conditions, un-spliced XBP1 mRNA (XBP1-u) is expressed. However, as ER stress is induced, a spliced form of XBP1 mRNA (XPB1-s) will be expressed. Thus, upregulation of XBP1-s mRNA is a marker of ER stress activation downstream of IRE1α (147).

Data Analysis

To determine statistical differences in protein and mRNA expression level between genotype (WT vs. ALS-Tg) and Age (70d, 90d and 120-140d) data were analyzed using two-way ANOVAs. Where interaction effects (genotype X age) were observed, the main effects are not reported. For significant interaction effects, Tukey post-hoc tests were used to determine differences across time points for ALS-Tg (i.e. 70d vs. 90d). T-tests were used to determine differences between WT and ALS-Tg at each time point. Statistical significance was accepted as $p<0.05$.

Results

ER stress pathway is induced in skeletal muscle of ALS mice. PERK and IRE1α are two ER stress sensors known to be upregulated when ER stress is induced. In our study, PERK protein level was upregulated 2.6 –fold in WG muscle of ALS-Tg vs. WT mice at 70d (p=0.01), 5.4-fold at 90d (p=0.025) and 5.2 fold at 120-140d (p=0.001) (Figure 1A and C). There was no difference in PERK level of ALS-Tg WG between 70, 90 and 120-140d (no main effect for age or genotype X age interaction). To assess the specificity of the antibody for total PERK, the antibody was pre-incubated with a PERK-antibody blocking peptide. Under these conditions, the protein band at ~140kDa identified as PERK was not visible (Figure 1B), confirming the specificity of the PERK antibody. Since activated PERK undergoes auto-phosphorylation, we also assessed the ratio of phospho-PERK to total PERK. The phospho-PERK/total PERK ratio was increased 2-fold in WG of ALS-Tg mice at 120-140d (p=0.012) indicating greater activation of existing PERK protein at the symptomatic age (Figure 1A and D). Previous studies have shown that PERK can activate eIF2α kinase, resulting in phosphorylation of eIF2α at Ser51 and suppression of protein synthesis during ER stress (147). We therefore assessed the downstream effects of activation of PERK. In WG muscle, the ratio of phospho-eIF2α/total eIF2α was increased 2.3-fold in ALS-Tg vs. WT at 70d (p=0.005), remained elevated at 90d (p=0.048) and increased further to 12-fold at 120-140d (p=0.011; Figure 2A and B). For phospho-eIF2α/total eIF2α there was a genotype X age interaction effects with the increase in ALS-Tg only increasing between 70d and 120-140d (70d vs. 90d; p=0.227; 70d vs. 120-140d p=0.018; 90d vs. 120-140 p=0.062). Total

eIF2α was not altered, just phosphorylation at Ser51, indicating inhibition of protein translation at these ages.

In addition to PERK, up-regulation of ER stress sensor IRE1α was also observed in WG of ALS-Tg mice by 70d. IRE1α protein levels were increased 2.5-fold at 70d ($p=0.043$) remained elevated at 90d ($p=0.0005$) and showed a further increase to 4.9 -fold WT levels at 120-140d ($p=0.0002$ vs. WT by t-test; $p=0.008$ for 70d vs. 120-140d for ALS-Tg by Tukey post-hoc) (Figure 3A and B). XBP1 mRNA splicing is commonly used to indicate upregulation of IRE1α since activation of IRE1α leads to mRNA splicing. Thus, we investigated transcript levels of the un-spliced (XBP-1u) and spliced XBP1 (XBP-1s) forms of XBP-1. In TA muscle, XBP-1s mRNA was increased to 1.3- and 1.4-fold at 90d ($p=0.001$) and 120-140d ($p<0.0001$). There was a genotype x age interaction effect with XBP1-s being higher at 90d vs. 70d ($p=0.002$) and at 120-140d vs. 70d ($p=0.002$). XBP1-u mRNA was not altered (Figure 3C and D).

Since cellular stress results in induction of ER chaperone proteins to handle misfolded and unfolded proteins, we examined changes in PDI and Grp78/BiP protein levels, two proteins involved in post-translational modification and known to be up-regulated with ER stress activation (9). Grp78/BiP was upregulated 2 -fold in WG of ALS-Tg vs. WT mice at 70d ($p=0.006$), remained elevated at 90d ($p=0.025$) and increased further to 6.7-fold at 120-140d ($p=0.005$) (Figure 4A and 4B). There was a genotype x age interaction effect with Grp78/BiP in ALS-Tg being different at 70d vs. 120-140d ($p<0.001$) and at 90d vs. 120-140d ($p<0.001$). Increased expression of PDI was also observed (2.2 -fold but only at 120-140d ($p=0.001$; Figure 4A and C). There was a genotype X age interaction effect for PDI with differences across all age groups for

ALS-Tg (70d vs. 90d, p=0.004; 70d vs. 120-140d, p=0.001; 90d vs. 120-140d, p<0.001). Taken together, these data show evidence of ER stress in skeletal muscle as early as 70d and further augmented at the symptomatic age in ALS-Tg mice.

To confirm antibody-based findings of the Grp78/BiP increase in skeletal muscle of ALS-Tg mice, we carried out relative protein quantification using LCMSMS and spectral counting compare Grp78/BiP protein levels between genotypes (Figure 5A). Grp78/BiP protein was identified by 11 exclusive unique spectra which contributed to the identification of 10 exclusive unique Grp78/BiP peptides (Figure 5B and C). Protein quantitative data analysis showed that Grp78/BiP was more abundant in skeletal muscle of ALS mice as spectral counting numbers were significantly higher in ALS-Tg versus WT mice (Figure 5D). Collectively, our label-free spectral counting-based protein quantitative data is consistent with western blot data, supporting our notion that ER stress is activated in skeletal muscle of ALS mice.

ER stress-specific cell death signal is induced in skeletal muscle of ALS mice. Several mechanisms have been suggested to link the ER stress pathway to cell death, including activation of the ER stress-specific cell death signal CHOP (9). In WG of ALS-Tg mice, CHOP was upregulated 1.8- fold at 70d (p=0.041), remained elevated at 90d (p=0.025) and further increased to 12-fold at 120-140d (p=0.019) (Figure 6A and B). There was a significant genotype X age interaction effects with ALS-Tg only being different at 70d vs. 120-140d (p<0.001) and at 90d vs. 120-140d (p<0.001). There were no changes in CHOP mRNA (data not shown), indicating that there is post-translational modification and increased stability of CHOP protein (172). In addition to evaluating CHOP induction in the limb muscle, we also investigated diaphragm muscle since

atrophy of this muscle results in respiratory failure and death in ALS mice (173). In DIA, CHOP protein expression was increased 1.7 -fold in ALS-Tg vs. WT mice at 70d (p=0.008), remained elevated at 90d (p=0.001) and then increased further to 9-fold at 120-140d but due to the high degree of variability in CHOP elevation, ALS-Tg vs. WT was not significant at 120-140d (p=0.10). there was a genotype X age interaction effect with CHOP showing an increase in ALS-Tg at 120-140d vs. 70d (p=0.004) and 120-140d vs. 90d (p=0.005) (Figure 6C and D).

Greater activation of ER stress pathway in glycolytic vs. oxidative muscle of ALS mice. On dissection we noted that the superficial gastrocnemius muscle was more red than white in the ALS-Tg mice (Figure 7A). Previous studies showed that fast type IIb motor units are affected first during ALS disease progression in the G93A*SOD1 mouse (174). Thus, we wanted to determine whether ER stress is activated to a greater extent in fast glycolytic vs. fast oxidative skeletal muscle by comparing two typical ER stress markers Grp78/BiP and CHOP between WG (fast glycolytic) and red gastrocnemius (RG; fast oxidative) muscle. At the symptomatic age (120-140d), both Grp78/BiP and CHOP were induced to greater extent in WG vs. RG (2.0- and 5.6-fold, respectively; p<0.05) (Figure 7B and C), indicating that ER stress activation is greater in fast glycolytic muscle.

ER stress markers are not induced in cardiac muscle and liver tissues of ALS mice. ER stress is activated when misfolded proteins accumulate in the ER lumen. One could argue that the ER stress activation we observed in our study may be a non-skeletal muscle specific event since the animal model we used is a whole-body SOD1 protein mutation and accumulation of mutant SOD1 could activate ER stress in all tissues, including skeletal muscle. Thus, we investigated the ER stress pathway in non-

pathological tissues such as cardiac muscle and liver. Two classical ER stress markers, Grp78/BiP and CHOP, were not different between WT and ALS-Tg mice for heart or liver at any age (see Figure 8). Therefore, ER stress activation is observed in skeletal but not cardiac muscle or other highly oxidative tissues like liver in ALS mice.

Discussion

In this study we show that ER stress is activated in skeletal muscle of G93A*SOD1 mice and thus may play a role in muscle atrophy in ALS. This is based on evidence that: i) ER stress is activated at 70d, an early pre-symptomatic age and is further upregulated at 120-140d, an age when mice are symptomatic; ii) skeletal muscle ER stress induces the cell death signal CHOP; iii) ER stress is activated to a greater extent in highly glycolytic muscles with primarily type IIb fibers which are affected by an early loss of fast fatigable motor axons; and iv) the ER stress activation is specific to skeletal vs. cardiac muscle. These data support the hypothesis that ER stress plays a role in muscle atrophy in ALS mice.

ER stress response in ALS

Our lab previously reported impairments in SR Ca^{2+} uptake, leading to elevations in resting cytosolic Ca^{2+} concentration in muscle fibers from G93A*SOD1 mice (7). We therefore hypothesized that altered intracellular Ca^{2+} in association with increased oxidative stress in muscle cells would lead to misfolded proteins and activate the UPR and ER stress responses. We propose a model (Figure 9) where age-dependent activation of ER stress sensors PERK and IRE1α in response to misfolded proteins leads to increases in protein chaperones Grp78/BiP and PDI in skeletal muscle. Prolonged oxidative stress (in this case due to mutant SOD1) and persistent accumulation of misfolded proteins further augments the ER stress response and activates the apoptotic signal CHOP leading to muscle atrophy. At 70d, an age where muscle grip function is still 100% of WT levels (7), there is already an ~2-fold increase in the ER stress markers PERK, IRE1α, Grp78/BiP and CHOP. By 84d grip function is reduced to 77% WT

levels and by 120-140d, when grip function is zero (i.e. mice are no longer able to grasp a metal grid) (7), there are further increases in IRE1α, Grp78/BiP and CHOP as well as increased phospho-PERK and phospho-eIF2α/total eIF2α. Based on these data we cannot determine if impaired Ca^{2+} regulation and ER stress are causative or a consequence of muscle atrophy, but only that they are associated. Using the same animal model, studies using MRI to asses muscle volume show significant muscle loss as early as 8 wks of age and continuous loss over the lifespan of these mice (175; 176). Collectively these data show muscle atrophy and weakness over the timeframe that we observed increases in markers of ER stress, suggestive of some involvement of protein misfolding, activation of the ER stress response and possibly apoptosis. The impairment in muscle protein translation as well as apoptosis would contribute to muscle cell atrophy and weakness which, in conjunction with motoneuron degeneration, would contribute to the pathophysiology and disease progression in ALS.

Proteins that require folding and post-translational modification, primarily secretory and membrane bound proteins, are processed in the ER. Proteins that do not fold properly are degraded by the ubiquitin proteasome pathway. If misfolded/unfolded proteins accumulate, the unfolded protein response is triggered to promote proper folding and autophagy is activated to support cell survival. However, if there is a persistent increase in misfolded/unfolded proteins that exceeds the capacity of the ER to regulate proper folding, then protein translation is inhibited to reduce protein load and there is activation of an ER stress-induced cell death pathway via upregulation of CHOP. Activation of the ER stress response is increasingly being recognized as a cellular mechanism in neurodegenerative as well as metabolic diseases such as diabetes (177;

178). The biological role of ER stress activation in motor neurons has been shown in one study in which deletion of an ER stress-induced pro-apoptotic signaling protein (puma) in ALS mice resulted in improved motor neuron survival and delayed disease onset and motor dysfunction (152). Although our study did not directly investigate the cellular consequences of ER stress activation in skeletal muscle of ALS mice, it is the first study to show the associated changes in ER stress markers in skeletal muscles across the lifespan of the G93A*SOD1 mouse.

Other studies with both ALS patients and transgenic G93A*SOD1 mice support the role of ER stress-related cellular dysfunction in ALS pathophysiology (21; 95; 150; 151; 153-155). Studies examining lumbar spinal cord sections of G93A*SOD1 mice, demonstrated significant upregulation of three ER stress sensors, PERK, IRE1α and ATF-6 as early as 60d, a time point at which these mice do not show any symptoms, suggesting they may trigger disease pathophysiology (153). In addition, the ER stress-specific cell death markers, CHOP and caspase-12, were activated, indicating apoptosis was induced before symptom onset (153). ATF6, IRE1α, CHOP, and caspase-12 were also shown to be up-regulated in the lumbar spinal cord sections of G93A*SOD1 mice at 90d, at a late pre-symptomatic stage of the disease (150). In yet other studies, a broad ER stress response occurred in spinal cords only in the end stage of ALS (~140d) when the mice were symptomatic which does not support the role of ER stress in ALS pathology (151). Levels of ER stress-related proteins including PERK, IRE1α, ATF6, XBP-1, Grp78/BiP, and CHOP were upregulated in motor neurons of the spinal cords of ALS patients (153). However, evidence from these studies is based on the association of ER stress markers with disease presence.

Impaired protein translation in muscle atrophy and ALS

Motor neurons and skeletal muscles are two targets of mutant SOD1-mediated toxicity in ALS. In skeletal muscle cells, ER stress leading to inhibition of protein translation and decreased protein synthesis could explain the reduction in muscle mass of the G93A*SOD1 mouse (4; 175; 176). We observed increases in PERK protein-kinase activity and increased phosphorylation of eIF2α on serine residue 51. Increased phospho-eIF2α has been shown to inhibit translation of messenger RNA into protein, effectively decreasing the protein load (96; 179). Inhibition of protein translation can alter both muscle protein synthesis during growth but also muscle plasticity in disease. We recently reported alterations in intracellular Ca^{2+} levels in skeletal muscle of the G93A*SOD1 mice and reductions in the Ca^{2+} buffering proteins SERCA1, SERCA2 and parvalbumin (7). SERCA1 is the SR/ER Ca^{2+} ATPase isoform expressed in fast glycolytic fibers and SERCA2 is expressed in fast oxidative and slow fibers (180). Due to the shift to more oxidative fibers in WG (181) and TA (169), we expected an increase in SERCA2 protein expression. However, SERCA2 protein was also decreased in skeletal muscle of ALS-Tg mice (7) despite a compensatory upregulation of SERCA2 mRNA (unpublished data). Thus, at least for SERCA2, we have observed transcriptional upregulation with no concurrent increase in protein translation. Our current data showing increased phospho-eIF2α/total eIF2α are consistent with this inhibition of protein translation as early as 70d. While there is an overall decrease in protein translation, this will specifically affect the secretory and transmembrane proteins that are processed in the ER (178) such as the SERCA pump proteins. However, the muscle is still capable of increased protein synthesis and can upregulate expression of the required ER stress proteins. Future studies

will be required to identify other muscle-specific proteins that are misfolded and that may contribute to atrophy and/or disease pathophysiology in ALS.

ER stress, muscle metabolic capacity and disease pathology

There are limited reports about ER stress pathways in skeletal muscles of motoneuron disease, although there are clinical reports of ER stress and UPR being activated in inclusion body myositis (122; 182), autoimmune myositis (123; 183), and myotonic dystrophy (124). It has also been shown that ER stress response proteins IRE1α, PDI, and other ER chaperones are upregulated in skeletal muscle of mice in response to high fat diet feeding which lead to a decrease in protein synthesis and insulin resistance (108). ER stress sensors and ER chaperones have also been shown to be upregulated in skeletal muscle following exercise (147; 184). Our study is consistent with these prior reports of ER stress response in diseases and under conditions of various cellular stresses such as altered metabolic substrate supply and changes in metabolic activity. Interestingly, our observation that ER stress was greater in WG compared to RG is consistent with the notion that an energetic stress contributes to activation of the ER stress response as glycolytic fibers are more likely to experience periods of hypoxia or perturbed energy homeostasis.

Previous studies have shown that glycolytic skeletal muscle is more susceptible to atrophy in response to hypoxia (185) and in disease states such as cancer cachexia (186; 187) and heart failure (188). The diaphragm, a muscle of mixed fiber type with high glycolytic capacity, had levels of ER stress comparable to the glycolytic WG. It thus appears that metabolic capacity rather than muscle fiber type per se (i.e. fast vs. slow contracting) is a crucial determinant of susceptibility to ER stress in skeletal muscle cells.

Muscles with a higher oxidative capacity have an increased capacity to respond to oxidative stress (187) and induce heat shock proteins (i.e. hsp70) (63; 189). This may render protection and provide a greater capacity to refold proteins in highly oxidative muscle fibers. We speculate that skeletal muscles with high glycolytic capacity and those with high repetitive use (i.e. diaphragm) are most susceptible to ER stress due to the greater metabolic stress with contractile activity and a reduced capacity to deal with misfolded proteins.

Potential limitations

In the current study we have assessed markers of ER stress using commercially available antibodies. The specificity and selectivity of antibodies for the protein ligand are critical to the interpretation of data from western blot analyses. We have confirmed the specificity of some of these protein markers using either a blocking peptide (PERK) or mass spectrometry (Grp78/BiP). Supporting our data, a recent study using proteomics and bioinformatics tools reported activation of stress responses in gastrocnemius muscle of ALS-Tg mice at 98d including Alpha-crystallin B chain (Cryab), Heat shock protein HSP 90-beta (Hsp90ab1) and protein disulfide-isomerase A3 (Pdia3) that suggest abnormalities in the ER protein folding machinery and activation of the UPR (167). Our observations of increased expression of proteins involved in UPR and ER stress are consistent with this report and illustrate that two independent techniques have been used to confirm the differential expression of ER stress protein markers in skeletal muscle.

Mutant SOD1, mitochondrial disruption and ER/SR dysfunction

Previous studies indicated that mutant SOD1 is present within the ER lumen which may account for activation of ER stress in SOD1-linked ALS cases (33). Mutant SOD1 also accumulates in mitochondria specifically in motoneurons (vs. sensory neurons) (190). Based on the ubiquitous expression of SOD1 (25) one would expect activation of the UPR and ER stress pathway from mutant SOD1 in all tissues. However, our results of two typical ER stress markers, Grp78/BiP and CHOP, showed that ER stress is not present in cardiac muscles or liver tissues. We speculate that this is due to the high oxidative capacity, and increased mitochondrial content in these tissues. Motoneurons and glycolytic skeletal muscle, however, have low mitochondrial content and thus mitochondrial impairment will be detrimental to survival of these cells. Decreased mitochondrial inner membrane potential and mitochondrial Ca^{2+} buffering have been observed in response to osmotic stress and plasma membrane depolarization in muscle fibers of G93A*SOD1 mice (48). The same group has shown that reduced mitochondrial membrane potential is greatest in muscle fibers at the neuromuscular junction region (168). Thus, changes in mitochondrial function leading to elevated cellular Ca^{2+} are specifically impaired at the skeletal muscle membrane nearest to its point of innervation. This may play an important role in the axonopathy associated with ALS (26; 191).

Vulnerable motoneurons also have reduced cytosolic Ca^{2+} buffering capacity and disrupted mitochondrial and ER Ca^{2+} buffering. Motoneurons with mutant (G93A) SOD1- had reduced mitochondrial membrane potential, lower ER Ca^{2+} release in response to a SERCA inhibitor and impaired mitochondrial Ca^{2+} buffering (192; 193). Thus, impairment of mitochondrial and ER Ca^{2+} storage is thought to be central to

motoneuron degenerative changes. Others have shown that mutant SOD1 aggregates with voltage dependent anion channels in mitochondria, specifically of motoneurons (34). In the latter study, ADP transport but not Ca^{2+} uptake by motoneuron mitochondria was diminished. There is emerging data on the importance of Ca^{2+} regulation, mitochondrial function and ER protein misfolding in various diseases (127; 194), but the tissue-specific mechanisms altered leading to muscle atrophy and weakness are still not clear. Further, the role of myocyte health in axonal survival and the putative retrograde cellular pathophysiology remains unresolved. Future studies will be required to determine the precise mechanisms by which proteins that regulate motoneuron and skeletal muscle interaction are affected by unfolded proteins and ER stress leading to muscle atrophy and weakness.

Conclusion

In summary, our findings show that ER stress is present in skeletal muscle of transgenic ALS mice starting at an early, pre-symptomatic age. The ER stress sensors (PERK, IRE1α), ER chaperones (Grp78/BiP, PDI), and ER stress-induced apoptotic mediator (CHOP) are activated and associated with disease pathophysiology and inhibition of protein translation in skeletal muscle. Additionally, we show that ER stress activation is greatest in glycolytic skeletal muscle and muscles of highest contractile activity demand. These data suggest that ER stress induces an early cellular pathology in skeletal muscle that may contribute to the atrophy in ALS.

Abbreviations

ALS, amyotrophic lateral sclerosis; SOD1, Cu/Zn superoxide dismutase; ER, endoplasmic reticulum; UPR, unfolded protein response; PERK, protein kinase RNA-activated (PKR)-like ER kinase; IRE1α, inositol-requiring kinase 1-alpha; eIF2α, eukaryotic initiation factor 2 alpha; PDI, protein disulfide isomerase; Grp78/BiP, 78 kDa glucose-regulated protein and immunoglobulin binding protein; CHOP, C/EBP-homologous protein; SDS-PAGE, dodecyl sulfate polyacrylamide gel electrophoresis; WG, white gastrocnemius; RG, red gastrocnemius DIA, diaphragm; HRT, heart; LIV, liver.

Conflict of Interest

ERC and DC are Inventors on a pending patent which includes some of these data. ERC is the Founder and Chief Scientific Officer of MyoTherapeutics, a University of Maryland-based start-up company.

Authors' contribution

ERC designed the study, established the G93A*SOD1 animal colony and completed animal dissections. DC assisted in maintaining colonies and completed muscle tissue analyses. YW advised on muscle sample preparation for mass spectrometry, completed mass spectrometry analysis and interpretation of MS data. DC, YW and ERC made figures, analyzed the data, and interpreted the findings. DC and ERC wrote the manuscript. DC, YW and ERC edited the manuscript. All authors read and approved the final manuscript.

Acknowledgements

We thank Brittany Jacobs, Davi A.G. Mazala and Samuel A. English for their contributions to data collections and analyses. The authors also thank Dr. Andrew T. Ludlow for his critical reading of the manuscript.

THIS WORK WAS SUPPORTED BY THE UNIVERSITY OF MARYLAND, COLLEGE PARK NEW INVESTIGATOR FUNDS TO ERC.

Figures:

Figure 3.1

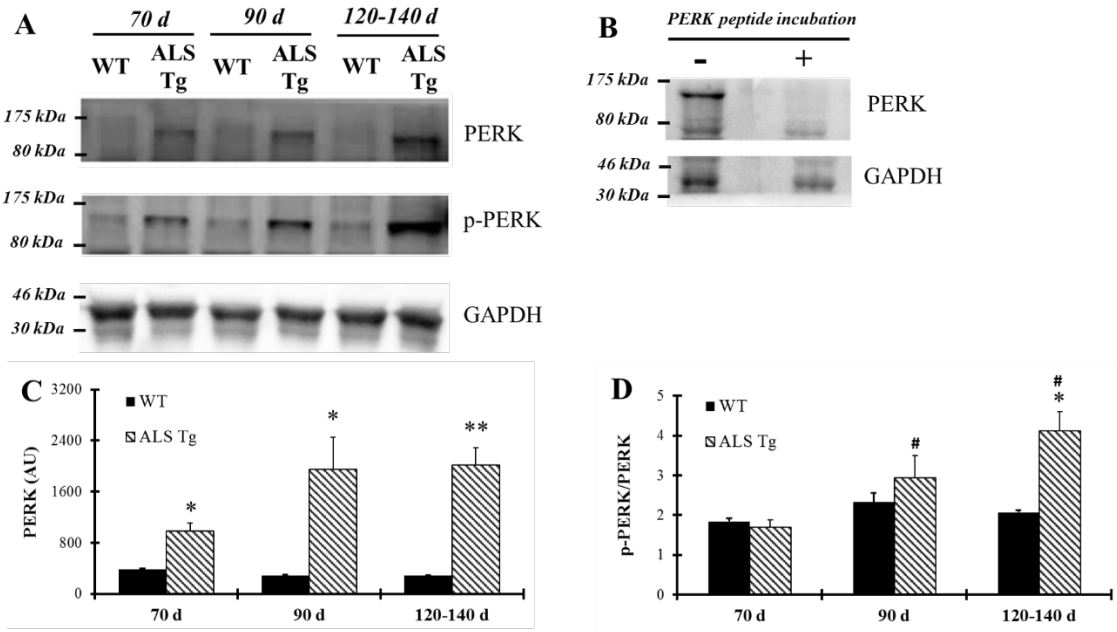

Figure 3.1. PERK and phospho-PERK are up-regulated in skeletal muscle of G93A*SOD1 ALS-Tg mice. (A) White gastrocnemius muscle tissues from different ages of wild-type (WT) and transgenic G93A*SOD1 (ALS-Tg) mice were collected to determine protein expression levels using western blot technique. Primary antibodies PERK, phospho-PERK, GAPDH were used and representative images are shown. Three postnatal ages were examined as follows: early pre-symptomatic (70d; n=3 each for WT and ALS-Tg), late pre-symptomatic (90d; n=5 each for WT and ALS-Tg), and symptomatic (120-140d; n=3 each for WT and ALS-Tg) mice. (B) Protein samples were incubated either with or without PERK peptides and then PERK protein levels were detected using western blots technique. **(C)** Analysis of average arbitrary units (AU) obtained by densitometry for PERK. **(D)** Analysis of average ratio of phosphor-PERK to

total PERK. Data in C and D are presented as mean ± S.E; *, $p < 0.05$; **, $p<0.01$ WT vs. ALS-Tg in the same age group. # $p<0.05$ vs. 70d.

Figure 3.2

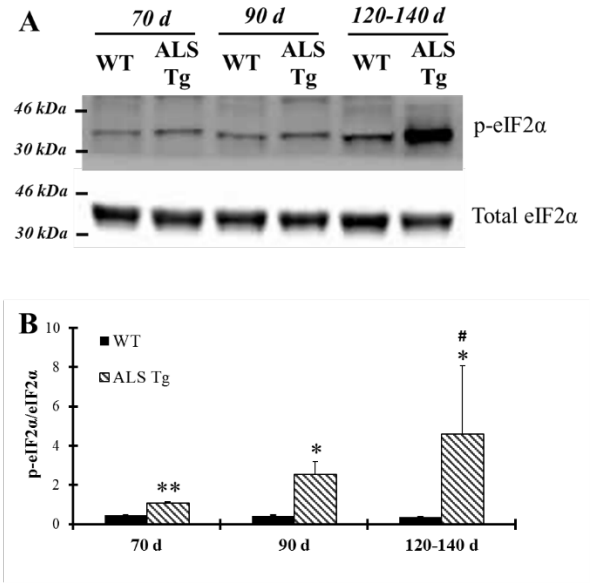

Figure 3.2. Phosphorylation of eIF2α is up-regulated in skeletal muscle of G93A*SOD1 ALS-Tg mice. (A) Total protein from white gastrocnemius muscle tissues was isolated from wild-type (WT) and transgenic G93A*SOD1 (ALS-Tg) mice. Western blots showed phospho-eIF2α (Ser51) and total eIF2α. Three different disease stages were used: early pre-symptomatic (70d; n=3 each for WT and ALS-Tg), late pre-symptomatic (90d; n=5 each for WT and ALS-Tg), and symptomatic (120-140d; n=3 each for WT and ALS-Tg) mice. **(B)** Analysis of ratio of phospho-eIF2α to total eIF2α. Data in B is presented as mean ± S.E; *, $p< 0.05$; **, $p<0.01$ WT vs ALS-Tg in the same age group. # $p<0.05$ vs. 70d.

Figure 3.3

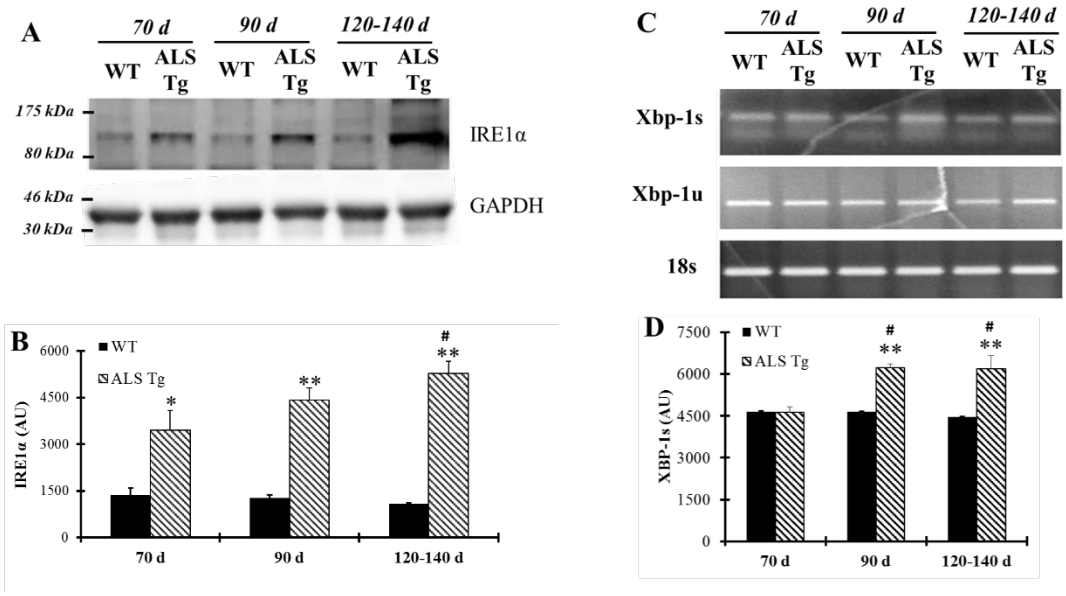

Figure 3.3. IRE1α protein level and spliced Xbp-1 transcriptional level are up-regulated in skeletal muscle of G93A*SOD1 ALS-Tg mice. (A) Protein was isolated from white gastrocnemius muscle of different ages of wild-type (WT) and transgenic G93A*SOD1 (ALS-Tg) mice and western blot was performed by using antibody specific for IRE1α. GAPDH was used as the total protein loading control. Three postnatal ages were examined as follows: early pre-symptomatic (70d; n=3 each for WT and ALS-Tg), late pre-symptomatic (90d; n=5 each for WT and ALS-Tg), and symptomatic (120-140d; n=3 each for WT and ALS-Tg) mice. **(B)** Analysis of average arbitrary units (AU) obtained by densitometry for IRE1α. **(C)** Total mRNA was isolated by using tibialis anterior muscle tissues and un-spliced (Xbp-1u) and spliced Xbp-1 (Xbp-1s) transcriptional levels were determined by using semi-quantitative PCR and PCR results are shown by running the products in 1.5% agarose gel. 18S was used as the internal control. Three different ages animals as mentioned previously were used. **(D)** Analysis of average arbitrary units (AU) obtained by densitometry for Xbp-1s. Data in B and D

are presented as mean ± S.E; *, p< 0.05; **, p<0.01 WT vs. ALS-Tg in the same age group.#p<0.05vs.70d.

Figure 3.4

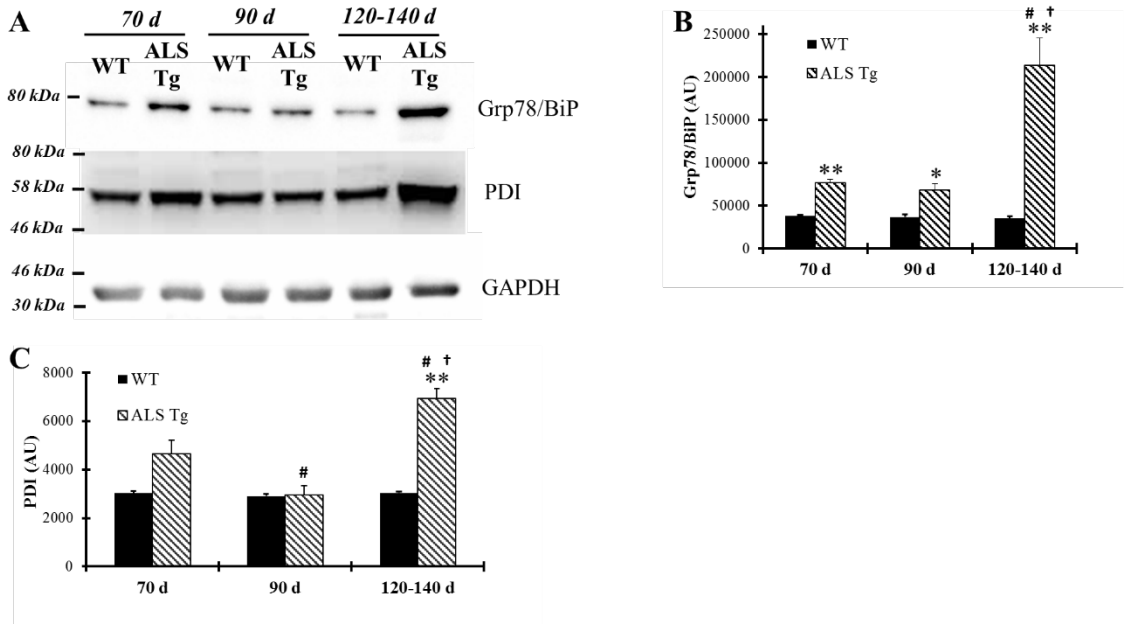

Figure 3.4. ER chaperones Grp78/BiP and PDI are up-regulated in skeletal muscle of G93A*SOD1 ALS-TG mice. (A) White gastrocnemius muscle tissues were used to determine Grp78/BiP and PDI expressions using western blot technique from different ages of wild-type (WT) and transgenic G93A*SOD1 (ALS-Tg) mice. Representative images of Grp78/BiP and PDI are shown. Three postnatal ages were examined as follows: early pre-symptomatic (70d; n=3 each for WT and ALS-Tg), late pre-symptomatic (90d; n=5 each for WT and ALS-Tg), and symptomatic (120-140d; n=3 each for WT and ALS-Tg) mice. **(B, C)** Analysis of average arbitrary units (AU) obtained by densitometry of PDI. Data in B are presented as mean ± S.E; **, $p<0.01$ WT vs. ALS-Tg in the same age group. # $p<0.05$ vs. 70d and † $p < 0.05$ vs. 90d.

Figure 3.5

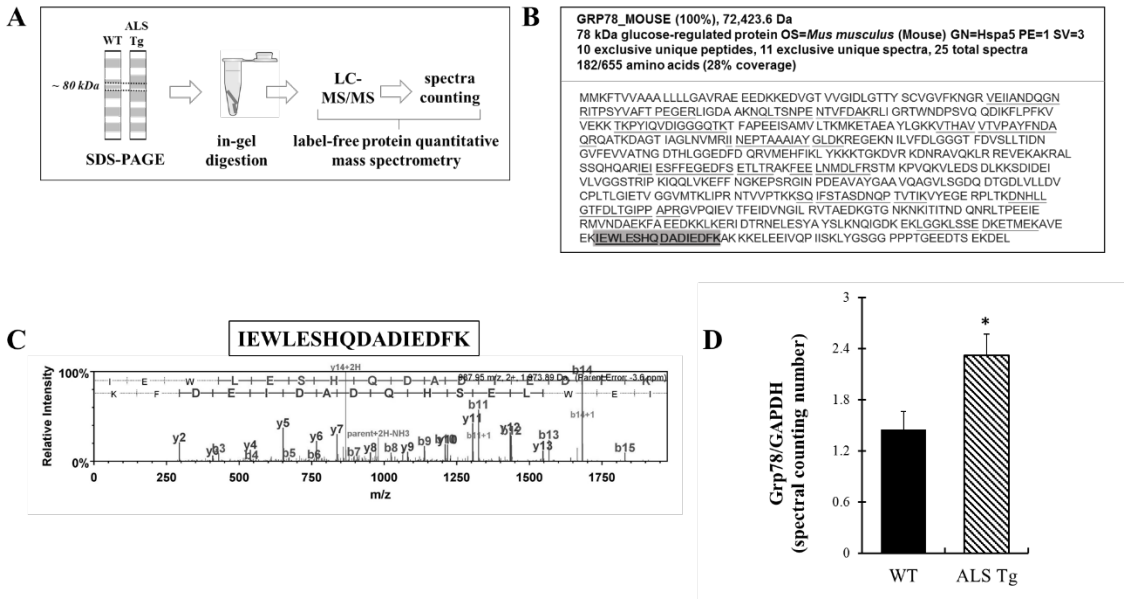

Figure 3.5. Grp78/BiP protein identification and quantitation using label-free spectral counting-based mass spectrometry. **(A)** Workflow of label-free spectral counting-based protein quantitative analysis using LC-MS/MS. Protein samples were separated using SDS-PAGE gel electrophoresis and gel pieces excised at ~80 kDa for the purpose of in-gel trypsin digestion and LC-MS/MS analysis. Protein quantitative data analysis was conducted using spectral counting and interpreted by normalized total spectra numbers. **(B)** Grp78/BiP protein identification and peptide coverage using LC-MS/MS. **(C)** Representative mass-to-charge ratio spectrum and b-/y ions fragmentation of Grp78/BiP peptide (highlighted in B). **(D)** Protein quantitative data analysis using the ratio of normalized total spectra numbers of Grp78/BiP to a house keeping protein GAPDH. Three independent muscles from 120-140d old wild type and ALS-Tg mice were analyzed. * $p < 0.05$, WT vs. ALS-Tg.

Figure 3.6

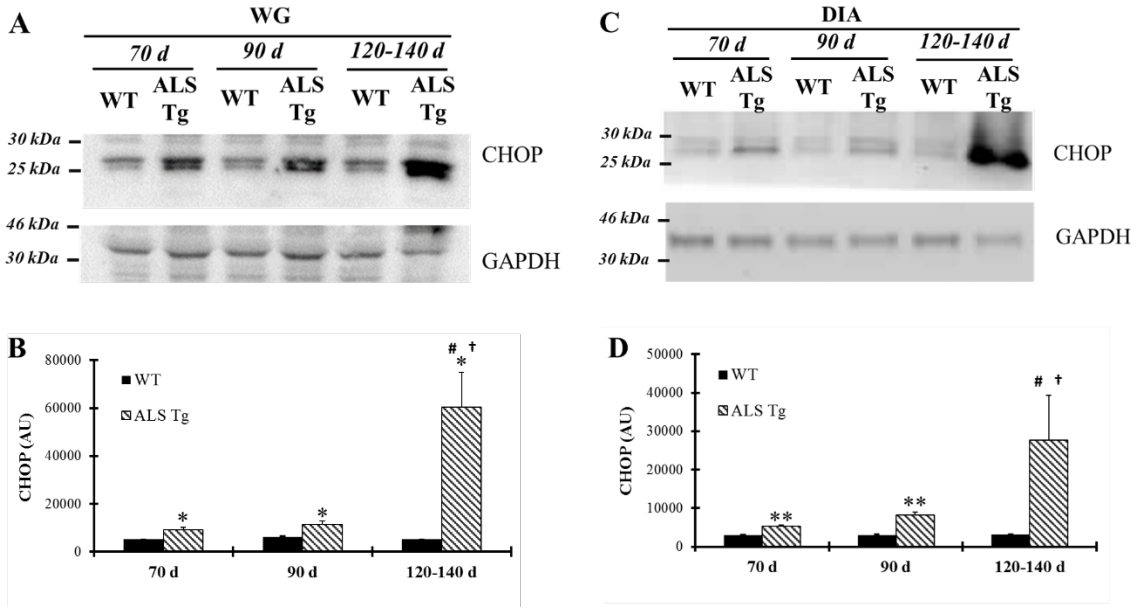

Figure 3.6. CHOP is up-regulated in skeletal muscles of G93A*SOD1 ALS-Tg mice. **(A)** White gastrocnemius (WG) muscle tissues were obtained from wild-type (WT) and transgenic G93A*SOD1 (ALS-Tg) mice of different ages and used to determine CHOP protein levels using western blot technique. GAPDH was used as the total protein loading control. Three postnatal ages were examined as follows: early pre-symptomatic (70d; n=3 each for WT and ALS-Tg), late pre-symptomatic (90d; n=5 each for WT and ALS-Tg), and symptomatic (120-140d; n=3 each for WT and ALS-Tg) mice. **(B)** Analysis of average arbitrary units (AU) obtained by densitometry of CHOP in WG. **(C)** Same as A, with diaphragm (DIA) muscle tissues used to assess CHOP protein level. **(D)** Analysis of average arbitrary units (AU) obtained by densitometry of CHOP in DIA. Data in B and D are presented as mean ± S.E; *, $p< 0.05$; **, $p<0.01$ WT vs. ALS-Tg in the same age group. # $p<0.05$ vs. 70d and † $p < 0.05$ vs. 90d.

Figure 3.7

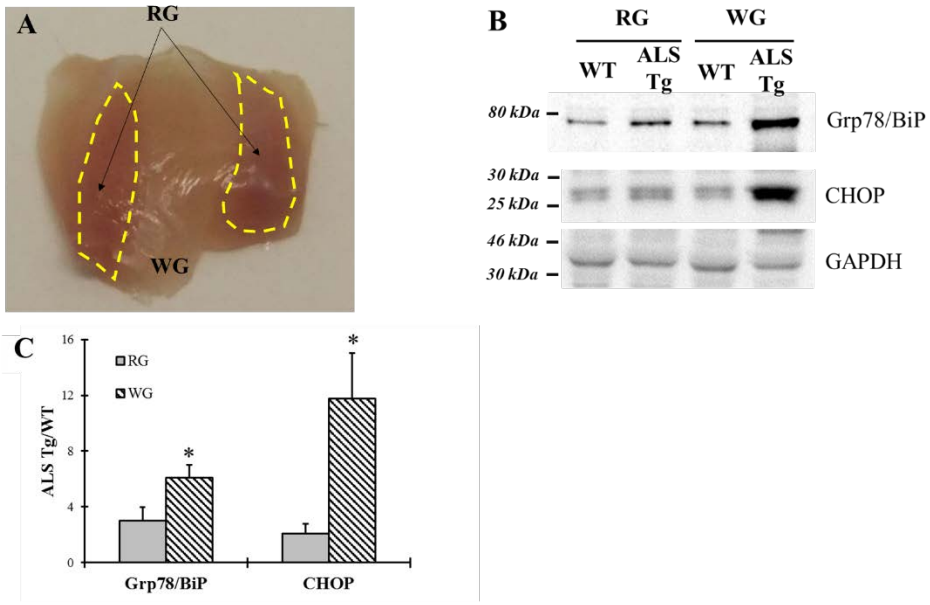

Figure 3.7. Comparison of Grp78/BiP and CHOP protein levels between white and red gastrocnemius muscle tissues of G93A*SOD1 ALS-Tg mice. (A) Image of deep portion of gastrocnemius muscle showing white and red gastrocnemius (yellow dashed areas) muscle region. **(B)** White (WG) and red (RG) gastrocnemius muscle tissues of symptomatic animals (120-140d; n=3 each for WT and ALS-Tg) were collected. Grp78/BiP and CHOP protein levels were determined using western blot technique. **(C)** Analysis of Grp78/BiP and CHOP average ratio of ALS-Tg to WT. Data in B is presented as mean ± S.E; *, $p< 0.05$; RG vs. WG.

Figure 3.8

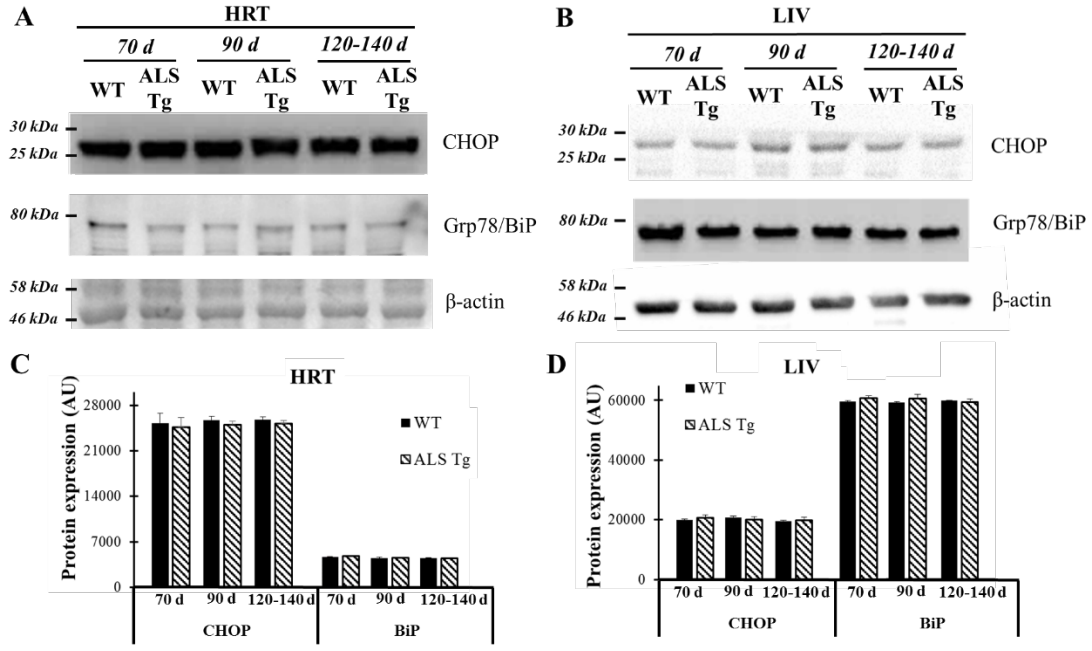

Figure 3.8. Grp78/BiP and CHOP protein levels in cardiac muscle and liver tissue of G93A*SOD1 ALS-Tg mice. (A) Cardiac muscle (HRT) was collected and protein levels determined using western blot technique. Grp78/BiP and CHOP antibodies were used and three postnatal ages were examined: early pre-symptomatic (70d; n=3 each for WT and ALS-Tg), late pre-symptomatic (90d; n=5 each for WT and ALS-Tg), and symptomatic (120-140d; n=3 each for WT and ALS-Tg) mice. **(B)** Liver tissues (LIV) was collected and protein levels were determined as described above. Analysis of average arbitrary units (AU) obtained by densitometry of Grp78/BiP and CHOP in HRT **(C)** and in LIV **(D).** Data in C and D are presented as mean ± S.E.

Figure 3.9

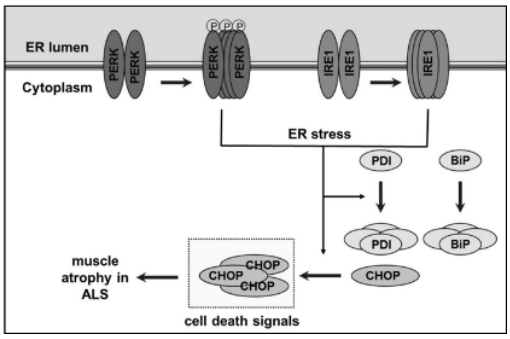

Figure 3.9. Schematic figure showing unfolded protein and endoplasmic reticulum (ER) stress pathway and its proposed role in skeletal muscle atrophy and weakness in ALS. In skeletal muscle of ALS-Tg mice, the G93A*SOD1 mutation leads to oxidative stress and protein misfolding. This leads to an age-dependent activation of ER stress sensors protein kinase RNA-activated-like ER kinase (PERK) and inositol-requiring kinase 1-alpha (IRE1α). Normally, these ER stress sensors physically interact with the ER chaperone immunoglobulin binding protein (Grp78/BiP) which suppresses their activation but accumulation of unfolded/misfolded proteins activates Grp78/BiP, including an upregulation of Grp78/BiP and protein disulfide isomerase (PDI) protein expression. Prolonged and severe ER stress can trigger apoptosis by ER stress-specific cell death signals, including C/EBP homologous protein (CHOP) and caspase-12, leading to muscle atrophy.

Chapter 4: SERCA1 overexpression in skeletal muscle preserves motor function and delays disease onset in a mouse model of ALS

The following is a manuscript that is in preparation. The work was performed at the University of Maryland.

SERCA1 overexpression in skeletal muscle preserves motor function and delays disease onset in a mouse model of ALS

D. Chen[1], Davi A. G. Mázala[1], Jeffery D Molkentin[3] and Eva R. Chin[1]

Department of Kinesiology[1], School of Public Health, University of Maryland, and [2]Department of Pediatrics, University of Cincinnati, Cincinnati Children's Hospital Medical Center.

Correspondence to: Dr. Eva Chin, School of Public Health, University of Maryland, 2134b SPH Building, College Park, MD 20742 USA, erchin@umd.edu

Running Title: SERCA1 attenuates ALS disease progression

Key words: Amyotrophic Lateral Sclerosis, ALS, SOD1, calcium, SERCA1, ER stress

Send correspondence: Dr. Eva R. Chin, School of Public Health, University of Maryland, College Park, MD 20742
Tel.: (301) 405-2478, Fax: (301) 405-5578
Email: erchin@umd.edu

Abstract

Intracellular Ca^{2+} homeostasis and induction of ER stress are pathophysiological features of skeletal muscle in amyotrophic lateral sclerosis (ALS). The purpose of this study was to investigate whether muscle-restricted overexpression of SERCA1 would improve motor function, disease progression and markers of ER stress in ALS mice. B6SJL-Tg(SOD1*G93A)1Gur/J (ALS) mice were bred with skeletal muscle α-actinin SERCA1 overexpressing mice to generate: i) wild type (WT; n=11); ii) SERCA1 overexpression (WT/+SERCA1; n=14); iii) SOD1*G93A ALS (ALS-Tg; n=7); iv) SERCA1 overexpressing SOD1*G93A ALS mice (AL-Tg/+SERCA1; n=11). Motor function (grip test) and time of symptom onset was assessed weekly and then skeletal muscles obtained to assess atrophy and markers of ER stress. SERCA1 expression and activity of the SR Ca^{2+} ATPase were decreased in quadriceps (QUAD) of ALS-Tg vs. WT mice (to 10% and 50% of WT, respectively) but rescued to WT levels in ALS-Tg/+SERCA1 GAS. This was associated with an attenuation of muscle atrophy in gastrocnemius and QUAD muscles. ALS-Tg/+SERCA1 mice had improved motor function at 14 weeks (111.4 ± 16.2 vs. 67.7 ± 13.1 sec; $p<0.05$) and 16 weeks (53.1 ± 11.8 vs. 8.9 ± 3.4 sec; $p<0.05$) compared to ALS-Tg and a delay in disease onset (101.9 ± 2.6 vs. 91.1 ± 4.7 days). The ER stress apoptotic signaling protein CHOP was upregulated in 2.6-fold in ALS-Tg but not attenuated in ALS-Tg/+SERCA1 GAS. These data indicate that SERCA1 overexpression in skeletal muscle improves motor function and slows disease progression in a mouse model of ALS but does not attenuate the ER stress response. We hypothesize that the improvements are due to improved muscle

health secondary to improved intracellular Ca^{2+} regulation but are not sufficient to overcome cellular ER stress in a transgenic overexpression model.

Introduction

Amyotrophic lateral sclerosis (ALS), also known as Lou Gehrig's disease, is a devastating neurodegenerative disease which affects 3 out of 100,000 people a year in the United States (1). The clinical features of ALS include upper and lower motor neuron degeneration leading to progressive muscle atrophy (1). Consequently, respiratory failure due to muscle weakness leads to death 3-5 years after disease onset (1). The underlying molecular defects in ALS are varied, with more than 50 genes identified (24). However, 90-95% of ALS cases are sporadic with unknown causes and only 5-10% of cases are familial ALS and linked to a genetic mutations (24). Among the genetic causes, mutations in the Cu/Zn superoxide dismutase 1 (SOD1) gene contribute to ~20% of all familial ALS cases (24). Transgenic mouse models representing SOD1 mutations have been developed (4), well characterized and greatly increased our understanding of the pathological mechanisms of ALS (24). The Glycine to Alanine at codon 93 (G93A) SOD1 mutation results in a "gain-of-function" toxicity from increased production of reactive oxygen species (i.e. H_2O_2) with several proposed downstream pathological mechanisms such as glutamate excitotoxicity, mitochondrial dysfunction, and intracellular calcium dysregulation that help to explain to muscle weakness (24; 37).

In skeletal muscle, there are rapid fluctuations in intracellular Ca^{2+} during muscle contraction, with levels increasing 40 to 100-fold during contractile activity (195). Consequently, both resting Ca^{2+} and Ca^{2+} release and reuptake events are tightly regulated by intracellular Ca^{2+} channels, pumps, and buffering proteins such as ryanodine receptor (RyR), sarco/endoplasmic reticulum Ca^{2+}-ATPase (SERCA), and parvalbumin (PV) (196). Redox modifications and impaired function of Ca^{2+} -handling proteins is

detrimental to their ability to bind or sequester Ca^{2+} (49). Thus, redox-modified proteins such as RYR and SERCA may contribute to elevations in Ca^{2+} and muscle pathology in various muscle diseases including ALS (7) and Duchenne Muscular Dystrophy (DMD) (13; 197). Forced overexpression of Ca^{2+} handling proteins that increase Ca^{2+} influx into muscle can induce a pathology that mimics DMD (198-200) while improvements in Ca^{2+} clearance by overexpression of the fast-twitch SERCA isoform (SERCA1) has been shown to rescue the muscle pathology and improve function in two models of DMD (13; 197). Thus, improving intracellular Ca^{2+} homeostasis may be beneficial for neuromuscular diseases where Ca^{2+} overload is part of the downstream muscle pathology.

Our lab has previous shown elevations in intracellular Ca^{2+} in single muscle fibers of the G93A*SOD1 mouse (12). This was associated with decreased levels of SERCA1, SERCA2 and PV protein in limb gastrocnemius muscle (12). We have also reported an increase in the unfolded protein response (UPR) and ER stress markers in skeletal muscle of the G93A*SOD1 mouse which are thought to be due to impaired ER intracellular Ca^{2+} regulation (10). Based on these findings we hypothesized that improving intracellular Ca^{2+} clearance capacity in skeletal muscle of ALS mice would preserve motor function, ameliorate muscle atrophy, and rescue the ALS phenotype. We also hypothesized that it would mitigate the ER stress response in skeletal muscle. Thus, the purpose of this study was to evaluate the motor function and the phenotype of skeletal muscle in G93A*SOD1 mice with muscle-specific overexpression of SERCA1. Our results show that SERCA1 overexpression preserved whole body motor function, delayed disease onset and attenuated the muscle atrophy in G93A*SOD1 mice. Surprisingly, SERCA1 overexpression did not attenuate markers of ER stress. Overall, our results indicate that

improving intracellular Ca^{2+} regulation in skeletal muscle can improve muscle health and motor function in ALS mice without alleviating myocellular ER stress.

Methods

Ethical Approval

All procedures were conducted under a protocol approved by the Institutional Animal Care and Use Committee (IACUC) of the University of Maryland, College Park.

Animals

Control (C57BL/6 SJL hybrid) female and C57BL/6 SJL-Tg SOD1*G93A (ALS-Tg) male mice were obtained from Jax Laboratories and bred to established a colony at the animal facility of University of Maryland, College Park as previously described (7). Male and female skeletal muscle SERCA1 overexpression mice were obtained from Cincinnati Children's Hospital Medical Center. SERCA1 overexpression is restricted to skeletal muscle by a modified human skeletal muscle α-actinin promoter (201). SERCA1 Tg breeders were then used to establish a colony of +SERCA1 mice at the University of Maryland Central Animal Research Facility as previously described (13). Male WT/+SERCA1 mice were bred with female ALS-Tg mice to obtain 4 genotypes: i) wild-type (WT); ii) SERCA1 overexpression (WT/+SERCA1); iii) G93A*SOD1 (ALS-Tg), and SERCA1 overexpressing G93A*SOD1 (ALS-Tg/+SERCA1). This study was designed to obtain 8-10 mice per genotype. All mice were weaned at 21 days and genotyped for expression of the G93A SOD1 mutation and for SERCA1 using primer sequences and methods previously described (7; 13). All mice were kept in the same room condition (typical ambient conditions 20.9% O_2 and 22 ± 1^{o}C) with equal access to food and water, bedding, and light cycles (12h light/12h dark).

Assessment of motor function and disease onset

Motor function of the mice was evaluated weekly from 9 weeks to 16 weeks of age with a grip test. Briefly, the grip test is the time the mice were able to hold their body weight while suspended from a wire mesh lid as previously described (7). In this study, each mouse was subjected to three trials with the maximum test time being 180 s and a 10 min rest period between trials. The average of three trials was used for reporting grip test performance. The test was conducted and analyzed in a blinded fashion. Disease onset was defined as the time corresponding to the first signs of myotonic symptoms such as muscle tremor or hindlimb stiffness. The rapid reduction in grip test performance was used as another criteria to evaluate the demonstration of disease onset.

Experimental Procedures

At 16 wks of age mice were euthanized by CO_2 inhalation followed by cervical dislocation. Skeletal muscles including gastrocnemius (GAS), tibialis anterior (TA) and quadriceps (QUAD) were removed and weighed by investigators who were blinded to the genotype of the mice. Muscle samples were then quick frozen in liquid nitrogen and stored at -80^{o}C until subsequent analyses. At the time of sacrifice, the flexor digitorum brevis (FDB) muscle was removed from a subset of mice (n=4 for each genotype; 3 females, 1 male each) and single muscle fibers isolated for assessing $[Ca^{2+}]_i$ levels.

Single muscle fiber isolation and free $[Ca^{2+}]_i$ measurements

Detailed methods for single muscle fiber isolation and $[Ca^{2+}]_i$ measurements have been previously described (202). Briefly, single muscle fibers were obtained from the FDB muscle by collagenase digestion with type 2 collagenase (Worthington) in minimal essential medium (MEM) with 10% fetal bovine serum (FBS) and 1% penicillin-streptomycin (Invitrogen). After incubation at 37°C in 95% O_2-5% CO_2, single muscle

fibers were obtained by trituration. Subsequently, fibers were maintained in MEM solution with 10% FBS at 37°C, 95% O_2-5% CO_2 until used for $[Ca^{2+}]_i$ assessment.

One day after dissection, fibers were loaded with Fura-2AM for 15 min. The Fura-2 ratio was measured in response to varying stimuli (see protocol below) as an index of $[Ca^{2+}]_i$. Fibers loaded with Fura-2AM were placed in a stimulation chamber containing parallel electrodes and the chamber was positioned on a Nikon TiU microscope stage. Muscle fibers were continuously perfused with a stimulating Tyrode solution (121.0 mM NaCl, 5.0 mM KCl, 1.8 mM $CaCl_2$, 0.5 mM $MgCl_2$, 0.4 mM NaH_2PO_4, 24.0 mM $NaHCO_3$, and 5.5 mM glucose) with 0.2% FBS (203). The solution was bubbled with 95% O_2-5% CO_2 to maintain a pH of 7.3 (203). Levels of $[Ca^{2+}]_i$ were assessed by the Fura-2 fluorescence ratio using an IonOptix Hyperswitch system with dual excitation, single emission filter set for Fura-2 (excitation 340 nm and 380 nm; emission 510 nm). Signals were captured and analyzed using the IonWizard software (IonOptix). Global Fura-2 ratio was measured in muscle fibers using trains of stimuli at 10, 30, 50, 70, 100, 120, and 150 Hz for 350 ms with fibers resting 1 min between frequencies. Peak Fura-2 ratios at each frequency were determined by the average ratio in the last 100 ms of the 350 ms tetanus, when Ca^{2+} Fura-2 should be at a steady state. All single muscle fibers were evaluated at room temperature. Fura-2 signals were measured in 7-9 fibers per mouse for a total of 28-33 fibers per genotype: WT (n=33); WT/+SERCA1 (n=33); ALS-Tg (n=28); ALS-Tg/+SERCA1 (n=33).

Muscle protein expression

The QUAD was used to confirm SERCA1 overexpression and to assess UPR and ER stress responses in skeletal muscle as previously described (7; 10). The ER stress

response was assessed by measuring protein expression of the ER stress sensors protein disulfide isomerase (PDI) and Grp78/BiP and the ER stress-specific cell death signaling protein C/EBP homologous protein (CHOP). Briefly, QUAD was homogenized in lysis buffer containing 20 mM Hepes buffer, 100 mM NaCl, 1.5 mM MgCl2, 0.1% Triton X-100, 20 % Glycerol, 1mM DTT and protease inhibitors (cOmplete mini EDTA-free protease inhibitor cocktail, Roche Diagnostics, Indianapolis, IN). After tissue homogenization, samples were kept at 4^{o}C for 20 min and then centrifuged at *20,000 g*. Supernatant was collected and frozen at -80^{o}C until used for protein expression analyses. Sample protein concentration was determined using a BCA assay (Thermo Fisher Scientific Inc., Rockford, IL). For assessing SERCA1, PDI, Grp78/BiP and CHOP protein levels, 30 μg of total protein was used. Protein samples were solubilized in 5 x loading buffered and denatured by incubation at 100^{o}C for 5 min. Denatured protein samples were loaded on 8% bis-acrylamide gels and separated by SDS-PAGE electrophoresis. After gel electrophoresis, proteins were transferred to PVDF membrane (EMD Millipore, Billerica, MA) and then blocked with 5% non-fat milk at room temperature for 1 h. The following antibodies and dilutions were used to determine protein expression levels: SERCA1 (1:2500, Thermo Fisher Scientific Inc., Rockford, IL) and PDI, Grp78/BiP and CHOP (1:1000, Cell Signaling Technology). GAPDH primary antibody (1:2000, Thermo Fisher Scientific Inc., Rockford, IL) was used as a total protein loading control. Protein levels were quantified by band densitometry (Bio-Rad Laboratories Inc., Hercules CA) and protein expression levels were expressed in arbitrary units (AU).

Determination of maximal SERCA1 ATPase activity

QUAD was used to determine maximal SERCA1 ATPase activity using the method described in Chin *et al.* 1994 (204) modified to a 96 well plate format (13). Briefly, QUAD was homogenized in muscle homogenizing media containing 200mM 200 mM Sucrose, 10 mM NaN_3, 1mM EDTA, and 40 mM L-histidine (pH 7.8) with a 1:20 ratio (w/v, 0.1 g tissue: 2mL buffer). The Ca^{2+}-ATPase reaction was measured in a crude homogenate in a reaction buffer which containing 20 mM Hepes buffer (pH 7.5), 200 mM KCl, 15mM $MgCl_2$, 10 mM NaN_3, 1mM EGTA, 5 mM ATP, 10mM phosphoenolpyruvate, 18U/mL lactate dehydrogenase, 18U/mL pyruvate kinase, 4 μM calcium ionophore A23187 and 0.3 mM NADH. Total ATPase activity was assessed by adding 1 mM $CaCl_2$ and basal ATPase was measured by adding 1 mM $CaCl_2$ and 5mM cyclopiazonic acid (CPA), which is a selective SERCAs ATPase inhibitor. The reaction was measured in triplicates in a 96-well plate at 37^{o}C and NADH absorbance was measured at 340 nm. Maximal SERCA1 ATPase activity was defined as the difference between total ATPase and basal ATPase activity.

Statistical Analysis

Values are expressed as mean ± standard error of the mean (SEM). To evaluate differences between WT, WT/+SERCA1, ALS-Tg and ALS-Tg/+SERCA1 mice, data were analyzed using Student's T-tests to compare between genotypes, with $p<0.05$ used to determine statistical significance.

Results

The body mass of mice used in this study are shown in Table 4.1. At 16 weeks, the average body mass of male mice was not different between any of the genotypes. However, for female mice, body mass of WT/+SERCA1, ALS-Tg and ALS-Tg/+SERCA1 mice were significantly lower compared to WT mice, averaging 85%, 68% and 72% of WT levels, respectively. Body mass of female ALS-Tg mice was also reduced (to 80%) compared to WT/+SERCA1 mice. Due to the low number of male ALS-Tg mice, the data for both sexes were combined. Combined, the body mass of WT and WT/+SERCA1 were not different, but the ALS-Tg and ALS-Tg/+SERCA1 mice were significantly reduced, to 75% and 78% of WT levels, respectively. All other data reported are for male and female mice combined unless otherwise specified.

*SERCA1 expression and maximal SR Ca^{2+} ATPase activity in skeletal muscle of ALS-Tg and +SERCA1 Tg mice***:** Western blot analysis was used to confirm SERCA1 overexpression in QUAD muscle of the WT/+SERCA1 and ALS-Tg/+SERCA1 Tg mice (Fig. 4.1A and 1B). SERCA1 protein levels were on average 1.8-fold higher in QUAD of WT/+SERCA1 compared to WT mice ($p<0.01$). Consistent with our previous report, SERCA1 protein levels were decreased in QUAD of ALS-Tg mice, to 10% of WT levels ($p<0.01$). SERCA1 overexpression resulted in 8.1 –fold higher SERCA1 protein levels in QUAD of ALS-Tg/+SERCA1 mice relative to ALS-Tg mice ($p<0.01$), to a level not different from WT. To determine whether the increase in SERCA1 protein level resulted in increased function of the Ca^{2+} ATPase, we measured muscle SR Ca^{2+} -ATPase activity (Fig. 4.1C). In QUAD muscle of ALS-Tg mice, maximum Ca2+ -ATPase activity was 50% of WT levels ($p<0.01$). SERCA1 overexpression increased maximal Ca2+ -ATPase

activity in QUAD of both WT/+SERCA1 (1.5-fold vs. WT; $p<0.05$) and ALS-Tg/+SERCA1 (1.8-fold vs. ALS-Tg; $p<0.05$) mice. These data confirm that SERCA1 protein levels as well as maximum SR Ca^{2+} ATPase activity was increased in skeletal muscle of WT/+SERCA and ALS-Tg/+SERCA mice.

*SERCA1 overexpression alters stimulation induced Ca^{2+} transients in ALS-Tg mice***:** In order to assess the effects of SERCA1 overexpression on skeletal muscle Ca^{2+} cycling during contraction and relaxation, we assessed $[Ca^{2+}]_i$ using Fura-2 ratio in single fibers during electrical stimulation. There was no significant difference in resting Fura-2 ratio, although there was a trend ($p=0.08$) for single fibers from ALS-Tg to be higher than an all other groups (Fig. 4.2A). Peak Fura-2 at all stimulation frequencies was not different in single fibers from WT and WT/+SERCA1 or between WT and ALS-Tg. There was, however, a significant reduction in Fura-2 ratio at all stimulation frequencies between ALS-Tg and ALS-Tg/+SERCA1, with peak ratios being 16% (10Hz), 22% (30Hz), 19% (50Hz), 17% (70Hz), 15% (100Hz), 14% (120Hz) and 11% (150Hz) lower in fibers from SERCA1 overexpressing ALS-Tg compared to ALS-Tg mice (Fig. 4.2B and 2C). These data suggest a reduction in releasable Ca^{2+} during contractile activity in ALS-Tg/+SERCA1 mice.

SERCA1 overexpression preserves motor function and delays disease onset in ALS-Tg mice: Deficits in motor function have been consistently observed with disease progression across the lifespan in G93A*SOD1 ALS-Tg mice (205; 206). To determine whether skeletal muscle-specific increases in SERCA1 would improve motor function, we assessed whole body motor performance using a grip test from 9 - 16 weeks of age (Fig. 4.3A). WT/+SERCA1 mice showed no signs of decreased motor function, with all

mice able to grip for the maximum 180 s, similar to WT. ALS-Tg and ALS-Tg/+SERCA1 mice showed normal motor function at an early age (up to 11 weeks). At 12 weeks, both ALS-Tg and ALS-Tg/+SERCA1 mice had decreased grip time compared to WT mice and this reduction continued until study termination (16 weeks). In spite of the rapid deterioration of motor function, SERCA1 overexpression was able to partially preserve motor function in ALS mice. Starting at 14 wks, grip time was longer for ALS-Tg/+SERCA1 mice compared to ALS-Tg with ALS-Tg/+SERCA1 at 62% of WT vs. ALS-Tg at 38% of WT levels ($p<0.05$). At 16 wks ALS-Tg/+SERCA1 mice were at 29% of WT compared to ALS-Tg at 5% of WT levels ($p<0.01$). These data indicate that SERCA1 overexpression could partially rescue the ALS phenotype by preserving motor function.

The G93A*SOD1 mice have a shortened life span of ~150d (4) with mice surviving ~2 wks after the first signs of disease onset (i.e. muscle tremor and hindlimb stiffness). To determine whether skeletal muscle-specific SERCA1 overexpression could delay disease onset, we recorded the age at which disease symptoms were first observed. In ALS-Tg mice, disease onset was observed at 91 ± 4.7 d. In contrast, ALS-Tg/+SERCA1 mice had a significant delay the disease onset in ALS/+SERCA1 mice (102 ± 2.6 d) (see Fig. 4.3B).

*SERCA1 overexpression attenuates skeletal muscle atrophy in ALS-Tg mice :*A decrease in muscle mass has been documented by MRI in G93A*SOD1 mice, starting as early as 60d (205). In this study we assessed muscle atrophy by measuring muscle mass at 16 wks (Figure 4). Muscle loss was seen in ALS-Tg, with muscle mass being 43% (GAS), 50% (TA) and 42% (QUAD) of WT levels ($p<0.01$). However, in ALS-

Tg/+SERCA1 mice there was an increase in muscle mass relative to ALS-Tg for all muscles: GAS was 141% vs. ALS-Tg ($p<0.01$), TA was 167% vs. ALS ($p<0.05$) and QUAD was 153% of ALS-Tg ($p<0.05$). Muscle mass in ALS-Tg/+SERCA1 was, however, still significantly less than WT levels for all muscle. Interestingly, the WT/+SERCA1 mice have a significant decrease in muscle mass compared to WT, being 58% (GAS), 78% (TA) and 58% (QUAD) of WT levels ($p<0.01$).

SERCA1 overexpression does not attenuate activation of the ER stress response in ALS-Tg mice: We previously reported an increase in ER stress sensors PDI and Grp78/BiP as well as ER apoptotic signaling protein CHOP in gastrocnemius muscle of ALS-Tg mice. In the current study, we did not detect an increase in PDI in QUAD muscle of ALS-Tg or any other group, with expression levels being similar to WT in all genotypes (Fig. 4.5A). The ER stress chaperone protein Grp78/BiP was elevated 3.5-fold in the ALS-Tg mice compared to WT ($p<0.05$; Fig. 4.5B). Grp78/BiP was not elevated in this set of ALS-Tg mice, but was 3.8-fold higher in ALS-Tg/+SERCA1 vs. WT ($p<0.01$) and 2.8-fold relative to the ALS-Tg genotype control ($p<0.01$). The apoptosis-signaling protein CHOP was not different between WT and WT/+SERCA1 QUAD muscle. But, CHOP was increased 2.6-fold in ALS-Tg muscle ($p<0.01$) and 2.5-fold in ALS-Tg/+SERCA1 mice ($p<0.01$) (Fig. 4.5C) indicating that activation of ER-stress induced apoptosis was not mitigated in skeletal muscle of ALS-Tg mice by SERCA1 overexpression.

Discussion

Intracellular Ca^{2+} plays an essential role in preserving skeletal muscle function and whole tissue integrity (12). Muscles use Ca^{2+} not only during contraction but also as a second messenger in regulating muscle gene expression (207). Ca^{2+} overload, defined as an elevation in resting intracellular Ca^{2+} level, leads to severe skeletal muscle damage via activation of Ca^{2+}- dependent proteases such as calpains, release of phospholipase A2, over production of reactive oxygen species, and mitochondrial Ca^{2+} overload (12). Therefore, abnormal intracellular Ca^{2+} levels are thought to be one of the factors contributing to skeletal muscle damage in various pathological conditions such as in over-training, trauma, tissue ischemia, muscle cachexia, and disease such as Duchenne muscular dystrophy and ALS (12). Considering the importance of preserving normal resting intracellular Ca^{2+} levels, skeletal muscle fibers have various ways of removing and buffering Ca^{2+} concentration in the cytoplasm such as plasma membrane Ca^{2+} pumps, cytosolic Ca^{2+} buffering proteins and Ca^{2+} regulatory proteins in the SR (13). The most significant of these is SERCA1, which is the SR/ER membrane Ca^{2+} ATPase responsible for the removal of Ca^{2+} into the SRduring muscle relaxation, following its release for muscle contraction (13). It can also reduce intracellular Ca^{2+} levels after a pathological overload (13). Overexpression of SERCA1 was shown to increase cytoplasmic clearance of Ca^{2+} and reduce mitochondrial swelling in response to Ca^{2+} exposure (197). It is now known that SERCA1 also plays an important role in mitigating skeletal muscle disease pathology (12; 13; 15).

The importance of SERCA1 in regulating Ca^{2+} signaling and skeletal muscle function in muscle disease pathology was shown in two recent studies where

overexpression of SERCA1 in skeletal muscle significantly improved the dystrophic phenotype (13; 197). In dystrophin deficient *mdx* mice, dystrophin and utrophin deficient (*mdx*/Utr$^{-/-}$) and Sarcoglycan null (Sgcd$^{-/-}$) mice, SERCA1 overexpression attenuated the pathological features such as central nucleation and muscle fibrosis in skeletal muscle and reduced creatine kinase, a serum markers of muscle damage (13; 200). And in both *mdx* and *mdx*/Utr$^{-/-}$ mice, SERCA1 overexpression improved force production in response to damage-inducing eccentric contractions (13). Thus, increased SERCA1 expression and improved intracellular Ca^{2+} clearance had profound effects on improving pathological and functional consequences in skeletal muscle (13; 15). These data support the hypothesis that Ca^{2+} dysregulation is the final pathological event in skeletal muscle diseases and that upregulation of SERCA1 protein level or increasing SERCA1 function is an attractive therapeutic strategy to treating these diseases.

Our previous study showed elevations in intracellular Ca^{2+} in single muscle fibers from G93A*SOD1 mice (12). This was associated with decreases in SERCA1 and SERCA2 as well as the Ca^{2+} buffering protein parvalbumin (7). Based on these findings, we hypothesized that decreased SERCA1 function could induce skeletal muscle pathology in ALS and that activation of SERCA1 function, by treating the animals with a small molecule activator of SERCA1 (6-gingerol), would improve muscle function. Indeed, our preliminary report of this study showed that 6-gingerol treatment significantly improved grip function in G93A*SOD1 mice and attenuated the ER stress protein markers PERK, PDI and Grp78/BiP and as well as the ER stress apoptotic signaling protein CHOP (15). These data suggested that increasing SERCA1 function can improve both motor function and reduce ER stress in skeletal muscle. To directly

assess the effects of increased SERCA1 activity in attenuating the ALS phenotype in skeletal muscle, in the present study, we crossed skeletal muscle-specific overexpressing SERCA1 mice with the G93A*SOD1 ALS-Tg mice. Our results clearly show that SERCA1 overexpression increases SR Ca^{2+} ATPase activity and results in improved Ca^{2+} handling in single muscle fibers of ALS-Tg mice. Most importantly, SERCA1 overexpression was shown to attenuate skeletal muscle atrophy, improve skeletal muscle function, and delay disease progression in the ALS-Tg mice. Our study support the notion that impaired SERCA1 function contributes to the skeletal muscle weakness and ALS pathogenesis.

Skeletal muscle atrophy is one of the main disease manifestations in ALS (12). However, it is still unclear whether muscle pathology is simply a consequence of motor neuron degeneration or a direct cause of the ALS phenotype (176). Notably, there is evidence indicating that skeletal muscle atrophy may precede changes in motor neurons (176). A magnetic resonance imaging (MRI) analysis of skeletal muscle volume of the G93A*SOD1 ALS-Tg showed a significant decrease in muscle as early as 8 weeks, 4 weeks before the mice become symptomatic (176; 208). Moreover, a decrease in motor function was observed as early as 50 days in ALS-Tg mice, much earlier than the mice showed clinical symptoms (176; 208). These results suggest that muscle weakness occurs in the early stages of ALS disease progression, prior to motor neuron loss. The role of skeletal muscle in the ALS phenotype has also been addressed in transgenic mice where mutant SOD1 proteins were only expressed in skeletal muscle (6). Mice with skeletal muscle-specific overexpression of mutant SOD1 also demonstrated severe muscle atrophy and progressive muscle paralysis, although disease progression was

delayed (6). Most importantly, distal degeneration was observed, strongly suggesting that skeletal muscle pathology plays an important role in ALS pathogenesis, possibly via a dying-back phenomenon (6). In our study, skeletal muscle-specific overexpression of SERCA1 recued skeletal muscle atrophy and improved motor function in ALS-Tg mice. Collectively these data support the importance of skeletal muscle in ALS disease progression and suggests that it has an important role in the ALS pathogenesis.

Our recent study showed that ER stress activation was present in skeletal muscle and could contribute, along with altered intracellular Ca^{2+} regulation, to mytocyte death in ALS-Tg mice (10). We previously showed that activation of ER stress is a skeletal muscle-specific event and is not induced in non-pathological tissues such as liver and cardiac muscle (10). Additionally, the ER stress-specific cell death signal CHOP was upregulated by 70d, prior to symptom onset, and to a greater extent in the later symptomatic stages of disease progression, suggesting that CHOP protein expression is important in ALS disease progression (10). Further, ER stress is activated to a greater extent in fast muscle, which shows an earlier decline in force in ALS-Tg mice (181), than slow type muscle fibers, suggesting that activation of ER stress is consistent with the severity of skeletal muscle pathology (10). In the current study, we tested the hypothesis that improving the skeletal muscle phenotype with SERCA1 overexpression would reduce the ER stress activation. Surprisingly, we found that the ER stress marker Grp78/BiP was upregulated in skeletal muscle of the SERCA1 Tg mice. we also found that SERCA1 overexpression failed to repress upregulation of Grp78/BiP and CHOP in skeletal muscle of ALS-Tg/+SERCA1 mice, indicating that ER stress *per se* was not involved in the improved of skeletal muscle phenotype. This result was unexpected since

Ca^{2+} handling is tightly associated with SR/ER function and we expected that improvements in Ca^{2+} homeostasis would help to preserve SR/ER function and suppress the activation of ER stress. However, considering that SERCA1 is the most abundant proteins in SR/ER, we cannot rule out the possibility that overexpression of SERCA1 could induce a temporary protein-overload in the ER lumen and thus activate ER stress even in the wild-type background. Further studies are needed to address the relationship between improved Ca^{2+} clearance capacity and ER homeostasis in skeletal muscle during ALS disease progression.

In summary, this study shows that skeletal muscle-specific overexpression of SERCA1 in ALS-Tg mice preserved muscle Ca^{2+} handling, improved motor function, delayed disease onset and attenuated muscle atrophy. Our results support the emerging notion that skeletal muscle pathology is a contributing factor in ALS pathogenesis. Our data also support targeting SERCA1 in skeletal muscle as a novel therapeutic strategy to treating ALS.

Conflict of Interest

ERC is the Founder and Chief Scientific Officer of MyoTherapeutics, a University of Maryland-based start-up company.

Acknowledgements

The authors thank Pai-Han Chen for his assistance with data collection and analysis. This work was supported by the University of Maryland, College Park new investigator funds to ERC. DAGM is supported by NIH Pre-doctoral Institutional Training Grant T32-AG000268 to J.M. Hagberg.

Table 4.1. Effects of SERCA1 overexpression on body mass of wild-type (WT) and G93A*SOD1 (ALS-Tg) mice.

	Male	Female	Male + Female Combined
WT	30.0 ± 1.2 (n = 7)	25.9 ± 1.1 (n = 4)	28.0 ± 1.0 (n = 11)
WT/+SERCA1	30.3 ± 1.2 (n = 7)	22.0 ± 1.8*† (n = 6)	26.5 ± 1.2 (n=13)
ALS-Tg	29.4 ± 11.5 (n = 2)	17.7 ± 0.9** (n = 5)	21 ± 3.5 * (n=7)
ALS-Tg/+SERCA1	26.4 ± 0.3 (n = 5)	18.5 ± 0.6** (n = 6)	21.7 ± 1.5 ** (n=11)

Body mass is shown in gram (g) with number of mice (n) per group are shown in parentheses. Data represent mean ± SEM. * $p < 0.05$ vs. WT; **$p < 0.01$ vs. WT; † $p < 0.05$ vs. ALS-Tg; †† $p < 0.01$ vs ALS-Tg.

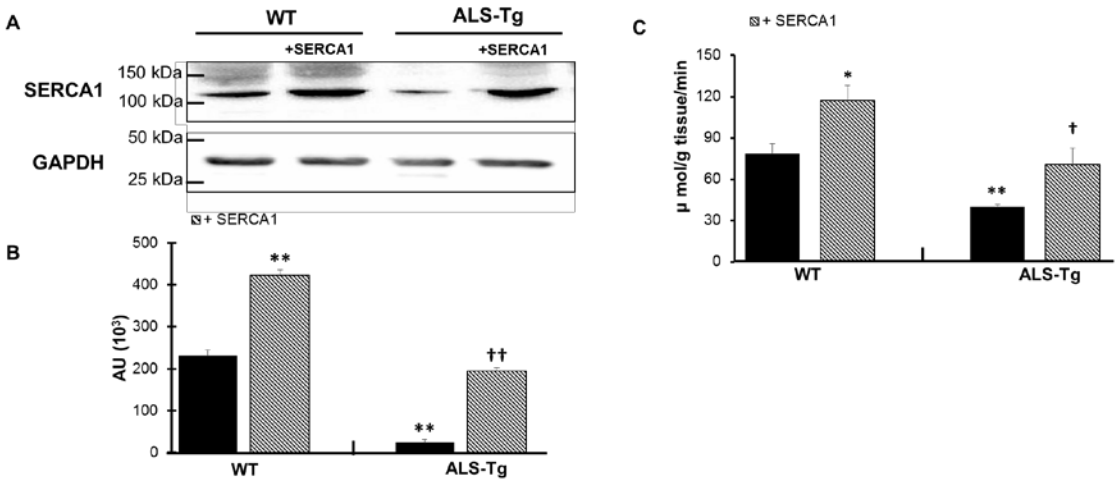

Figure 4.1. SERCA1 overexpression increases SERCA1 protein levels and maximum SR Ca^{2+} ATPase activity in quadriceps muscles in ALS-Tg mice. A) Representative western blot image for SERCA1 protein level in quadriceps muscle from WT and ALS-Tg mice with and without SERCA1 overexpression. B) Quantitative analysis of western blot images by densitometry. Data shown are in arbitrary units (AU) for WT (n=4; 1 male and 3 female), WT/+SERCA1 (n=4; 1 male and 3 female), ALS-Tg (n=4; 1 male and 3 female) and ALS-Tg/+SERCA1 (n=4; 1 male and 3 female). C) Maximal SR Ca^{2+} ATPase activity of quadriceps muscle of WT (n=4), WT/+SERCA1 (n=4), ALS-Tg (n=4) and ALS-Tg/+SERCA1 (n=4). Average data (B, C) represent mean ± SEM.. **$p < 0.01$ vs. WT, ††$p < 0.01$ vs. ALS-Tg.

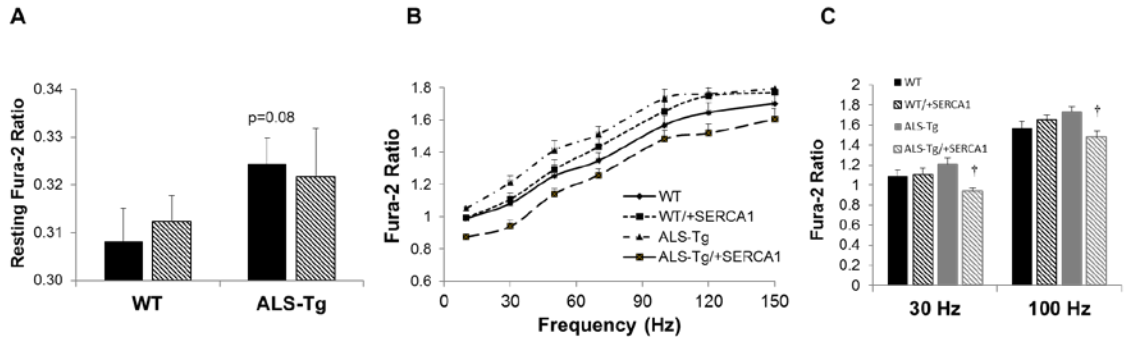

Figure 4.2. SERCA1 overexpression alters stimulation induced Ca^{2+} transients in skeletal muscle of ALS-Tg mice. (A) Data qualification of the Fura-2 ratio, which represents single muscle fiber resting intramuscular $[Ca^{2+}]_i$. (B) The Fura-2 ratio was measured in muscle fibers using trains of stimuli at 10, 30, 50, 70, 100, 120, and 150 Hz for 350 ms with fibers resting 1 min between frequencies. (C) Data qualification of The Fura-2 ratio measured in muscle fibers using trains of stimuli at 30 and 150 Hz. $^{\dagger}p < 0.05$ vs. ALS. Values shown are mean ± SEM.

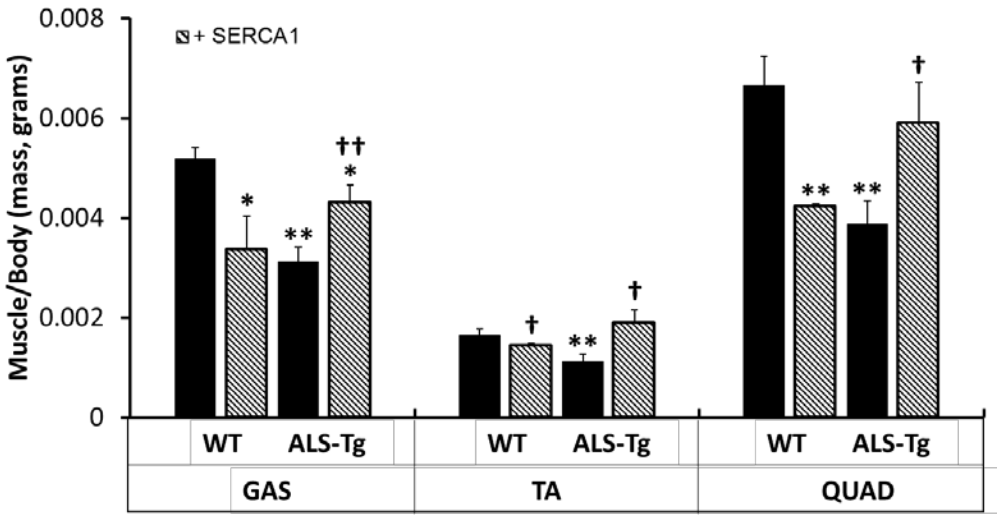

Figure 4.3. SERCA1 overexpression in skeletal muscle attenuates muscle atrophy in ALS-Tg mice. Muscle mass is shown by absolute mass (mg) for gastrocnemius (GAS), tibialis anterior (TA), and quadriceps (Quad). *$p < 0.05$ vs. WT, **$p < 0.01$ vs. WT; † $p < 0.05$ or ††$p < 0.01$ vs. ALS-Tg. Values shown are mean ± SEM.

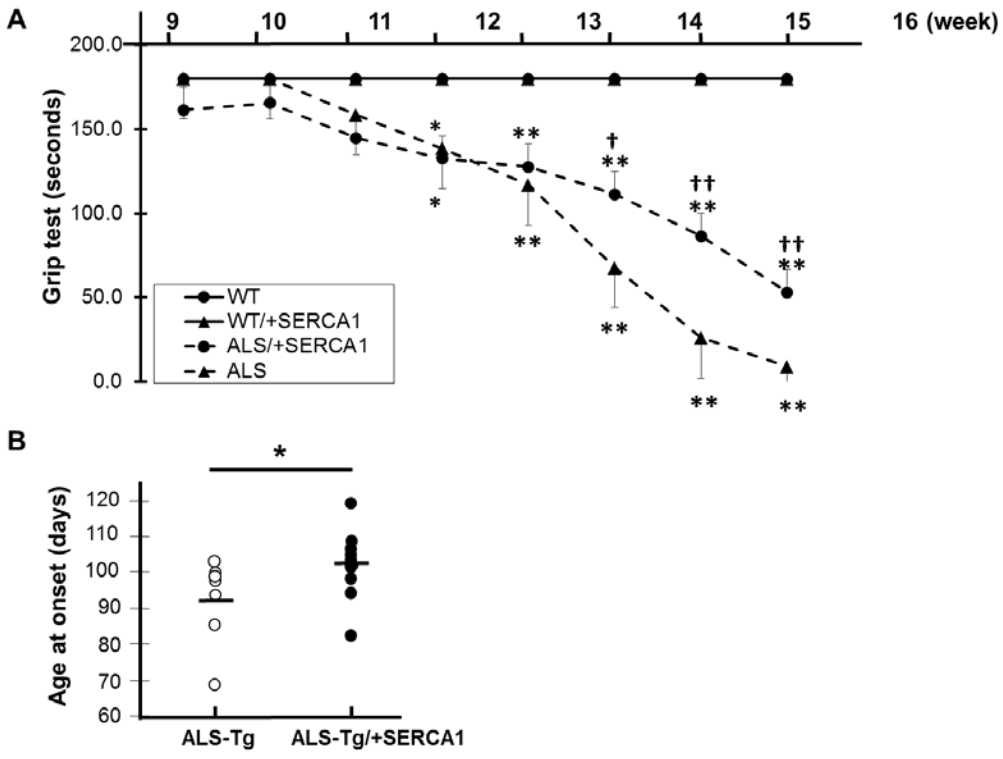

Figure 4.4. SERCA1 overexpression in skeletal muscle improves motor function and attenuates disease progression in ALS-Tg mice. (A) Data analysis of grip test. (B) Data analysis of disease onset.). *$p < 0.05$ vs. WT, **$p < 0.01$ vs. WT; † $p < 0.05$ or ††$p < 0.01$ vs. ALS-Tg. Values shown are mean ± SEM.

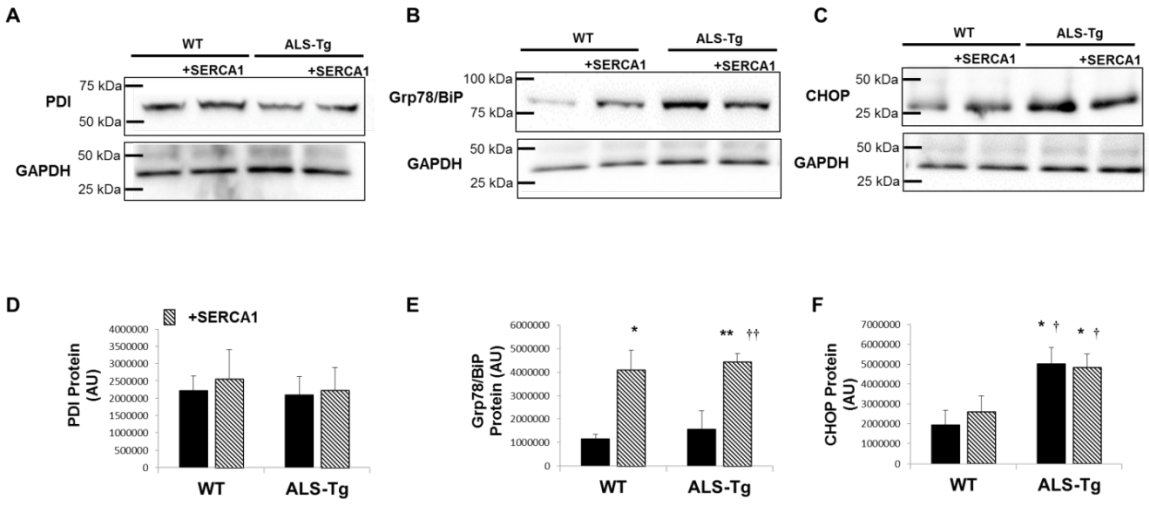

Figure 4.5. SERCA1 overexpression in skeletal muscle did not repress ER stress markers in skeletal muscle of **ALS-Tg mice.** Representative wester blots images for ER stress markers PDI (A), Grp78/BiP (B), and CHOP (C). Quantitative analysis of western blot images by densitometry of PDI (D), Grp78/BiP (E), and CHOP (F). WT (n=4), WT/+SERCA1 (n=4), ALS-Tg (n=4) and ALS-Tg/+SERCA1 (n=4). Average data represent mean ± SEM. *$p < 0.05$ vs. WT, **$p < 0.01$ vs. WT; † $p < 0.05$ or ††$p < 0.01$ vs. WT-Tg. Values shown are mean ± SEM.

Chapter 5: The role of ER stress in skeletal muscle Atrophy in amyotrophic lateral sclerosis

The following is a manuscript in preparation based on my final dissertation research project.

The role of ER stress in skeletal muscle Atrophy in amyotrophic lateral sclerosis

Dapeng Chen[1], Yan Wang[2] Eva R. Chin[1,3]

School of Public Health, University of Maryland, College Park, MD

1, School of Public Health, University of Maryland, College Park, MD 20742.
2, College of Computer, Mathematics and Natural Sciences, University of Maryland, College Park, MD 20742.
3, Send correspondence: Dr. Eva R. Chin, School of Public Health, University of Maryland, College Park, MD 20742
Tel.: (301) 405-2478, Fax: (301) 405-5578
Email: erchin@umd.edu

Abstract

Amyotrophic lateral sclerosis (ALS) is a devastating disease which affects both motor neurons and skeletal muscle. Skeletal muscle atrophy and dysfunction is one of the main features of disease progression and is suggested to contribute to ALS pathogenesis. Our preliminary data showed that ER stress was induced in skeletal muscle of ALS mice and could contribute to skeletal muscle atrophy. The purpose of this study was to investigate the molecular mechanisms of ER stress in skeletal muscle atrophy in ALS. For this purpose, we utilized affinity-based protein mass spectrometry and cell culture model approaches. Antibody co-immunoprecipitation studies show that Grp78/BiP interacts with ATPase synthase subunits and pavalbumin proteins in skeletal muscle of ALS-Tg but not wild type mice. Grp78/BiP also interacted with SERCA1 and SR Ca^{2+} ATPase activity function was reduced when Grp78/BiP was neutralized. In C2C12 myotubes, H_2O_2-induced oxidative stress reduced SR Ca^{2+} ATPase activity from 138.5 ± 22.1 to 9.6 ± 1.7 μ mole/mg protein/min. Inhibition of ER stress using 4-PBA attenuated the H_2O_2-induced decrease in in SR Ca^{2+} ATPase by 34% and catalase reversed it 100% . These data indicate that Grp78/BiP has binding partners in multiple cellular organelles and in the SR plays a protective role by attenuating oxidative stress-induced declines in SR Ca^{2+} regulation. These data further suggest that inhibition of ER stress could be an effective therapeutic way to rescue skeletal muscle dysfunction in ALS.

Keywords: ER stress, oxidative stress, skeletal muscle atrophy, ALS.

Introduction

Amyotrophic lateral sclerosis (ALS) is a devastating disease which affects both motor neurons and skeletal muscle (1). Skeletal muscle atrophy/dysfunction is one of the main features of ALS pathology and ALS patients generally die from respiratory failure within a few years of diagnosis (1). Although most ALS cases are sporadic without family history, 5-10% of the ALS cases are linked to genetic mutations with family history and thus termed as familial ALS (1). Among familial ALS cases, mutations in human Cu/Zn superoxide dismutase 1 (SOD1) proteins were first identified (32). Animal models expressing human SOD1 mutations reproduce several key phenotypes of ALS patients and have been widely used to study pathological mechanisms in ALS (4). It is suggested that mutant SOD1 proteins induce their cellular effects via a "gain-of-function" mechanism (33). However, it is still largely unknown how "gain-of-function" of mutant SOD1 proteins induces cellular toxicity. Nevertheless, several hypotheses have been proposed to suggest potential pathways for ALS pathogenesis such as oxidative stress, mitochondrial dysfunction, and unfolded protein response (21).

Unfolded protein response, or endoplasmic reticulum (ER) stress, is known to contribute to tissue pathology in various neurodegenerative diseases including ALS (21). ER is the main site for protein synthesis and newly synthesized peptides are folded properly in the ER lumen. However, various pathological conditions can cause accumulation of misfolded or unfolded proteins in the ER lumen and induce the ER stress pathway (9). Activation of ER stress involves in three ER stress sensors located on the ER membrane: protein kinase RNA activated-like ER kinase (PERK), inositol-requiring kinase 1-alpha (IRE1α), and activating transcription factor 6 (ATF6) (9). Under normal

conditions, those three ER sensors are repressed by an ER chaperone called glucose-regulated 78kDa protein/immunoglobulin binding protein (Grp78/BiP) (9). However, upon accumulation of misfolded or unfolded proteins, Grp78/BiP proteins preferentially bind to these abnormal proteins and thus activates the ER stress sensors (9). Short-term or moderate activation of ER stress is critical to preserving cellular homeostasis but long-term or prolonged activation of ER stress contributes to cell death via upregulation of ER stress-specific cell death signals such as C/EBP homologous protein (CHOP) and caspase-12 (9).

Our previous studies suggest that a disruption of ER homeostasis could play a detrimental role in inducing skeletal muscle dysfunction in ALS mice (10). Elevated intramuscular calcium level was observed in single muscle fibers of ALS mice (12). Concurrently, sarcoplasmic/endoplasmic reticulum Ca^{2+} ATPase isoform 1 (SERCA1), which is a key ER membrane calcium-handling protein, was shown to be downregulated in skeletal muscle of ALS mice, leading to our speculation that downregulation of SERCA1 proteins could results in interrupted calcium homeostasis in skeletal muscle of ALS mice (12). Indeed, SR Ca^{2+} ATPase activity, a functional measure which is more physiologically relevant, was dramatically reduced in skeletal muscle of ALS mice (12). More importantly, SERCA1 overexpression in skeletal muscle of ALS mice resulted in improvements in the disease phenotypes including improved motor function, increased muscle mass, and a delay in disease onset, indicating that increasing SR Ca^{2+} ATPase activity and maintaining calcium homeostasis can preserve skeletal muscle function in ALS mice (Chapter 4).

Our recent studies showed that ER stress was activated in skeletal muscle of ALS and suggested that this cellular stress pathway could play a pathological role in inducing muscle atrophy and dysfunction in ALS (10). Therefore, in the current study, we focused on the molecular mechanisms by which ER stress induces skeletal muscle dysfunction. Since the "gain-of-function" of SOD1*G93A mutation results in increase H_2O_2 production (17), we hypothesized that that H_2O_2 is the reactive oxygen species (ROS) that activates ER stress in skeletal muscle. We also hypothesized that H_2O_2 is responsible for the decrease in SR Ca^{2+} ATPase activity in skeletal muscle of ALS. In order to further investigate the molecular mechanism for Grp78/BiP function in skeletal muscle, we tried to identify novel binding partners through a protein-immunoprecipitation/pull down approach and identification of binding partners via protein mass spectrometry.

Methods

Ethics Statement: All animal procedures were conducted under a protocol approved by the Institutional Animal Care & Use Committee (IACUC) of the University of Maryland, College Park.

Animals: Control C57BL/6 SJL hybrid female and transgenic ALS B6SJL-Tg (SOD1 G93A) Gur/J (G93A*SOD1) male mice were obtained from The Jackson Laboratory. Wild-type control (WT) and transgenic G93A*SOD1 heterozygote (ALS-Tg) mice were bred to establish a colony at our animal care facility at the University of Maryland. Mice were weaned at postnatal day 21 and genotyped. At time of use, animals were euthanized by CO_2 inhalation followed by cervical dislocation. Skeletal muscles tissues were harvested, quickly frozen in liquid nitrogen and stored at 80^oC.

C2C12 Cell Culture and drug treatment: C2C12 cells are removed from liquid nitrogen and quickly thawed at 37^oC. After defrost, cells are moved to 25 mL flask and suspended with 10 mL growth media (GM) containing 20% fetal bovine serum, 80% DMEM, and 1% 100 x Pen/strep. C2C12 mouse myoblast were cultured in an incubator at 37^oC with 5% CO_2. After cultured in DMEM/10% FBS for 48 h, cell numbers are counted and 1.0×10^6 cells/well are moved to 12-well plates (1.0×10^5 cells/well for 24-well plate) and cultured in differentiation medium containing 2% horse serum medium, 98% DMEM, 10 ug/mL transferrin, 10 ug/mL human recombinant insulin, and 1% 100 x Pen/strep. After 96 h of myotube differentiation, cells were treated with either hydrogen peroxide (H_2O_2), thapsigargin (TG), or appropriate vehicles (water for hydrogen peroxide and 4-PBA, DMSO for thapsigargin, glycerol for catalase). C2C12 myotubes were

harvested after 24 hours after treatment for the purpose of determining SR Ca^{2+} ATPase activity and 48 hours after treatment for the purpose for western blots analysis.

Total Protein Extraction: Either skeletal muscle tissues or cell culture product samples were homogenized on ice using a polytron at 50% maximal power for three 10 s bursts, separated by 30 s in ice cold lysis buffer (20 mM Hepes, pH = 7.5, 150 mM NaCl, 1.5 mM $MgCl_2$, 0.1% Triton X-100, 20% Glycerol) containing 1 mM DTT and protease inhibitor cocktail (cOmplete mini EDTA-free Protease Inhibitor Cocktail, Roche). After 20 min of incubation at 4^{o}C followed by centrifugation for 5 min at 20,000 x g, the supernatant was collected, quick frozen in liquid nitrogen and stored at 80^{o}C until required. A BCA protein assay kit (Thermo Scientific) was used to determine protein concentration in the samples.

Western Blots: To determine protein expression levels in the sample, total protein samples were prepared with 5 x loading buffer and then heated at 100^{o}C for 5 min. After cooled down on the ice, protein samples were loaded onto bis-acrylamide gels and separated using polyacrylamide gel electrophoresis (PAGE). Samples were then transferred to PVDF membrane (Millipore) and blocked with 5% (w/v) non-fat dry milk in Tris-buffered saline (pH 8.0) for 1 h. The appropriate primary antibodies were added and incubated with membranes at 4^{o}C overnight. After primary antibody incubation, membranes were washed briefly with 1 x TBST buffer. Either anti-mouse or anti-rabbit secondary antibodies were added and incubated with membranes for 1 hour at room temperature. Secondary antibody signals were detected using either HRP-linked chemiluminescence with SuperSignal West Dura Chemiluminescence Substrate (Thermo Scientific) or Clarity^{TM} ECL western blotting substrate. The signal for the target protein

of each sample was quantified using Image Lab Software (5.0) and expressed in arbitrary unit (AU).

Cross-link Magnetic Co-immunoprecipitation (Co-IP): Quadriceps muscle was used for the purpose of Co-IP and a protein Co-IP kit was obtained commercially and Grp78/BiP protein Co-IP was conducted accordingly to the manual. Briefly, protein magnetic beads were prepared and incubated with Grp78/BiP antibody for 30 min at room temperature. After incubation, bead-antibody products were collected. For the purpose of cross linking, diluted discuccinimidyl suberate (DSS) were added and incubated with bead-antibody for 30 min at room temperature. After cross linking, the products were washed briefly and collected. Then, total protein samples were prepared and incubated with cross-linking products at 4^{o}C overnight. After protein sample incubation, Grp78/BiP protein complexes were washed off using elution buffer. After sample elution, the samples were neutralized by adding neutralization buffer and the sample pH were set as 7.0. The final elution contains Grp78/BiP and its protein interacting partners.

Mass Spectrometry-based Protein Identification & Quantity: In-solution enzymatic digestion and bottom-up protein mass spectrometry strategy were used to identify proteins in Grp78/BiP Co-IP products. For this purpose, Grp78/BiP Co-IP products were reduced with 5 mM DTT and then alkylated with 55 mM iodoacetamide. Then, Grp78/BiP Co-IP produces were incubated with trypsin (1 ug) at 37^{o}C overnight. Mass spectrometry-based protein identification and quantity method has been described previous. Briefly, after trypsin digestion, peptide products were collected and analyzed by nano LC-MS/MS analysis using LTQ Orbitrap mass spectrometer coupled to a

Shimadzu 2D Nano HPLC system. Peptides were loaded with an autosampler into an Zorbax SBC18 trap column (0.3 x 5.0 mm) (Agilent Technologies, Palo Alto, CA, USA) at 10 mL/min with solvent A (97.5% water, 2.5% ACN, 0.1% formic acid) for 10 min, then eluted and separated at 300 nL/min with a gradient of 0–35% solvent B (2.5% water, 97.5% ACN, 0.1% formic acid) in 30 min using a Zorbax SB-C18 nano column (0.075 x 150 mm). The mass spectrometer was set to acquire a full scan at resolution 60,000 (m/z 400) followed by data dependent MSMS analysis of top 10 peaks with more than one charge in the linear ion trap at unit mass resolution. The resulting LC-MS/MS data were searched against a mouse protein database generated from *uniprot* and a common contaminant database using Mascot (v2.3) and Sequest search engines through Proteome Discoverer (v1.4). Carbomidomethylation at Cys was set as fixed modification. Methionine oxidation and asparagine and glutamine deamidation were set as variable modification. Spectral counting with normalized total spectra was carried out using *Scaffold* software, (Proteome Software, Inc). Protein probability >99% and at least one unique peptide with a probability score >95% were set to as minimum requirement for protein identification (10).

SR Ca^{2+} ATPase Activity Assay: SR Ca^{2+} ATPase activity was measured in C2C12 lysates and in isolated SR vesicles. SR vesicles from skeletal muscle were a kind gift of R. Bloch. The methods for measuring SR Ca^{2+} ATPase activity has been described previously (13; 204) and this was applied to C2C12 myotube lysates. Briefly, for testing SR Ca^{2+} ATPase activity in the cell lysates, myotubes were collected and homogenized in homogenizing media containing 200mM 200 mM Sucrose, 10 mM NaN_3, 1mM EDTA, and 40 mM L-histidine (pH 7.8). The SR Ca^{2+} ATPase reaction was

measured in a myotube lysates in a reaction buffer containing 200 mM KCl, 20 mM HEPES, 10 mM NaH_3, 1 mM EGTA, 15 mM $MgCl_2$, 5 mM ATP, and 10 mM phophoenolpyruvate (PEP). To measure the Ca^{2+} ATPase activity 18 U/mL each of lactate dyhydrogenase (LDH), pyruvate kinase (PK), and 2M calcium ionophore A23187 were added to the assay buffer. SR Ca^{2+} ATPase activity was measured at different calcium concentrations: 0.1, 0.5, 1.0, 2.0, and 5.0 mM $CaCl_2$. SR Ca^{2+} ATPase activity reaches the maximal activity at 1.0 mM $CaCl_2$, whereas higher calcium concentration, such as 5.0 mM $CaCl_2$, inhibits SR Ca^{2+} ATPase activity. The reaction is driven by adding 0.4 uM NADH and the absorbance of NADH is measured at 340 nm every 30 s for 40 min. Specific SR Ca^{2+} ATPase activity is calculated using total ATPase activity at 1mM $CaCl_2$ minus basal ATPase activity, which is generated by adding 10 μM cyclopiazonic acid (CPA), which is a selective SERCA inhibitor.

For testing SR Ca^{2+} ATPase activity using SR vesicles, vesicles were added into SR Ca^{2+} ATPase activity buffer activity measured under different calcium concentrations as described above. Both cell lysates and SR vesicles determination of SR Ca^{2+} ATPase activity were performed in 96-well plates.

Statistical Analysis: All results were expressed as means ± S.E. For protein validation using western blots of Grp78/BiP co-IP products and maximal SR Ca^{2+} ATPase activity determination in SR vesicles, a Student t-test was used. For cell culture experiments, one-way ANOVA was used. The statistical significance was set as $p<0.05$.

Results

Identification of Grp78/BiP protein-protein interactions using antibody-based protein precipitation and protein mass spectrometry. A systematic series of methods coupling antibody-based protein co-immunoprecipitation with protein mass spectrometry has been developed and optimized in this study with the aim of identifying Grp78/BiP binding partners in skeletal muscle of wild (WT) and transgenic SOD1*G93A (ALS-Tg) mice (Figure 5.1 A). To validate the Grp78/BiP antibody used in our study, Grp78/BiP co-IP products from 2 sets of WT and ALS-Tg mice were loaded onto an 8% polyacrylamide gel and prepared for the SDS-PAGE electrophoresis. After gel electrophoresis, total protein was stained with a Coomassie blue kit and our results showed that Grp78/BiP bands were visualized at ~80 kDa size (black arrow, Figure 5.1 B). To further confirm the specificity of the Grp78/BiP antibody, we excised the bands and analyzed by protein mass spectrometry. Grp78/BiP protein was successfully identified in Grp78/BiP co-IP samples, indicating that the Grp78/BiP antibody was specific and appropriate for the purpose of doing protein-protein interaction analysis (supplementary Figure 5.1) (17).

In this study, we used quadriceps muscle tissue (QUAD) collected from 4 sets of WT and ALS-Tg mice. Skeletal muscle total protein was obtained and Grp78/BiP and its interacting proteins were enriched using the Grp78/BiP antibody-based co-precipitation method. To acquire solid peptide information from protein mass spectrometry analysis, we took advantage of different sample preparation strategies such as bottom-up and middle-down proteomics (209). Trypsin digestion usually generates small peptides and is used for the purpose of bottom-up proteomics. In contrast, clostripain (Arg-C) and Asp-

N endoproteinases digestion have been commonly used for the purpose of middle-down proteomics since they cleave either the C-terminus of arginine residues or N-terminus of aspartic and cysteic acid residues respectively, resulting in larger peptides and to the ability to acquire additional peptide information. The workflow would enable us to acquire protein ID as well as protein quantification information based on label-free spectral counting analysis. Finally, western blots were completed to confirm protein quantification data from protein mass spectrometry.

Identification of Grp78/BiP protein binding partners using protein mass spectrometry. Protein mass spectrometry analysis identified 182 proteins in our Grp78/BiP co-IP products (WT, n=4; ALS, n=4). As expected, Grp78/BiP was identified as the most abundant protein (Table 5.1 and Figure 5.2). Besides Grp78/BiP protein, several proteins on the top of the list (most abundant) are: Glyceraldehyde-3-phosphate dehydrogenase (GAPDH, Supplementary Figure 5.3), Sarcoplasmic/endoplasmic reticulum calcium ATPase 1 (SERCA1, Supplementary Figure 5.4), creatine kinase M-type (MCK) and ADP/ATP translocase (ANT-1, Supplementary Figure 5.5). In addition, label-free spectral counting analysis was conducted and protein quantification analyzed (Table 5.1). Our results indicated that SERCA1 and ANT-1 were in higher abundance in the Grp78/BiP complex from ALS-Tg muscle samples when compared to WT samples while GAPDH was not altered (Table 5.1, red highlight). Western blot analysis confirmed that there was a significant increase in ANT-1 (Figure 5.3B) and SERCA1 (Figure 5.3C) (~ 7-fold and ~ 40-fold, respectively) in this Grp78/BiP complex of ALS-Tg samples. In contrast, GAPDH did not show significant difference between WT and ALS-Tg (Figure 5.3D).

Protein subcellular locations were also analyzed (Table 5.2). Grp78/BiP is an ER-located chaperone and our western blots analysis confirmed that Grp78/BiP was interacting with SR -located proteins such as SERCA1. However, in ALS-Tg samples where ER stress was activated, we found that Grp78/BiP also interacted with non-SR/ER-located proteins such as ATP synthase subunits that are located in mitochondrial inner membrane. These data suggest that Grp78/BiP may translocate to some other subcellular components under ER stress conditions. Other studies in human cancer cell lines have shown that Grp78/BiP was localized in cell surface, cytoplasm, and mitochondria under cellular stress conditions (129). Collectively, our results are consistent with previous findings and suggest that Grp78/BiP undergoes an intracellular relocalization in ER stress-induced skeletal muscle.

Effect of Grp78/BiP and SERCA1 interaction on SR Ca^{2+} ATPase activity. Our IP/protein mass spectrometry and western blots analysis showed that Grp78/BiP was interacting with SERCA1 in the Grp78/BiP co-IP products. For this study, we used SR vesicles from skeletal muscle where SERCA1 was the most abundant protein (~100 kDa, Figure 5.4 A). In addition, Grp78/BiP was identified in the SR vesicle samples, further confirming the potential interaction between Grp78/BiP and SERCA1 proteins (Figure 5.4 B). To assess the functional effects of Grp78/BiP-SERCA interaction, we assessed SR Ca^{2+} ATPase activity with and without Grp78/BiP neutralization with the Grp78/BiP antibody.

We confirmed maximal ATPase activity at 1 mM $CaCl_2$ and inhibition at high levels (Figure 5.5 B). To test the effect of Grp78/BiP and SERCA1 protein interaction on maximal SR Ca^{2+} ATPase activity, SR Ca^{2+} ATPase activity was measured under three

different conditions: no Grp78/BiP antibody pre-incubation, with Grp78/BiP antibody pre-incubation, and control antibody pre-incubation (rabbit IgG, Figure 5.5 A). There was a significant decrease (25.6%) in SR Ca^{2+} ATPase activity when SR vesicles were incubated with Grp78/BiP antibody (Figure 5.5 C). To rule out the possibility of a non-specific antibody effect, a rabbit IgG was used. There was no effect of rabbit IgG on SR Ca^{2+} ATPase activity (Figure 5.5 C). These data indicate that disruption of the Grp78/BiP - SERCA1 interaction with antibody pre-incubation decreased maximal SR Ca^{2+} ATPase activity.

Activation of ER stress markers with hydrogen peroxide treatment in C2C12 myotubes. We hypothesized that oxidative stress is an important factor in inducing ER stress in skeletal muscle in ALS-Tg mice. To test this notion, we used C2C12 cell culture system and induced oxidative stress using H_2O_2. Both 100 μM and 200 μM H_2O_2 treatment upregulated Grp78/BiP and CHOP protein expression in C2C12 myotubes (~2-fold and ~1.7-fold, respectively) (Figure 5.6). Moreover, Grp78/BiP and CHOP protein expression did not show significant changes when myotubes were pre-treated with100 U/mL catalase (Figure 5.6). Thapsigargin (TG) treatment was used as a positive control to induce ER stress (9). Both 1 nM and 5 nM TG significantly upregulated Grp78/BiP and CHOP protein levels (~2.2-fold for Grp78/BiP and ~8-fold and 10-fold for CHOP) in C2C12 myotubes (Figure 5.7). To determine if 4-PBA pre-treatment could inhibit H_2O_2-induced activation of ER stress, C2C12 myotubes were pre-treated with 10 mM 4-PBA prior to H_2O_2 exposure. 4-PBA attenuated the increase in Grp78/BiP expression but did not have an effect on CHOP expression, indicating that 4-PBA pre-treatment could only partially attenuate the activation of ER stress in C2C12 myotubes (Figure 5.8).

Collectively, these results are consistent with a previous study in which H_2O_2 was shown to induce both gene and protein expression of ER stress markers in C2C12 myotubes (22).

The effects of oxidative stress and ER stress on maximal SR Ca^{2+} ATPase in C2C12 myotubes. Based on previous observations, we hypothesized that oxidative stress and ER stress would decrease SR Ca^{2+} ATPase activity. As expected, both H_2O_2 and TG treatment of C2C12 myotubes dramatically decreased maximal SR Ca^{2+} ATPase activity (Supplementary Figure 5.6 and Figure 5.9). Compared to the vehicle treatment, 100 μM H_2O_2 and 1 nM TG treatment decreased maximum SR Ca^{2+} ATPase activity by 86% and 93%, respectively (Supplementary Figure 5.6 and Figure 5.9). To evaluate the effect of oxidative stress and ER stress on maximal SR Ca^{2+} ATPase activity, we pre-treated cells either with 100 U/mL catalase or 10 mM 4-PBA. Pre-treatment with 100 U/mL catalase rescued the decrease in SR Ca^{2+} ATPase activity (Figure 5.9). Pre-treatment with 10 mM 4-PBA also rescued the TG-induced decrease in SR Ca^{2+} ATPase activity (Supplementary Figure 5.6). However, 10 mM 4-PBA failed to fully rescue maximal SR Ca^{2+} ATPase activity with H_2O_2 treatment (~34% of maximal ATPase activity with vehicle treatment) (Figure 5.9). Collectively, these data show that both oxidative stress and ER stress diminished maximum SR Ca^{2+} ATPase activity in C2C12 myotubes. Suppression of oxidative stress can fully prevent inhibition of maximal SR Ca^{2+} ATPase activity but attenuation of ER stress only showed partially rescued the decrease in SR Ca^{2+} ATPase activity with H_2O_2 treatment. These data suggest that factors other than ER stress contribute to the H_2O_2-induced the decrease in maximal SR Ca^{2+} ATPase activity.

Discussion

Here we have demonstrated that Grp78/BiP preferentially binds to cytoplasm and mitochondria proteins under ER stress conditions in skeletal muscle of ALS-Tg mice. We also identified SERCA1 as a Grp78/BiP –interacting protein and our show that Grp78/BiP is critical to preserving SERCA function in skeletal muscle. Both oxidative stress and ER stress could induce a dramatic decrease in SERCA SR Ca^{2+} ATPase activity in C2C12 myotubes. However, inhibition of ER stress only partially rescued the decrease in SR Ca^{2+} ATPase activity induced by oxidative stress.

Applying protein mass spectrometry technology to investigation of protein-protein interactions. Mass spectrometry-based proteomics has been shown to be a powerful tool to decode protein information such as protein site mutations, protein post-translational modifications, protein-protein interactions, and protein signaling networks (209). Proteins function, in part, by assembling protein complexes (protein-protein interactions), which are tightly associated with their cellular activity. Therefore, it is critical to understand what proteins are interacting and the cellular localization of these interacting proteins. In this case, protein mass spectrometry has a profound impact to the protein-protein interactions analysis.

Mass spectrometry-based proteomics analysis of protein-protein interactions usually contains three key components: antibody affinity-based target protein enrichment, protein mass spectrometry analysis, and data validation (210). For the purpose of *protein-of-interest* enrichment, the protein co-immunoprecipitation strategy is widely used. Before using it for the purpose of co-IP, the specificity of the antibody should be tested and validated. Theoretically, antibodies used for co-IP could bind to endogenous

proteins that function as the bait and enable the capture and isolation of specific proteins and their binding partners. However, there are no such exclusive antibodies produced and many antibodies either show poor affinity or yield non-specific protein binding. Consequently, non-specific protein binding and lack of specificity still exist and the MS data should be evaluated carefully. To overcome this, gene engineering strategies were used to express a "tag" on the protein interested and the antibody is produced specifically to the "tag" (210). However, those strategies have only been applied in a limited numbers of species and still show limitations in animal models. Moreover, many biological and physiological relevant protein-protein interactions are transient and their affinity capacity is largely dependent on the specific subcellular environment. Therefore, during the mass spectrometry analysis, only a part of the large group of protein-protein interactions was identified.

Before being analyzed by mass spectrometry, proteins in co-IP products are denatured, alkylated, and digested with proteases (10). Bottom-up mass spectrometry-based proteomics strategy has been widely used for the purpose of protein analysis. In this strategy, proteins enriched from various biological resources are digested into small peptides and analyzed with mass spectrometry. Trypsin-driven bottom-up proteomics strategy has its advantage since tryptic peptides are relatively stable and can be easily analyzed by mass spectrometer. Moreover, tryptic peptides would be readily fragmented and detected, providing satisfactory information for the purpose of protein sequence identification. However, trypsin digestion usually yields very small peptides and some peptides could be the same or not considerably different. Consequently, those small peptides could be either under the detection or miss their correlation to protein database

during mass spectrometry analysis. In this case, middle-down mass spectrometry-based proteomics will be a beneficial compensation (211). The principle of middle-down proteomics is to product relatively large peptides and provides more protein coverage information. In our strategy, we took advantage of those two strategies and applied them to the identification of Grp78/BiP interacting proteins.

After mass spectrometry analysis, protein IDs and quantification data could be assessed using analysis tools such as label free spectral counting protein qualification method. To confirm the mass spectrometry data analysis, western blot technique can be used to validate protein quantification data. Protein database information shows that Grp78/BiP interacts with a variety of ER-located proteins including heat shock protein 70 kDa family members and calcium handling proteins such as calreticulin and calnexin (*Uniprot.org*). However, changes in Grp78/BiP protein complexes under activation of ER stress have not been investigated. Recently, we showed ER stress was induced in skeletal muscle of ALS mice (10). Moreover, using a non-denaturing gel electrophoresis strategy, we showed that there was a dramatic change in Grp78/BiP protein complex in ER stress-induced skeletal muscle (Supplement figure 5.1). A better understanding of changes in Grp78/BiP protein complex is critical to reveal the role of Grp78/BiP in modulating ER stress signals in skeletal muscle of ALS-Tg mice. Therefore, we combined co-IP and protein mass spectrometry methods to characterize Grp78/BiP protein-protein interactions in skeletal muscle of ALS mice. To further validate our protein qualification data, we selected several protein targets identified on the top of our MS data list, such as GAPDH, SERCA1, and ANT-1. Our western blots analysis was consistent with the protein mass spectrometry results.

Relocalization of Grp78/BiP under ER stress activation. Grp78/BiP has long been recognized as an ER-located protein and induced under ER stress conditions (9). The first piece of evident showing the relocalization of Grp78/BiP to cell surface was reported in cancer cells, where Grp78/BiP was suggested to serve as a receptor to conduct cell surface signaling (131). Later on, the re-localization of Grp78/BiP event has also been reported in other cell types such as in proliferating endothelial cells and monocytic cells (130; 131). It was shown that Grp78/BiP was bound to cytoskeletal proteins such as major histocompatibility complex class I and GPI-anchored T-cadherin, suggesting that Grp78/BiP could have a role in regulating cell survival as a cell surface receptor (130). The mechanisms inducing cell surface re-localization of Grp78/BiP are still largely unknown but studies indicated Grp78/BiP protein posttranslational modifications could be involved (18).

A recent study showed that an alternative splicing form of Grp78/BiP was surprisingly expressed in the cytoplasm and mitochondria (130). Our mass spectrometry data analysis was consistent with previous studies showing the relocalization of Grp78/BiP to cytoplasm and mitochondria. In our study, five proteins identified in the Grp78/BiP co-IP products with our mass spectrometry analysis, which were only present in ALS-Tg muscle samples, included ATP synthase subunits and parvalbumin. Moreover, subcellular location analysis bioinformatics tools showed that these proteins are non-ER located proteins but expressed on mitochondrial inner membranes or within the cytoplasm. Although we did not directly image Grp78/BiP localization by immunohistochemical technqiues in skeletal muscle of ALS-Tg mice, our results are

consistent with previous studies indicating the relocalization of Grp78/BiP proteins to some other cellular components under ER stress activation (212).

Previous studies suggested that cytoplasmic Grp78/BiP proteins interact with other cytoplasmic proteins to initiated activation of the ER stress response (9). Notably, previous studies in cancer cells showed that Grp78/BiP was interacting with P58IPK, which is an inhibitor of PERK pathway (18). The protein interaction between Grp78/BiP and P58IPK would attenuate the inhibitory effect of P58IPK on PERK pathway, which is essential for cell survival, and thus protected cancer cells from initiating cell death pathway (18). Besides being expressed in the cytoplasm, Grp78/BiP proteins were also found in mitochondria (130). This notion is further supported by the fact that the ER and the mitochondria physically interact (213) and this subcellular connection is critical to preserving mitochondrial function (214). In mitochondria, Grp78/BiP was found in the mitochondrial inner membrane and matrix locations (130). Consistent with this finding, we also reported that Grp78/BiP interacts with proteins located in mitochondrial inner membrane such as ATP synthase subunits. The physiological outcome of Grp78/BiP and mitochondrial inner membrane proteins has been reported. It suggested that Grp78/BiP protected stress-induced cell injury by regulating intracellular calcium flux, decreasing the production of radical oxygen species, and preserving mitochondrial respiratory activity (215). Our finding as well as previous studies supported the notion that Grp78/BiP interacts with mitochondrial proteins and protects mitochondrial function from stress-induced cellular dysfunction.

Grp78/BiP - Isthmin-1 - ADP/ATP translocase interactions. Recent studies showed that upon activation of ER stress, Grp78/BiP proteins were expressed on the cell

surface and served as a receptor that modulated extracellular signaling (130). The biological outcomes of cell surface expression of Grp78/BiP were suggested to induce cell death pathway such as apoptosis (130). Grp78/BiP was found to be highly expressed on the cell surface and showed strong affinity to a secreted protein called Isthmin-1, which plays a role in inducing cell death in certain types of cells such as in endothelial cells (130). Under cellular stress conditions, Grp78/BiP were expressed on the cell surface and responsible for shuttling extracellular Isthmin-1 proteins into the cytoplasm in a clathrin-dependent way (130). Upon movement into the cell, Isthimin-1 interacted with Grp78/BiP and ADP/ATP translocase forming a protein complex in mitochondria (130). The final effect is to decrease ADP/ATP translocase capacity to initiate ADP/ATP turnover (130). Consequently, disruption of ADP/ATP transport induced mitochondrial dysfunction and resulted in apoptosis. Bases on these observations, either adding Grp78/BiP antibody or isthmin-1 antibody showed rescue effect on cell survival. Therefore, Grp78/BiP - Isthmin-1 - ADP/ATP translocase has been presented as a novel pathway to induce apoptosis and isthmin-1 was served as a novel cytokine involved in the initiation of cell death. Our mass spectrometry data and western blots validation data clearly showed that Grp78/BiP interacts with ADP/ATP translocase and we expect that Isthmin-1 could be a novel secreted factor that induces cell death and muscle atrophy in the animal model of ALS under ER stress activation.

Grp78/BiP and SERCA1 protein-protein interaction in skeletal muscle. Grp78/BiP is a member of heat shock protein 70 kDa family (hsp70s). A previous study showed that hsp70 interacts with SERCA1 in skeletal muscle (20). The biological consequence of those protein-protein interactions was investigated and it was suggested

that hsp70s had a protective role in SERCA1 function under heat stress challenge (20). SERCA1 is an ATP-dependent calcium pump located on the SR membrane and responsible for taking up calcium from cytoplasm to the ER lumen. SR Ca^{2+} ATPase activity is critical to preserving skeletal muscle function not only because it is the most abundance protein in the SR/ER but also because muscle contraction is known to induce a dramatic change in intramuscular calcium level (~300-fold) (195).

To evaluate the biological consequence of Grp78/BiP and SERCA1 interaction, we developed an *in vitro* assay to determine SR Ca^{2+} ATPase activity with and without Grp78/BiP antibody. Considering the protective role of hsp70s proteins in preserving SERCA1 function under heat stress, we hypothesized that disruption of this protein-protein interaction would decrease SR Ca^{2+} ATPase activity. Our results showed that there was a ~20% of decrease in maximal SR Ca^{2+} ATPase activity with Grp78/BiP antibody pre-incubation, supporting the notion that Grp78/BiP could interact with SERCA1 and thereby preserve maximal SR Ca^{2+}ATPase activity. Our results imply that Grp78/BiP and SERCA1 interaction is critical to maintaining SR Ca^{2+} ATPase activity under conditions of ER stress. However, further studies need to be conducted to investigate the cellular outcomes of Grp78/BiP and SERCA1 protein-protein interaction under cellular stress conditions.

The role of oxidative stress and ER stress in regulating SR Ca^{2+} ATPase activity in C2C12 myotubes. Skeletal muscle contraction is driven by the dramatic elevation of intracellular calcium upon release from the SR/ER. After muscle contraction, intracellular calcium levels are returned to resting levels by the SR Ca^{2+} ATPase (SERCA1 and SERCA2). A prolonged increase in intracellular calcium level is harmful

and previous studies suggested higher resting intracellular calcium levels could induce cell death and cause pathological conditions in muscle-related diseases (56). Intracellular calcium level is tightly controlled by various calcium handling proteins such as SERCA1, which is an ATP-dependent calcium pump located on ER membrane and responsible for taking up calcium back into the SR/ER after muscle contraction. The ATPase activity of SERCA1 is critical to preserving intracellular calcium balance and cellular homeostasis. Decreased SR Ca^{2+} ATPase activity in skeletal muscle is known to contribute to muscle pathology such as in muscular dystrophy and muscle atrophy (12; 216). Our lab recently reported that maximal SR Ca^{2+} ATPase activity was decreased in skeletal muscle of the G93A*SOD1 ALS mouse model and could induce skeletal muscle function (12). Indeed, both treatment with a small molecule activator of SERCA and transgenic overexpression of SERCA1 in skeletal muscle have been shown to improve skeletal muscle function and attenuate disease phenotypes in ALS mice (unpublished data and Chapter 4). These data suggested to us that SR Ca^{2+} ATPase activity is critical to preserving muscle function and attenuating disease progression in ALS mice.

Pathological factors inducing skeletal muscle dysfunction in ALS are still largely unknown. However, mutant SOD1 protein-mediated oxidative stress is suggested to be a primary candidate due to its immediate connection with overproduction of hydrogen peroxide (17). We hypothesized that oxidative stress and ER stress would decrease SR Ca^{2+} ATPase activity in the skeletal muscle and inhibition of these two cellular stress pathways would attenuate the decreased in SR Ca^{2+} ATPase activity. For this purpose, we took advantage of the C2C12 myotube culture model and oxidative stress and ER stress were induced using *in vitro* pharmacological treatments, hydrogen peroxide (H_2O_2)

and thapsigargin (TG) treatment respectively. Our results showed that both H_2O_2 and TG treatment dramatically reduced maximal SR Ca^{2+} ATPase activity. Moreover, pre-treatment of myotubes with 4-PBA, which is a chemical chaperone and represses ER stress response, was shown to attenuate the decrease in SR Ca^{2+} ATPase activity induced by TG. However, 4-PBA pre-treatment only partly prevented the decrease in maximal SR Ca^{2+} ATPase activity induced by H_2O_2 treatment. These data indicate that inhibition of ER stress could be a therapeutic method to rescue skeletal muscle damage. Additionally, besides ER stress, other factors are suggested to contribute to the decrease in maximal SR Ca^{2+} ATPase activity induced by oxidative stress.

In summary, by studying the Grp78/BiP protein-protein interactions we have shown that Grp78/BiP interacts with proteins expressed in the cytoplasm and mitochondria, suggesting the cellular relocalization of Grp78/BiP under ER stress activation. Moreover, Grp78/BiP interacts with SERCA1 in skeletal muscle and appears to be protective in terms of maintaining SR Ca^{2+} ATPase function. We also show that oxidative stress and ER stress dramatically reduce maximal SR Ca^{2+} ATPase activity and that inhibition of ER stress could be beneficial in preventing this decline. Overall these data suggest that inhibition of ER stress could be beneficial for treating skeletal muscle in ALS. However, other factors also contribute to the oxidative stress-induced decrease in SERCA function.

Acknowledgements

We thank Patrick F. Desmond and Robert J. Bloch, University of Maryland School of Medicine for the SR vesicle preparation. We thank Davi A.G. Mazala and Harry Li for their contributions to muscle tissue collections and analyses. This work was supported by the University of Maryland, College Park new investigator funds to ERC.

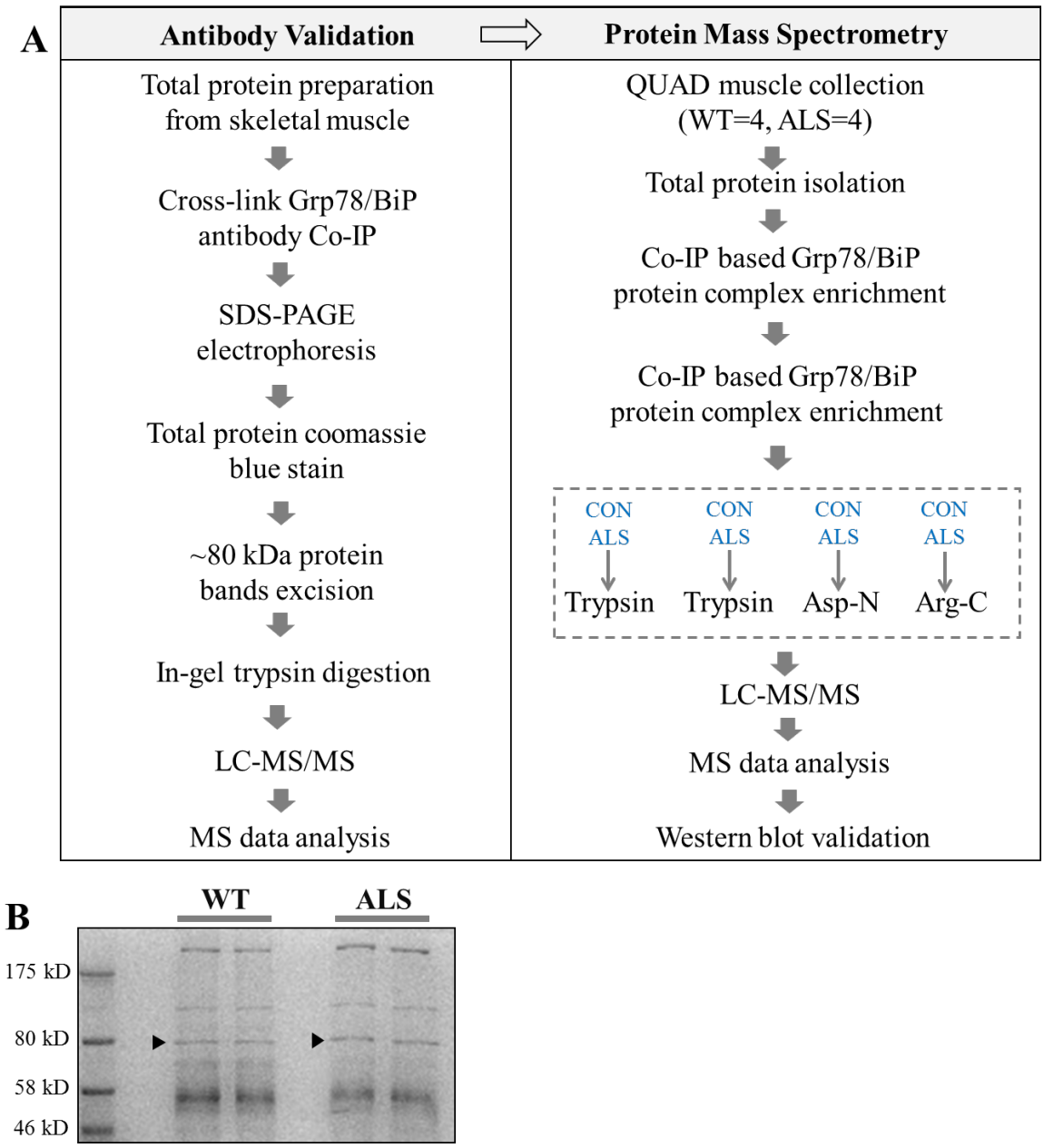

Figure 5.1: Identification of Grp78/BiP protein-protein interactions using co-immunoprecipitation and protein mass spectrometry. (A) Skeletal muscle total protein from four sets of wild type and ALS animals was isolated. Grp78/BiP and its binding proteins were enriched with Grp78/BiP protein co-immunoprecipitation (co-IP). Before being sent to mass spectrometry, co-IP protein products were digested with different proteases. Liquid chromatography-tandem mass spectrometry was used for the

purpose of protein identification and western blots were used to validate protein mass spectrometry data. (B) 30 ug of total muscle protein from wild type and ALS mice were loaded on 8% sodium dodecyl sulfate polyacrylamide gel (SDS-PAGE). After SDS-PAGE gel electrophoresis, the protein gel was washed briefly with water and incubated with coomassie blue stain buffer. Grp78/BiP (black arrow) and other protein bands were visualized using our imaging system.

Table 5.1. Top seven proteins identified in the Grp78/BiP co-precipitation products using protein mass spectrometry.

Protein list	Quantitative Value (Normalized Total Spectra)	
	WT	ALS
Heat shock 70kD protein 5 (Glucose-regulated protein) OS=Mus musculus GN=Hspa5 PE=3 SV=1	101	67
Glyceraldehyde-3-phosphate dehydrogenase OS=Mus musculus GN=Gapdh PE=1 SV=2	10	13
Sarcoplasmic/endoplasmic reticulum calcium ATPase 1 OS=Mus musculus GN=Atp2a1 PE=2 SV=1	2	15
Creatine kinase M-type OS=Mus musculus GN=Ckm PE=1 SV=1	4	7
ADP/ATP translocase=Mus musculus GN=Alb PE=1 SV=3	0	8
Pterin-mimicking anti-idiotope heavy chain variable region (Fragment) OS=Mus musculus PE=4 SV=1	9	5
ATP synthase subunit alpha, mitochondrial OS=Mus musculus GN=Atp5a1 PE=1 SV=1	0	7

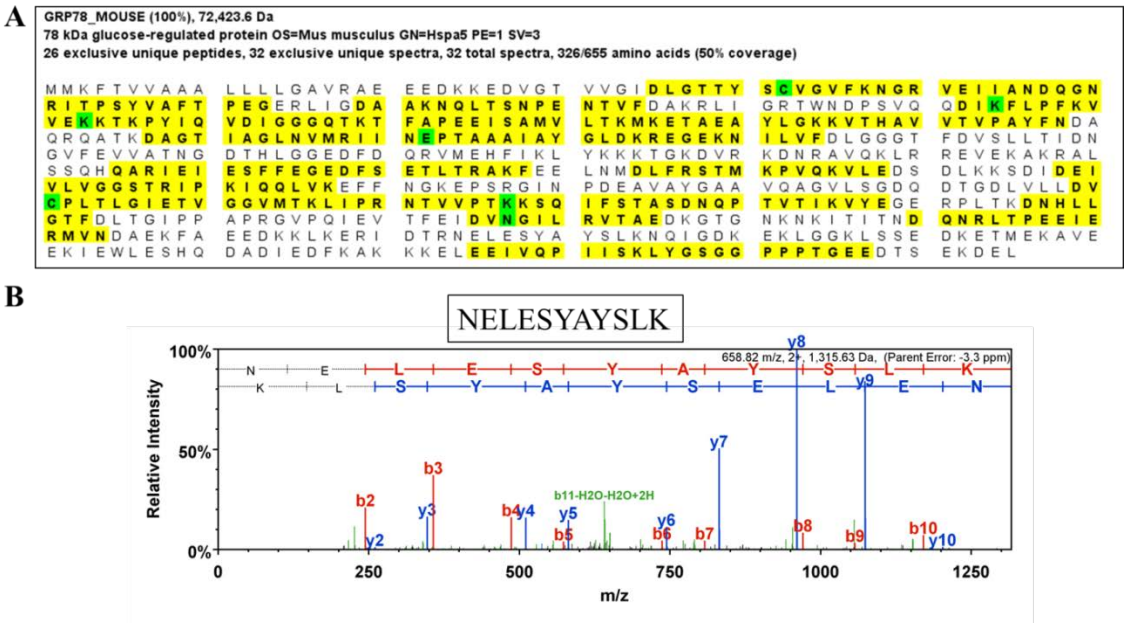

Figure 5.2: Identification of Grp78/BiP protein in Grp78/BiP co-IP products using LC-MS/MS. A) Grp78/BiP was identified in one of our samples with ~50% peptide coverage (yellow highlight), 26 exclusive unique peptides, and 32 total spectra. B) *b*- and *y*- ion fragmentation of a peptide NELESYAYSLK was presented.

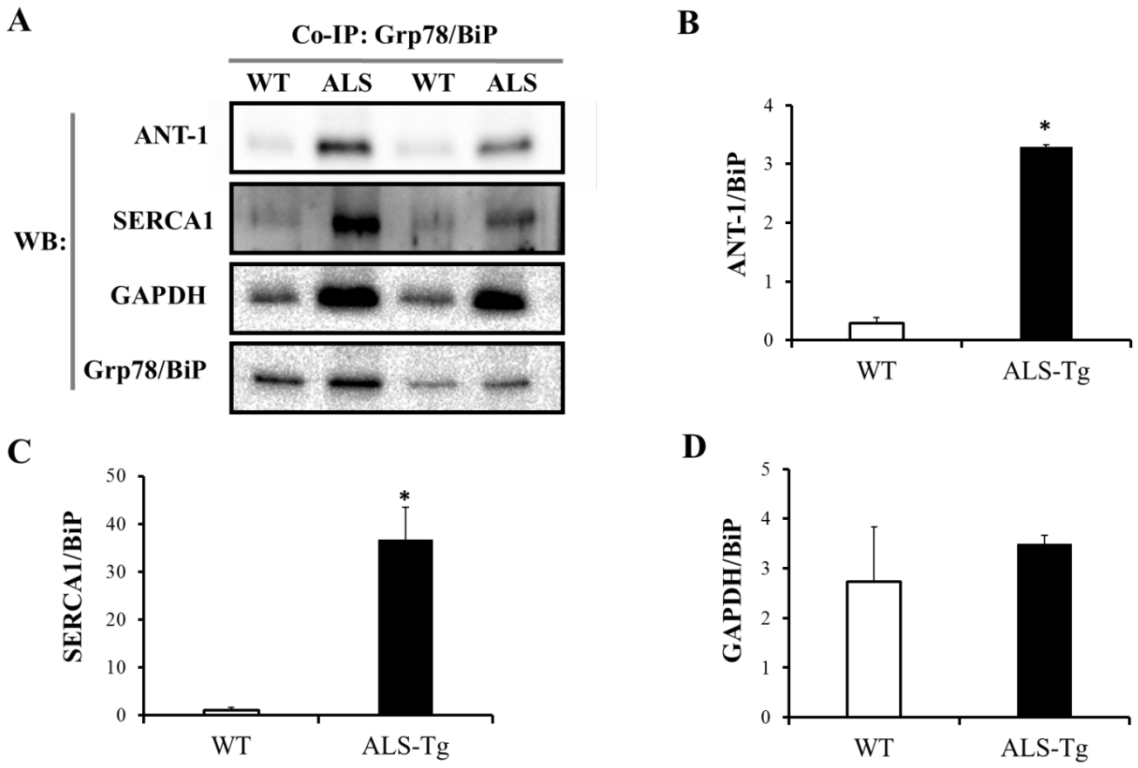

Figure 5.3: Validation of ANT-1, SERCA1, GAPDH proteins by western blots in Grp78/BiP co-IP products. (A) Grp78/BiP co-IP products from wild type (WT, n=4) and SOD1*G93A (ALS-Tg, n=4) samples were prepared for the purpose of doing western blots. The representative western blots results of ANT-1, SERCA1, GAPDH, and Grp78/BiP were shown. Data analysis of ANT-1 (B), SERCA1 (C), GAPDH (D) was presented as the ratio of target protein to Grp78/BiP. * $p<0.05$ vs. WT.

Table 5.2. Proteins identified in Grp78/BiP co-IP products using protein mass spectrometry.

Identified proteins	ALS/WT(spectral-counting numbers)	Subcelluar locations
ATP synthase subunit alpha, mitochondrial OS=Mus musculus GN=Atp5a1 PE=1 SV=1	Only identified in ALS	Mitochondrion inner membrane
ATP synthase subunit O, mitochondrial OS=Mus musculus GN=Atp5o PE=1 SV=1	Only identified in ALS	Mitochondrion
Q3SZR3 SWISS-PROT:Q3SZR3 Alpha-1-acid glycoprotein precursor	Only identified in ALS	Secreted
Pavalbumin alpha OS=Mus musculus GN=Pvalb PE=1 SV=3	Only identified in ALS	Cytoplasm
Putative uncharacterized protein OS=Mus musculus GN=slc25a4 PE=2 SV=1	Only identified in ALS	Mitochondrion inner membrane
Sarcoplasmic/endoplasmic reticulum calcium ATPase 1 OS=Mus musculus GN=Atp2a1 PE=2 SV=1	12	Endoplamic reticulum membrane
Ceatine kinase M-type OS=Mus musculus GN=Ckm PE=1 SV=1	2	cytoplasm
Glyceraldehyde-3-phosphate dehydrogenase OS=Mus musculus GN=Gapdh PE=1 SV=2	1	cytoplasm
MCG10806 OS=Mus musculus GN=RpI23a PE=2 SV=1	1	Ribosome

Protein qualification was analyzed with spectral-counting numbers and its subcellular locations were shown in the table.

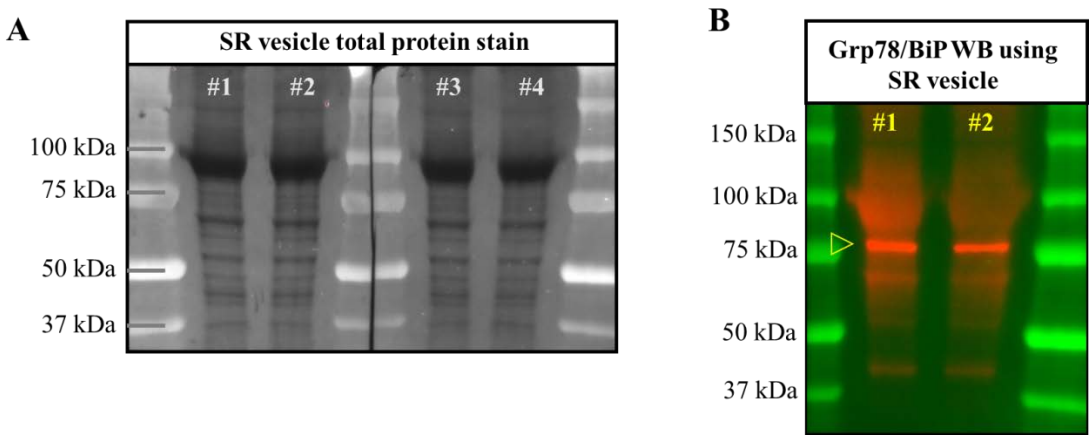

Figure 5.4. Identification of SERCA1 and Grp78/BiP proteins in SR vesicles. (A) Four SR vesicle samples were loaded on 8% sodium dodecyl sulfate polyacrylamide gel (SDS-PAGE). After SDS-PAGE gel electrophoresis, the protein gel was washed briefly with water and stained with coomassie blue. SERCA1 was shown to be the most abundant protein in the SR vesicles (~100kDa). (B) Two SR vesicle samples were prepared for SDS-PAGE gel electrophoresis and analyzed with western blots. Grp78/BiP protein (yellow open arrow and red bands) were shown.

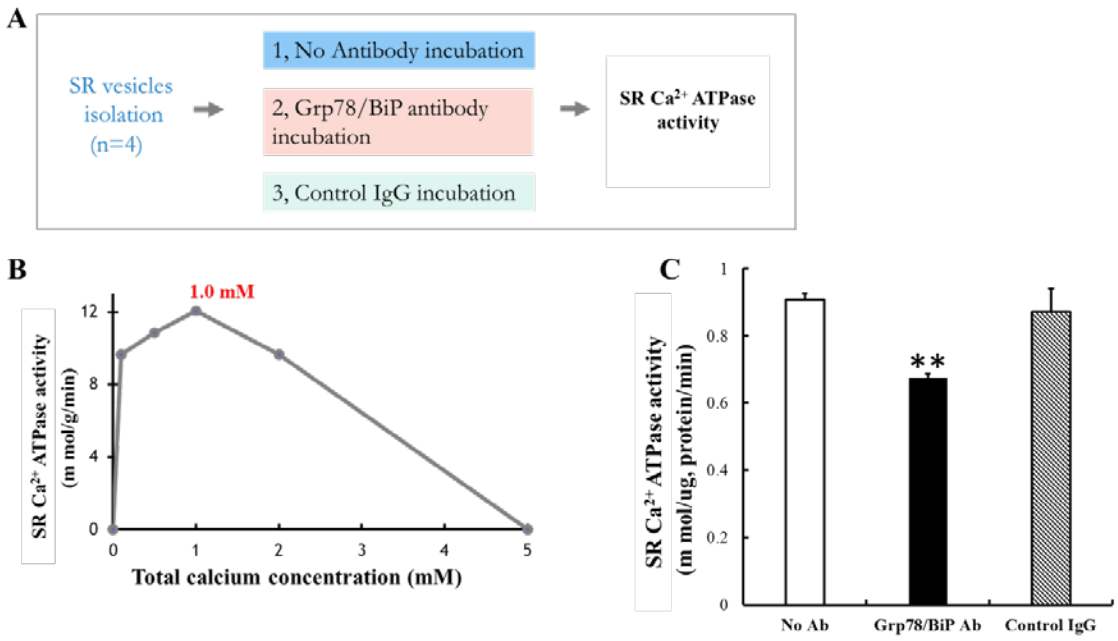

Figure 5.5. Decreased SR Ca^{2+} ATPase activity with Grp78/BiP antibody incubation in SR vesicles. (A) Maximal SERCA1 ATPase activity was determined in three conditions: no Grp78/BiP antibody incubation (No Ab), Grp78/BiP incubation (Grp78/BiP Ab), and control rabbit IgG incubation (Control IgG). (B) Maximal SERCA1 ATPase activity was shown at 1.0 mM free calcium concentration (red). (C) Maximal SERCA1 ATPase activity was determined and data analysis was presented as m mol/ug, protein content/min. Data was presented as means ± S.E.. ** $p<0.01$ vs. No Ab.

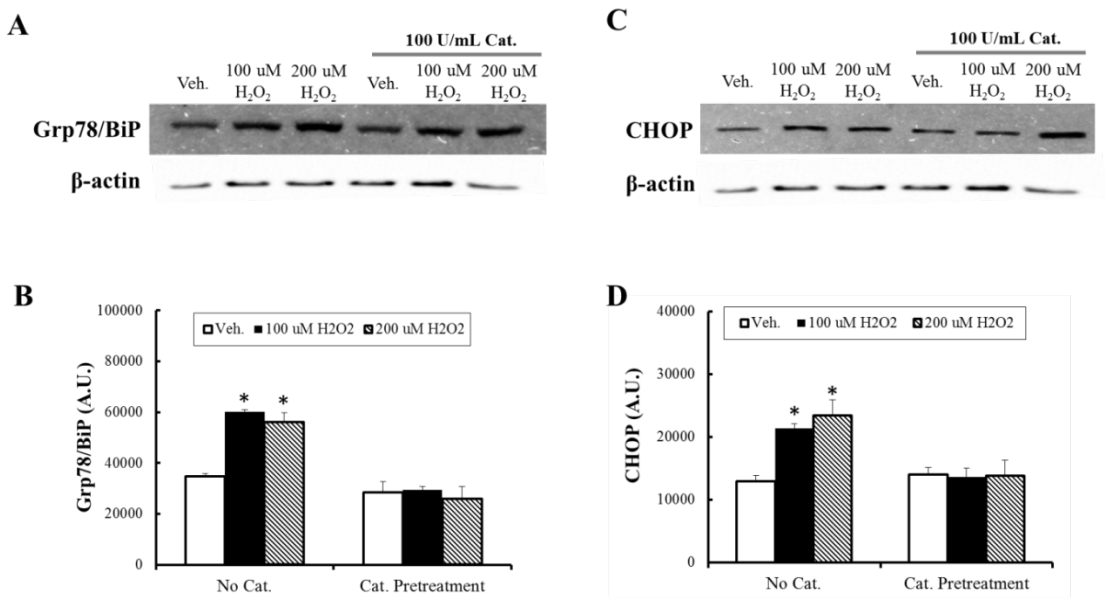

Figure 5.6. Activation of ER stress in C2C12 myotubes with hydrogen peroxidate treatment. C2C12 myotubes were treated with 100 mM and 200 uM hydrogen peroxide (H_2O_2). 100 U/mL catalase (Cat.) pre-treatment was used to neutralize the effect of hydrogen peroxide. After treatment, cells were collected and prepared for western blots analysis. The protein level of Grp78/BiP and CHOP was tested and β-actin was used as the total protein loading control (A and C). (B) The protein qualification of Grp78/BiP and CHOP was presented as arbitrary units (B and D). Data was presented as means ± S.E. *p<0.05 vs. vehicle treatment (Veh.).

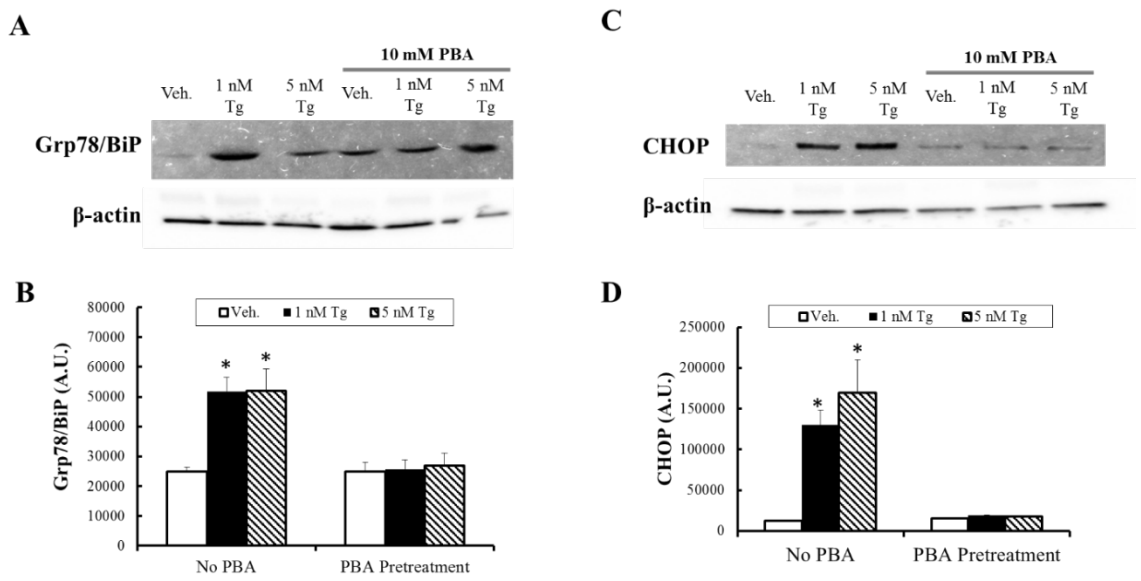

Figure 5.7. Activation of ER stress in C2C12 myotubes with thapsigargin treatment. C2C12 myotubes were treated with 1 nM and 5 nM thapsigargin (Tg). To test the effect of 4-PBA (PBA) on ER stress markers Grp78 and CHOP, cells were pre-treated with 10 mM 4-PBA before adding thapsigargin. After treatment, cells were collected and prepared for western blots analysis. The protein level of Grp78/BiP and CHOP was tested and β-actin was used as the total protein loading control (A and C). (B) The protein qualification of Grp78/BiP and CHOP was presented as arbitrary units (B and D). Data was presented as means ± S.E. *p<0.05 vs. vehicle treatment (No PBA).

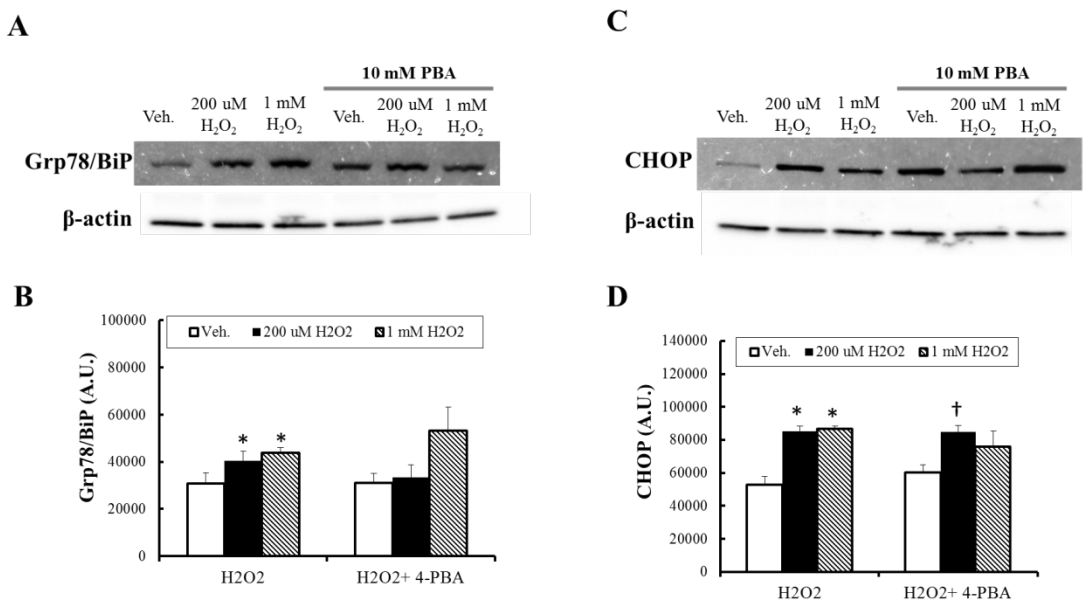

Figure 5.8. The effect of 4-PBA (PBA) pre-treatment attenuated hydrogen peroxide-induced ER stress activation. C2C12 myotubes were treated with 200 mM and 1 mM hydrogen peroxide (H_2O_2). To test the effect of 4-PBA (PBA) on ER stress markers Grp78 and CHOP, cells were pre-treated with 10 mM 4-PBA before adding hydrogen peroxide. After treatment, cells were collected and prepared for western blots analysis. The protein level of Grp78/BiP and CHOP was tested and β-actin was used as the total protein loading control (A and C). (B) The protein qualification of Grp78/BiP and CHOP was presented as arbitrary units (B and D). Data was presented as means ± S.E. *p<0.05 vs. hydrogen peroxide-only vehicle treatment (Veh.). †p<0.05 vs. PBA pre-treatment vehicle.

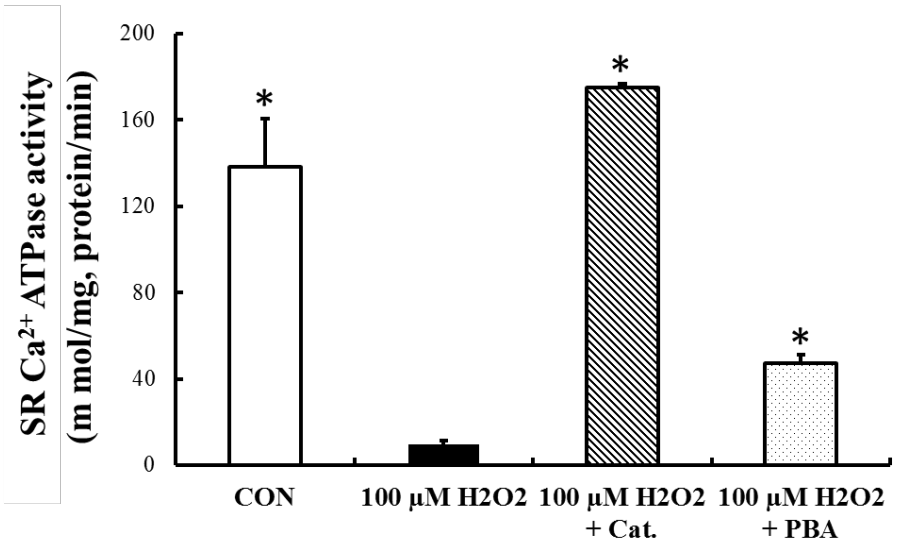

Figure 5.9. The effect of oxidative stress and 4-PBA treatment on maximal SR Ca^{2+} ATPase activity. Hydrogen peroxide (100 µM H_2O_2) was used to induce oxidative stress in C2C12 myotubes. To evaluate the effect of catalase and 4-PBA on maximal SERCA1 ATPase activity, C2C12 myotubes were pre-treated either with control vehicle (CON), 100 U/mL catalase (Cat.) or 10 mM 4-PBA (PBA). After treatment, myotubes were collected and maximal SERCA1 ATPase activity was tested. Data was presented as means ± S.E. *$p<0.05$ vs. 100 µM H_2O_2 treatment.

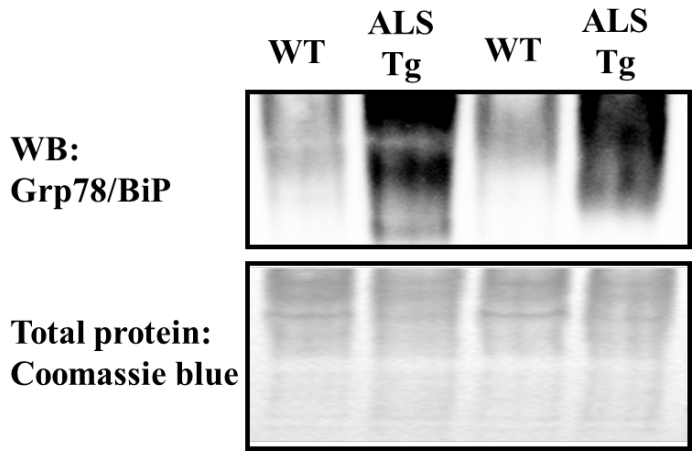

Supplementary Figure 5.1. Identification of Grp78/BiP protein complexs using denaturing gel electrophoresis. Quadriceps muscle tissues were collected from wild type (QT, n=2) and SOD1*G93A (ALS Tg, n=2) mice and prepared for the purpose of doing denaturing gel electrophoresis. After gel electrophoresis, proteins were transferred to PVDF and then incubated with Grp78/BiP antibody. After primary antibody incubation, the secondary antibody was used and the protein bands were visualized using our imaging system. Total protein stain with coomassie blue was used for protein loading normalization.

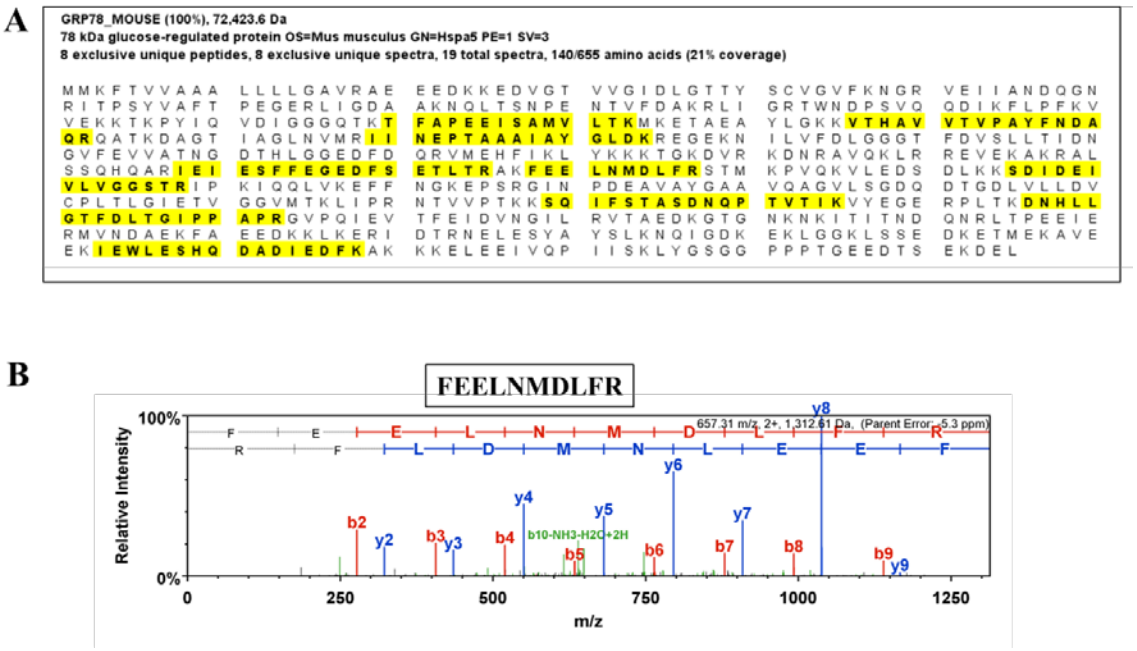

Supplement figure 5.2: Identification of G78/BiP protein in the protein bands excised from Grp78/BiP co-IP products. A) Grp78/BiP was identified in one of our samples with ~21% peptide coverage (yellow highlight), 8 exclusive unique peptides, and 19 total spectra. B) *b*- and *y*- ion fragmentation of a peptide FEELNMDLFR was presented.

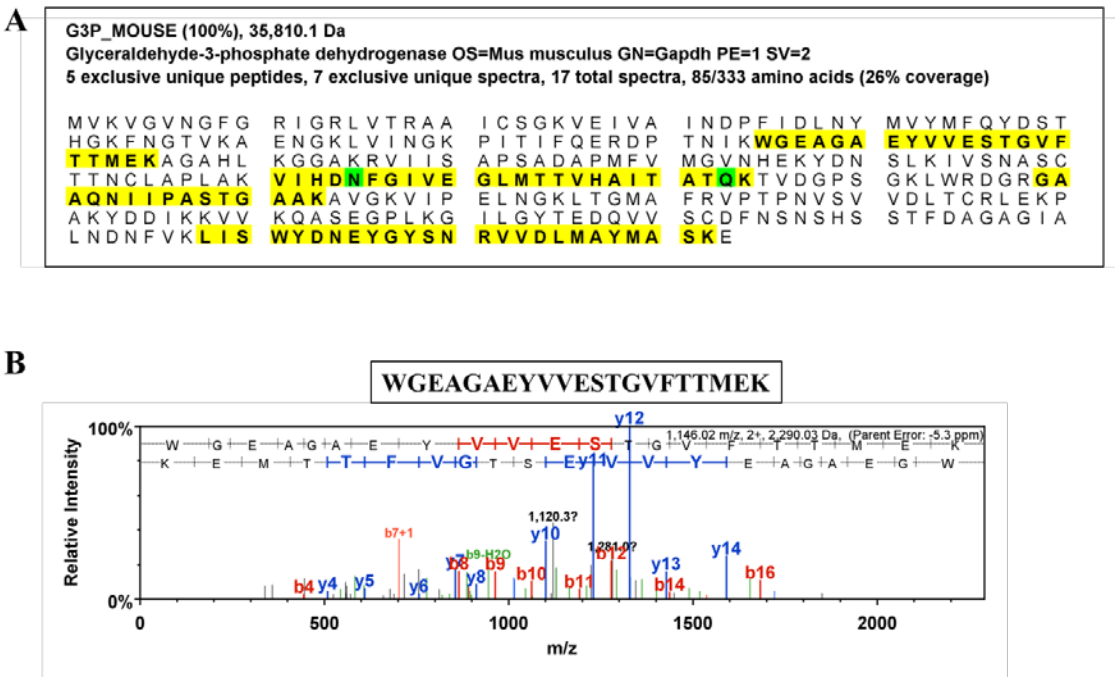

Supplement figure 5.3: Identification GAPDH protein Grp78/BiP co-IP products used for protein mass spectrometry analysis. A) GAPDH was identified in one of our samples with ~26% peptide coverage (yellow highlight), 7 exclusive unique peptides, and 17 total spectra. B) *b*- and *y*- ion fragmentation of a peptide WGEAGAEYVVESTGVFTTMEK was presented.

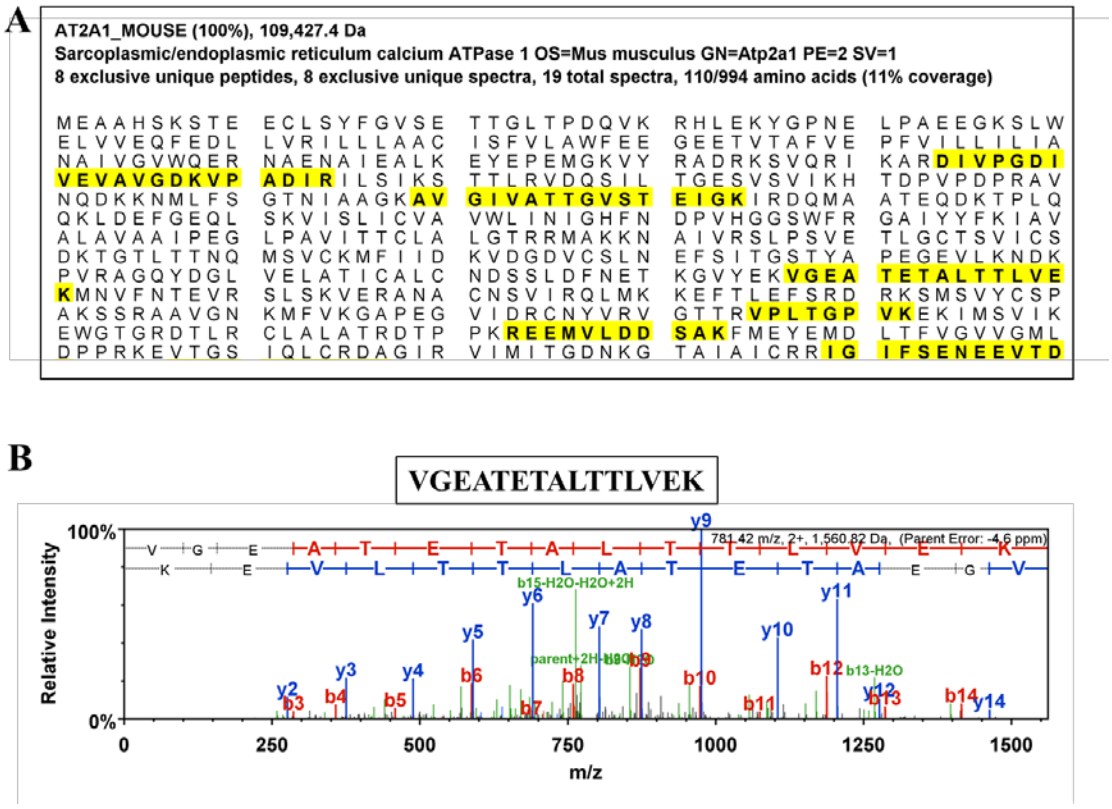

Supplement figure 5.4: Identification SERCA1 protein Grp78/BiP co-IP products used for protein mass spectrometry analysis. A) SERCA1 was identified in one of our samples with ~26% peptide coverage (yellow highlight), 8 exclusive unique peptides, and 19 total spectra. B) *b*- and *y*- ion fragmentation of a peptide VGEATETALTTLVEK was presented.

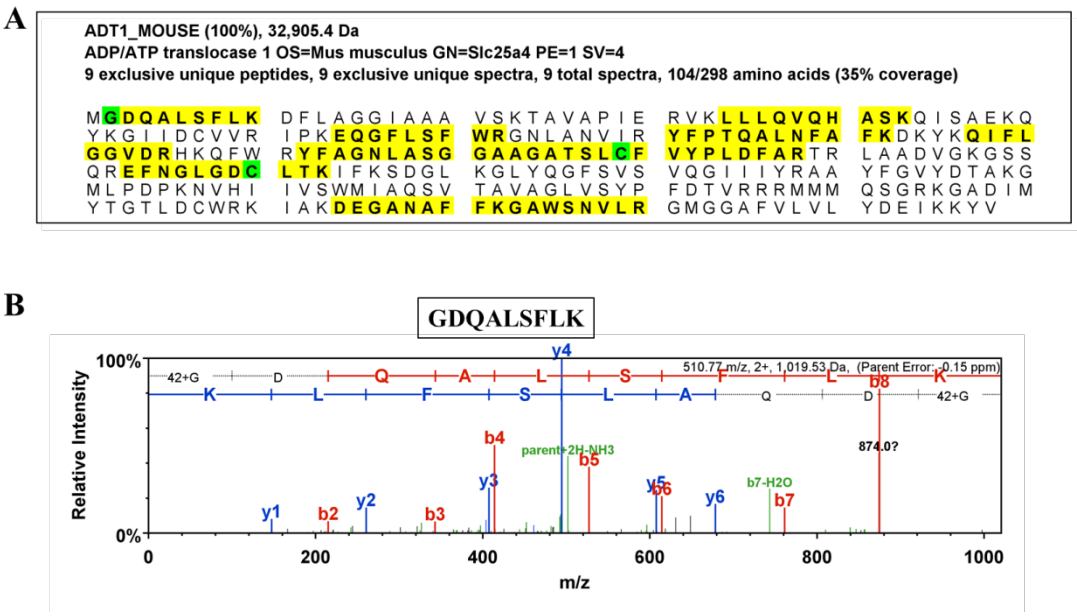

Supplement figure 5.5: Identification ANT-1 protein Grp78/BiP co-IP products used for protein mass spectrometry analysis. A) ANT-1 was identified in one of our samples with ~26% peptide coverage (yellow highlight), 9 exclusive unique peptides, and 9 total spectra. B) *b*- and *y*- ion fragmentation of a peptide GDQALSFLK was presented.

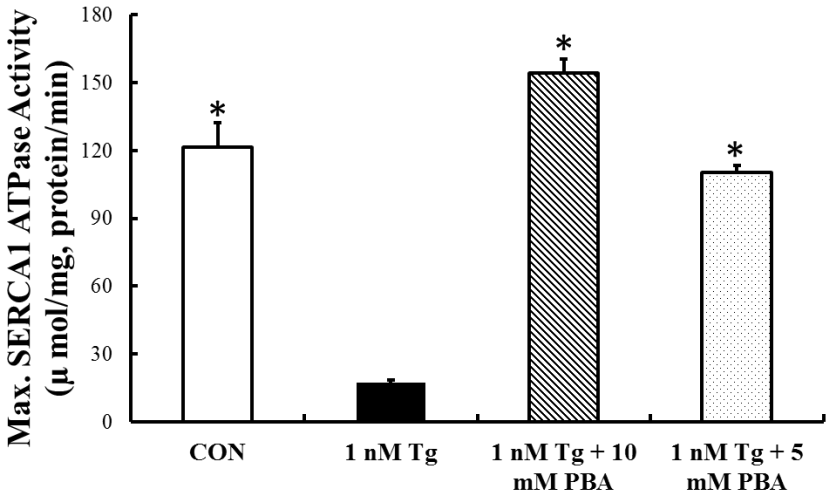

Supplement figure 5.6. The effect of 4-PBA treatment on maximal SERCA1 ATPase activity with ER stress. Thapsigargin (1 nM Tg) was used to induce ER stress in C2C12 myotubes. To evaluate the effect of 4-PBA on maximal SERCA1 ATPase activity, C2C12 myotubes were pre-treated with either control vehicle (CON), 10 mM or 5 mM 4-PBA (PBA). After treatment, myotubes were collected and maximal SERCA1 ATPase activity was tested. Data was presented as means ± S.E. *$p<0.05$ vs. 1 nM Tg treatment.

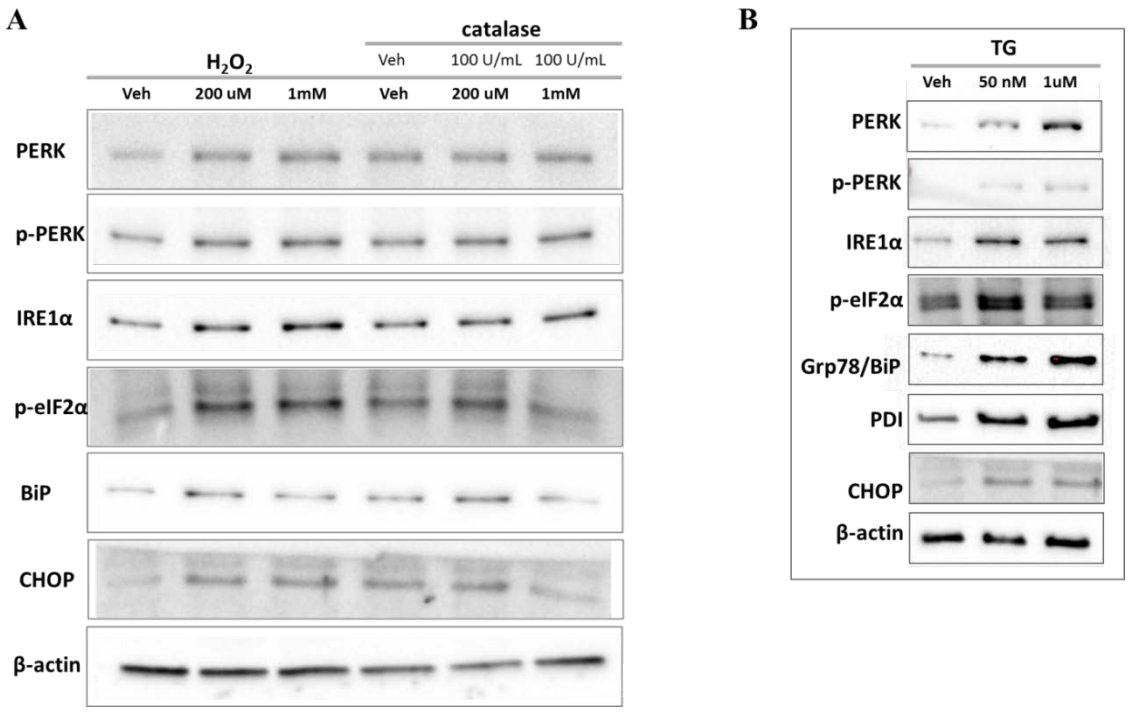

Supplementary Figure 5.7. Activation of ER stress in C2C12 myotubes with hydrogen peroxide (H_2O_2) and thapsigargin (TG) treatment. (A) C2C12 myotubes were treated with either of H_2O_2 or 100 U/mL catalase plus H_2O_2. After treatment, cells were collected and prepared for the western blots analysis. (B) C2C12 myotubes were treated with either different concentration of Tg and then collected and prepared for the western blots analysis. PERK, p-PERK, IRE1α, p-eIF2α, Grp78/BiP, and CHOP were selected for ER stress markers. β-actin was used as the total protein loading control.

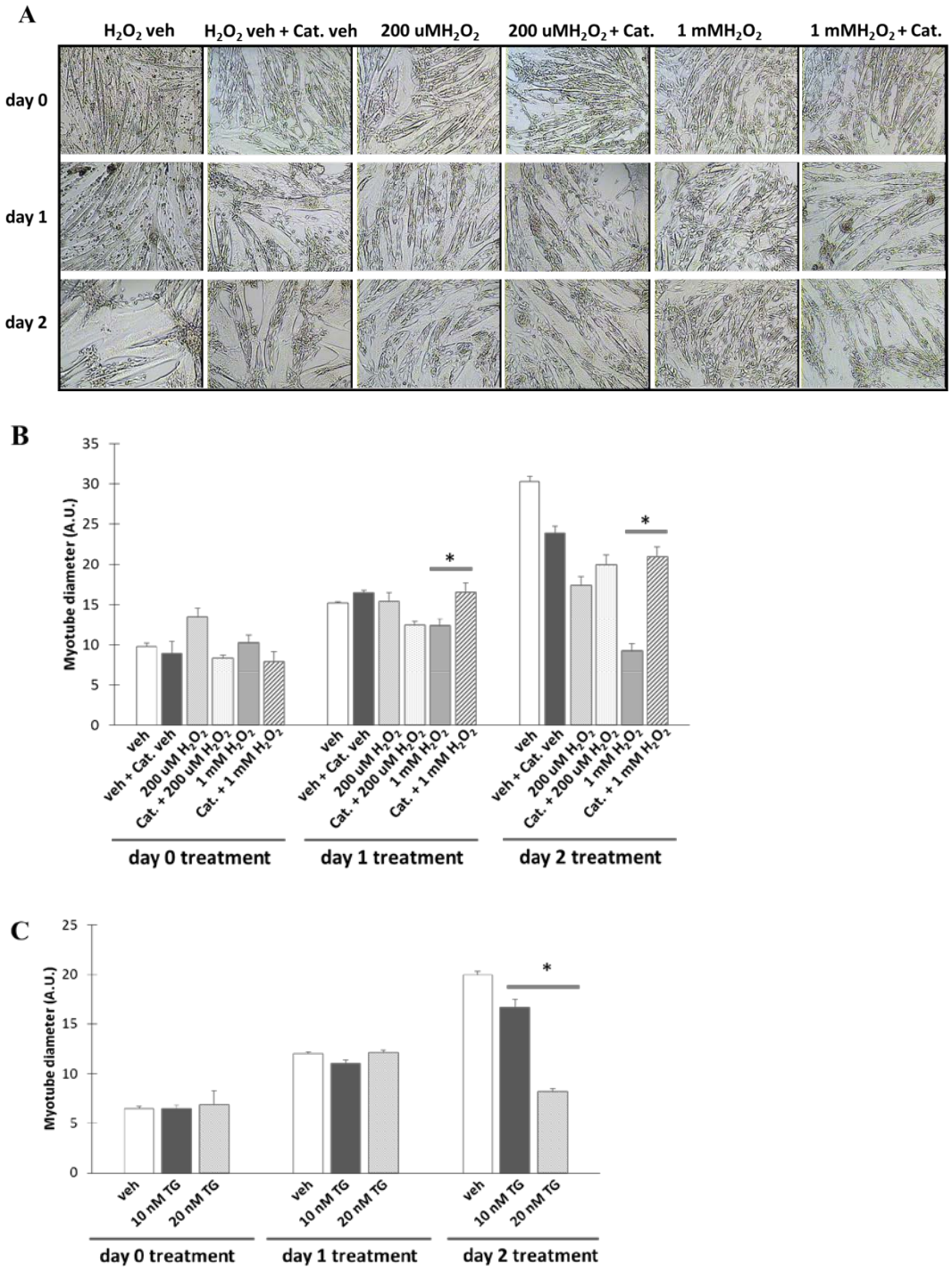

Supplementary Figure 5.8. Oxidative stress and ER stress induced C2C12 myotube atrophy. (A) H_2O_2 was used for the purpose of inducing oxidative stress in C2C12 myotubes. C2C12 myotubes were treated with either different concentration of H_2O_2 or

100 U/mL catalase (Cat.) plus H_2O_2 for two days. Images were taken before drug treatment (day 0), in the end of first day treatment (day 1) and second day treatment (day 2). (B) C2C12 myotube diameter was analyzed using Image J and presented as arbitrary units (A.U.). Data was presented as Mean ± s.e. *$p<0.05$ vs. 1mM H_2O_2 treatment at each time point.

Chapter 6: Summary and Future Directions

We conducted three independent studies to interpret the potential molecular causes underlying ER stress-induced skeletal muscle dysfunction and atrophy in ALS.

In the Study #1, we investigated ER stress pathway in skeletal muscle of ALS. Our results for the first time showed that ER stress was activated in skeletal muscle of ALS mice (10). Moreover, we suggested that prolonged activation of ER stress could contribute to skeletal muscle atrophy in ALS mice based on several lines of evident. First, ER stress-specific cell death signal CHOP was induced dramatically in the late stage of ALS disease progression. Second, ER stress activation was only present in skeletal muscle and motor neurons. Considering motor neurons and skeletal muscle are two primary targets in ALS, we suggested ER stress activation is highly relevant to disease pathology. Further, ER stress markers were induced to a greater extent in muscles with predominantly fast fibers compared with muscles with predominantly slow fibers, indicating that ER stress activation is associated with skeletal muscle pathogenesis (10).

Our previous study showed that there was an elevated resting intramuscular calcium level in muscle fibers of ALS mice and we suspected that decreased SERCA1 protein expression level contributed to the calcium dysregulation in skeletal muscle of ALS (12). Therefore, in Study #2 we took advantage of a transgenic gain of function strategy in which SERCA1 was specifically overexpressed in skeletal muscle of ALS-Tg mice. Our results showed that overexpression of SERCA1 in skeletal muscle was beneficial to ALS-Tg mice and indicated that increased SERCA SR Ca^{2+} ATPase activity leads to improved skeletal muscle function in ALS-Tg mice. Considering the potential role of ER stress in inducing skeletal muscle atrophy in ALS mice, we also determined

ER stress markers in this study. Surprisingly, overexpression of SERCA1 in skeletal muscle did not repress activation of ER stress in ALS mice. Our results indicated that: 1) the SERCA1 rescue effect on the skeletal muscle phenotype in ALS is independent of repressing ER stress pathway; and 2) overexpression of SERCA1 could induce temporary activation of ER stress in skeletal muscle of both wild type and ALS mice.

Considering the important role of oxidative stress and ER stress in inducing skeletal muscle dysfunction and atrophy in ALS mice, for Study #3, we developed an antibody affinity-based protein mass spectrometry strategy to investigate Grp78/BiP protein-protein interaction patterns in skeletal muscle of wild type and ALS-Tg mice. In this study, Grp78/BiP antibody was used for the purpose of protein precipitation. Consequently, Grp78/BiP and its protein complex were enriched and analyzed by mass spectrometry. Several highly abundant identified proteins from mass spectrometry analysis were validated using western blot. Grp78/BiP is known as an ER lumen-located protein. However, our MS data analysis showed that Grp78/BiP protein was preferentially bound to non-ER proteins such as ATP synthase subunits, which are located in mitochondria, and parvalbumin, a cytoplasm-located protein in muscle from ALS-Tg mice. Moreover, our previous study showed that ER stress was specifically activated in skeletal muscle of ALS. Collectively, our results are consistent with previous studies showing the subcellular translocation of Grp78/BiP protein under cellular stress conditions (130). SERCA1 is known as an ATPase located on the SR/ER membrane and responsible for calcium uptake from cytoplasm to ER lumen after a bout of calcium release such as during muscle contraction. Interestingly, our MS data analysis showed that Grp78/BiP interacted with SERCA1 in skeletal muscle of both wild type and

ALS mice. To determine the functional importance of this protein-protein interaction, we tested SERCA1 ATPase activity with Grp78/BiP antibody incubation. Our results showed that Grp78/BiP antibody pre-incubation induced a 20% decrease in SR Ca^{2+} ATPase activity, which was not seen with control rabbit IgG incubation, indicating that preservation of this protein-protein interaction could be critical to SERCA1 function. Finally, considering the important role of SERCA1 function in preserving skeletal muscle function, we used a muscle cell model to investigate oxidative stress/ER stress/SR Ca^{2+} ATPase activity. Our cell culture study indicated that oxidative stress was not a single factor inducing ER stress and suggested that other factors contribute to activation of ER stress in ALS.

Limitations

In Study #1, although we showed that ER stress was activated in skeletal muscle of ALS, our study did not directly test the causal role of ER stress in inducing skeletal muscle atrophy in ALS mice. In this case, specific deletion of ER stress-induced cell death signal CHOP would be a solution, which is addressed in the future direction. In Study #2, although we studied muscle mass and disease progression, we did not determine if improvement of skeletal muscle phenotype could rescue the motor neuron atrophy based on the "dying-back" model of ALS. In this case, tissue histology could be used to investigate if there are any improvements in motor neuron survival in the spinal cord withSERCA1 overexpression in ALS-Tg mice. In Study #3, although Grp78/BiP interaction mass spectrometry data indicated that Grp78/BiP proteins interact with proteins from other cellular locations, a more physiology-relevant condition should be used to validate the mass spectrometry data. For example, a skeletal muscle histology

strategy can be used to visualize Grp78/BiP proteins in the cross-section of skeletal muscle of wild type and ALS-Tg mice.

Future direction

Isthmin-1: a novel cytokine inducing cell death in skeletal muscle under ER stress?

Isthmis-1 (ISM-1) was identified as a 60 kDa secreted protein containing two functional sequences: thrombospondin type 1 repeat domain (TSP-1) and adhesion-associated domain in MUC4 and other proteins domain (AMOP) (217). Both protein domains are typically located in secreted proteins and responsible for cell adhesion and cell migration, indicating its potential role as a cytokine involved in modulating cellular signaling (217). ISM-1 was firstly identified as a novel inhibitor of endogenous angiogenesis. In *in vitro* studies, ISM-1 was shown to inhibit angiogenesis during endothelial cell capillary network formation as well as induce apoptosis (218). In animal studies, ISM-1 overexpression was shown to inhibit tumor growth (219). Moreover, knockout of ISM-1 in zebrafish embryos resulted in abnormal intersegmental vessel formation (218). It is clear that ISM-1 induces apoptosis and represses angiogenesis (218). However, the potential molecular mechanism for how extracellular ISM-1 directs signals into the cell and initiates the anti-angiogenenic action is still unknown. Recently, a mass spectrometry-based protein receptor assay showed Grp78/BiP interacted with ISM-1 (218). Binding affinity assay showed that cell surface Grp78/BiP had a very high affinity to ISM-1, further confirming this protein-protein interaction (130). Consequently, the mechanism of how ISM-1 initiates its pro-apoptotic effect was revealed. In this model, Grp78/BiP translocated to cell surface under cellular stress conditions, where Grp78/BiP

worked as a protein receptor and modulated the cellular re-localization of ISM-1 from the extracellular space to the cytoplasm in a clathrin-dependent endocytosis fashion (130). Once translocated into the cell, ISM-1/Grp78/BiP was shown to interact with ADP/ATP translocase, which is a mitochondrial membrane protein and shuttles ATP from mitochondria to cytoplasm (130). Once binding to ADP-ATP translocase, ISM-1/Grp78/BiP inhibited ADP/ATP turnover, resulting in mitochondrial dysfunction, and thus inducing mitochondria-dependent cell death (130). Those studies reveal several clues about the role of IMS-1 in integrating cell signals. First, ISM-1 could be a novel cytokine initiating extracellular and intracellular signals to induce cell death and tissue dysfunction. Second, although the role of ISM-1 in driving apoptosis has been revealed, several questions still need to be answered such as in which tissue ISM-1 proteins get secreted and how ISM-1 protein translocates into the cell (e.g., protein posttranslational modifications)? Finally, ISM-1 could also induce apoptosis in some other cell types such as myocytes.

Our primary data indicated that Grp78/BiP interacted with the mitochondrial protein ADP/ATP translocase under activation of ER stress, leading us to ask these questions in the future: 1) Is Grp78/BiP is expressed in the cell surface in skeletal muscle fibers of ALS-Tg mice? 2) Does Grp78/BiP bind to ISM-1 in skeletal muscle of ALS-Tg mice? 3) Is ISM-1 a novel cytokine to induce skeletal muscle atrophy under ER stress activation?

In vivo determination of ER stress inducing muscle atrophy in ALS

Activation of ER stress contributes to muscle pathology in various muscle diseases such as in sporadic inclusion-body myositis, cancer cachexia induced skeletal

muscle wasting, muscular dystrophy, stroke-induced myopathy, and neurodegenerative diseases (124). The causal role of ER stress in inducing muscle pathology is further established in both transgenic animal models and pharmacological drug treatment studies. For example, a study conducted by Moorwood *et al* (149) showed that several ER stress markers including Grp78/BiP, CHOP, and caspase-12, were induced in skeletal muscle in a mouse model of Duchenne muscular dystrophy (DMD). Caspase-12 is identified as an ER stress-specific induced cell death signal. When caspase-12 from DMD mice was deleted, ER stress was inhibited (149). Moreover, an improved phenotype was observed in this study including improvements in skeletal muscle function and attenuation in muscle degeneration (149). This study suggested that ER stress activation contributes to muscle dysfunction in DMD mice and that inhibition of the ER stress apoptotic pathway offers a novel therapeutic method to treat muscle pathology in DMD (149).

Inhibition of ER stress pathway was suggested as an effective strategy to delay disease progression in ALS-Tg mice (152). Studies conducted by Kieran et al showed that treating ALS mice with arimoclomol, which is a coinducer of heat shock proteins and represses ER stress activation, could improve muscle function, preserve motoneuron survival, and increase lifespan in ALS mice (152). Although activation of ER stress in motoneruons is also a main feature and arimoclomol treatment could attenuate disease progression by improving motoneuron function in ALS-Tg mice, this study provided the first line of evidence that there is a link between inhibition of ER stress and improved muscle function in ALS-Tg mice (152). Our study further confirmed the notion that activation of ER stress is causally associated with ALS disease progression. In our study, ALS-Tg mice treated with 6-gingerol, a small molecular previously shown to activate the

SR Ca^{2+} ATPase pump, showed improvements in muscle function. Most importantly, ER stress markers were repressed with drug treatment (unpublished data).

Although several therapeutic treatments have been proposed to address the role of ER stress in initiating disease pathology in ALS-Tg mice (152), to fully determine the role of ER stress activation in inducing skeletal muscle dysfunction, a better model such as transgenic animals should be used for this purpose. Previous studies indicated that either upregulation of ER chaperones, such as hsp70s, or deletion of ER stress-specific cell death signals such as CHOP and caspase-12 was an attractive strategy to repress the activation of ER stress (149). As a transcriptional factor, CHOP is suggested to integrate cell death signals induced by ER stress such as pro-apoptotic regulator Bcl-2-associated x proteins (9). Therefore, CHOP knockout animal models have been used to investigate ER stress-induced organ dysfunction (220). Caspase-12 knockout strategy has been also presented in several studies. However, caspase-12 is not present in human, wakening its role as an appealing therapeutic target for treating human diseases. Therefore, to study the role of ER stress in inducing skeletal muscle atrophy in ALS, skeletal muscle-specific deletion of CHOP could be used and crossed with ALS mice. Outcome determinations include skeletal muscle function, muscle mass, disease onset, and disease progression. This study will address several key points regarding pathological mechanism in ALS. In the first place, this study will fully evaluate the role of ER stress activation in inducing skeletal muscle atrophy and dysfunction in ALS. In the second place, our study will address the primary role of muscle pathology in inducing ALS pathophysiology. Previous studies presented the principle of “dying-back” model in ALS disease, in which ALS pathophysiology is thought to stem from skeletal muscle or neuron-muscle junctions.

However, early pathological events in skeletal muscle of ALS are still unknown. Here we presented that ER stress activation in skeletal muscle not only resulted in muscle pathology but also could contribute to muscle-induced whole body ALS phenotype. In the last, our study will provide a piece of evidence that can be used in treating some other types of ER stress-involved muscle dysfunction/diseases. It should be noted that skeletal muscle function is tightly associated with muscle metabolism and several lines of evidence indicated that activation of ER stress contributed to metabolic defects in skeletal muscle and it will be interesting to ask if inhibition of ER stress, which preserves skeletal muscle function, would generate a better metabolic phenotype in skeletal muscle.

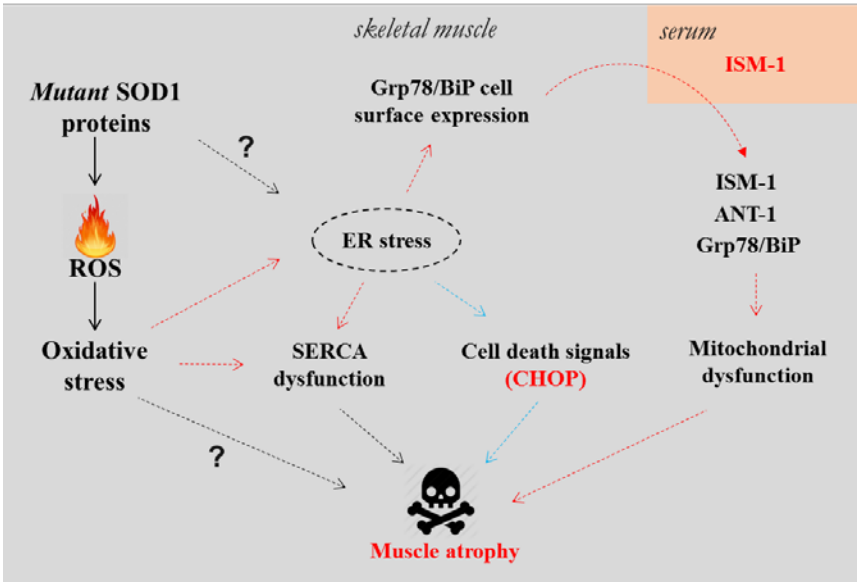

Figure 6.1. *"All Roads Lead to Rome"*- the schematic model of skeletal muscle atrophy in ALS. . Based on our three independent studies, proposed model is proposed with various potential mechanisms inducing skeletal muscle atrophy and dysfunction in ALS from Study #1 (blue-dots line), Study #2 (black-dots line), and Study #3 (red-dots line). Study #1 investigated ER stress pathway and we suggested that ER stress-specific cell signal CHOP could induce myocyte death and induce skeletal muscle atrophy in ALS. Study #2 investigated the effect skeletal muscle overexpressing SERCA1 on skeletal muscle function and atrophy in ALS-Tg mice. SERCA1 preserved skeletal muscle function and improved the ALS phenotype in ALS-Tg mice. Study #3 investigated the molecular mechanisms underlying ER stress-induced skeletal muscle atrophy in ALS. Oxidative stress and ER stress could induce muscle dysfunction by regulating SERCA function. Furthermore, we proposed the hypothesis that ISM-1 could play a role as a novel cytokine to induce mitochondrial dysfunction and tissue atrophy by interacting Grp78/BiP under ER stress conditions.

Literature Cited

1. Rowland LP, Shneider NA: Amyotrophic lateral sclerosis. N Engl J Med 2001;344:1688-1700

2. Rosen DR, Siddique T, Patterson D, Figlewicz DA, Sapp P, Hentati A, Donaldson D, Goto J, O'Regan JP, Deng HX, et al.: Mutations in Cu/Zn superoxide dismutase gene are associated with familial amyotrophic lateral sclerosis. Nature 1993;362:59-62

3. Deng HX, Tainer JA, Mitsumoto H, Ohnishi A, He X, Hung WY, Zhao Y, Juneja T, Hentati A, Siddique T: Two novel SOD1 mutations in patients with familial amyotrophic lateral sclerosis. Hum Mol Genet 1995;4:1113-1116

4. Gurney ME, Pu H, Chiu AY, Dal Canto MC, Polchow CY, Alexander DD, Caliendo J, Hentati A, Kwon YW, Deng HX: Motor neuron degeneration in mice that express a human Cu,Zn superoxide dismutase mutation. Science 1994;264:1772-1775

5. Baker MR: ALS--dying forward, backward or outward? Nat Rev Neurol 2014;10:660

6. Wong M, Martin LJ: Skeletal muscle-restricted expression of human SOD1 causes motor neuron degeneration in transgenic mice. Hum Mol Genet 2010;19:2284-2302

7. Chin ER, Chen D, Bobyk KD, Mazala DA: Perturbations in intracellular Ca2+ handling in skeletal muscle in the G93A*SOD1 mouse model of amyotrophic lateral sclerosis. Am J Physiol Cell Physiol 2014;307:C1031-1038

8. Kania E, Pająk B, Orzechowski A: Calcium homeostasis and ER stress in control of autophagy in cancer cells. Biomed Res Int 2015;2015:352794

9. Xu C, Bailly-Maitre B, Reed JC: Endoplasmic reticulum stress: cell life and death decisions. J Clin Invest 2005;115:2656-2664

10. Chen D, Wang Y, Chin ER: Activation of the endoplasmic reticulum stress response in skeletal muscle of G93A*SOD1 amyotrophic lateral sclerosis mice. Front Cell Neurosci 2015;9:170

11. Hegedus J, Putman CT, Gordon T: Time course of preferential motor unit loss in the SOD1 G93A mouse model of amyotrophic lateral sclerosis. Neurobiol Dis 2007;28:154-164

12. Chin ER, Chen D, Bobyk KD, Mázala DA: Perturbations in intracellular Ca2+ handling in skeletal muscle in the G93A*SOD1 mouse model of amyotrophic lateral sclerosis. Am J Physiol Cell Physiol 2014;307:C1031-1038

13. Mazala DA, Pratt SJ, Chen D, Molkentin JD, Lovering RM, Chin ER: SERCA1 overexpression minimizes skeletal muscle damage in dystrophic mouse models. In *Am J Physiol Cell Physiol* United States, 2015 the American Physiological Society., 2015, p. C699-709

14. Kruman II, Pedersen WA, Springer JE, Mattson MP: ALS-linked Cu/Zn-SOD mutation increases vulnerability of motor neurons to excitotoxicity by a mechanism involving increased oxidative stress and perturbed calcium homeostasis. Exp Neurol 1999;160:28-39

15. Chin E, DAG M, D C: Improvements in motor function, Ca^{2+} clearance and markers of endoplasmic reticulum stress with 6-gingerol treatment in G93A*SOD1 mice. Amyotrophic Lateral Sclerosis and Frontotemporal Degeneration 2014;15:203

16. Kim JK, Kim Y, Na KM, Surh YJ, Kim TY: [6]-Gingerol prevents UVB-induced ROS production and COX-2 expression in vitro and in vivo. In *Free Radic Res* England, 2007, p. 603-614

17. Cookson MR, Menzies FM, Manning P, Eggett CJ, Figlewicz DA, McNeil CJ, Shaw PJ: Cu/Zn superoxide dismutase (SOD1) mutations associated with familial amyotrophic lateral sclerosis (ALS) affect cellular free radical release in the presence of oxidative stress. Amyotroph Lateral Scler Other Motor Neuron Disord 2002;3:75-85

18. Hendershot LM: The ER function BiP is a master regulator of ER function. Mt Sinai J Med 2004;71:289-297

19. Li J, Ni M, Lee B, Barron E, Hinton DR, Lee AS: The unfolded protein response regulator GRP78/BiP is required for endoplasmic reticulum integrity and stress-induced autophagy in mammalian cells. Cell Death Differ 2008;15:1460-1471

20. Tupling AR, Gramolini AO, Duhamel TA, Kondo H, Asahi M, Tsuchiya SC, Borrelli MJ, Lepock JR, Otsu K, Hori M, MacLennan DH, Green HJ: HSP70 binds to the fast-twitch skeletal muscle sarco(endo)plasmic reticulum Ca2+ -ATPase (SERCA1a) and prevents thermal inactivation. J Biol Chem 2004;279:52382-52389

21. Ilieva EV, Ayala V, Jové M, Dalfó E, Cacabelos D, Povedano M, Bellmunt MJ, Ferrer I, Pamplona R, Portero-Otín M: Oxidative and endoplasmic reticulum stress interplay in sporadic amyotrophic lateral sclerosis. Brain 2007;130:3111-3123

22. Pierre N, Barbé C, Gilson H, Deldicque L, Raymackers JM, Francaux M: Activation of ER stress by hydrogen peroxide in C2C12 myotubes. Biochem Biophys Res Commun 2014;450:459-463

23. Tadic V, Prell T, Lautenschlaeger J, Grosskreutz J: The ER mitochondria calcium cycle and ER stress response as therapeutic targets in amyotrophic lateral sclerosis. Front Cell Neurosci 2014;8:147

24. Kiernan MC, Vucic S, Cheah BC, Turner MR, Eisen A, Hardiman O, Burrell JR, Zoing MC: Amyotrophic lateral sclerosis. Lancet 2011;377:942-955

25. Hirano A: Cytopathology of amyotrophic lateral sclerosis. Advances in Neurology 1991;56:91-101

26. Fischer LR, Culver DG, Tennant P, Davis AA, Wang M, Castellano-Sanchez A, Khan J, Polak MA, Glass JD: Amyotrophic lateral sclerosis is a distal axonopathy: evidence in mice and man. Exp Neurol 2004;185:232-240

27. Correction to: epidemiology of amyotrophic lateral sclerosis in Emilia Romagna Region (Italy): a population based study. Amyotroph Lateral Scler Frontotemporal Degener 2015;16:141

28. Prevalence of amyotrophic lateral sclerosis - United States, 2010-2011. Am J Public Health 2015;105:e7-9

29. Ajroud-Driss S, Siddique T: Sporadic and hereditary amyotrophic lateral sclerosis (ALS). Biochim Biophys Acta 2015;1852:679-684

30. Ash S, Olm C, McMillan CT, Boller A, Irwin DJ, McCluskey L, Elman L, Grossman M: Deficits in sentence expression in amyotrophic lateral sclerosis. Amyotroph Lateral Scler Frontotemporal Degener 2015;16:31-39

31. Caller TA, Andrews A, Field NC, Henegan PL, Stommel EW: The Epidemiology of Amyotrophic Lateral Sclerosis in New Hampshire, USA, 2004-2007. Neurodegener Dis 2015;

32. Rosen DR: Mutations in Cu/Zn superoxide dismutase gene are associated with familial amyotrophic lateral sclerosis. Nature 1993;364:362

33. Karch CM, Prudencio M, Winkler DD, Hart PJ, Borchelt DR: Role of mutant SOD1 disulfide oxidation and aggregation in the pathogenesis of familial ALS. Proc Natl Acad Sci U S A 2009;106:7774-7779

34. Israelson A, Arbel N, Da Cruz S, Ilieva H, Yamanaka K, Shoshan-Barmatz V, Cleveland DW: Misfolded mutant SOD1 directly inhibits VDAC1 conductance in a mouse model of inherited ALS. Neuron 2010;67:575-587

35. Rojas F, Gonzalez D, Cortes N, Ampuero E, Hernández DE, Fritz E, Abarzua S, Martinez A, Elorza AA, Alvarez A, Court F, van Zundert B: Reactive oxygen species trigger motoneuron death in non-cell-autonomous models of ALS through activation of c-Abl signaling. Front Cell Neurosci 2015;9:203

36. Brooks BR: ALS-Plus - where does it begin, where does it end? J Neurol Sci 2014;345:1-2

37. Blasco H, Mavel S, Corcia P, Gordon PH: The glutamate hypothesis in ALS: pathophysiology and drug development. Curr Med Chem 2014;21:3551-3575

38. Bucchia M, Ramirez A, Parente V, Simone C, Nizzardo M, Magri F, Dametti S, Corti S: Therapeutic development in amyotrophic lateral sclerosis. Clin Ther 2015;37:668-680

39. Zhu Y, Fotinos A, Mao LL, Atassi N, Zhou EW, Ahmad S, Guan Y, Berry JD, Cudkowicz ME, Wang X: Neuroprotective agents target molecular mechanisms of disease in ALS. Drug Discov Today 2015;20:65-75

40. Lindal S: Mitochondria and neurodegenerative diseases--is there a link? The role of mitochondria in the pathogenesis of amyotrophic lateral sclerosis (ALS). Ultrastruct Pathol 2002;26:1-2

41. Cozzolino M, Ferri A, Valle C, Carrì MT: Mitochondria and ALS: implications from novel genes and pathways. Mol Cell Neurosci 2013;55:44-49

42. Cozzolino M, Rossi S, Mirra A, Carrì MT: Mitochondrial dynamism and the pathogenesis of Amyotrophic Lateral Sclerosis. Front Cell Neurosci 2015;9:31

43. Ehinger JK, Morota S, Hansson MJ, Paul G, Elmér E: Mitochondrial dysfunction in blood cells from amyotrophic lateral sclerosis patients. J Neurol 2015;262:1493-1503

44. Martin LJ, Fancelli D, Wong M, Niedzwiecki M, Ballarini M, Plyte S, Chang Q: GNX-4728, a novel small molecule drug inhibitor of mitochondrial permeability transition, is therapeutic in a mouse model of amyotrophic lateral sclerosis. Front Cell Neurosci 2014;8:433

45. Pehar M, Beeson G, Beeson CC, Johnson JA, Vargas MR: Mitochondria-targeted catalase reverts the neurotoxicity of hSOD1G^{93}A astrocytes without extending the survival of ALS-linked mutant hSOD1 mice. PLoS One 2014;9:e103438

46. Palomo GM, Manfredi G: Exploring new pathways of neurodegeneration in ALS: the role of mitochondria quality control. Brain Res 2015;1607:36-46

47. Nguyen KT, García-Chacón LE, Barrett JN, Barrett EF, David G: The Psi(m) depolarization that accompanies mitochondrial Ca2+ uptake is greater in mutant SOD1 than in wild-type mouse motor terminals. Proc Natl Acad Sci U S A 2009;106:2007-2011

48. Yi J, Ma C, Li Y, Weisleder N, Rios E, Ma J, Zhou J: Mitochondrial calcium uptake regulates rapid calcium transients in skeletal muscle during excitation-contraction (E-C) coupling. J Biol Chem 2011;286:32436-32443

49. Prell T, Lautenschläger J, Grosskreutz J: Calcium-dependent protein folding in amyotrophic lateral sclerosis. Cell Calcium 2013;54:132-143

50. Kawahara Y, Sun H, Ito K, Hideyama T, Aoki M, Sobue G, Tsuji S, Kwak S: Underediting of GluR2 mRNA, a neuronal death inducing molecular change in sporadic ALS, does not occur in motor neurons in ALS1 or SBMA. Neurosci Res 2006;54:11-14

51. Kawahara Y, Kwak S, Sun H, Ito K, Hashida H, Aizawa H, Jeong SY, Kanazawa I: Human spinal motoneurons express low relative abundance of GluR2 mRNA: an implication for excitotoxicity in ALS. J Neurochem 2003;85:680-689

52. Pollari E, Goldsteins G, Bart G, Koistinaho J, Giniatullin R: The role of oxidative stress in degeneration of the neuromuscular junction in amyotrophic lateral sclerosis. Front Cell Neurosci 2014;8:131

53. Vehviläinen P, Koistinaho J, Gundars G: Mechanisms of mutant SOD1 induced mitochondrial toxicity in amyotrophic lateral sclerosis. Front Cell Neurosci 2014;8:126

54. An T, Shi P, Duan W, Zhang S, Yuan P, Li Z, Wu D, Xu Z, Li C, Guo Y: Oxidative stress and autophagic alteration in brainstem of SOD1-G93A mouse model of ALS. Mol Neurobiol 2014;49:1435-1448

55. Sierra V, Oliván M: Role of mitochondria on muscle cell death and meat tenderization. Recent Pat Endocr Metab Immune Drug Discov 2013;7:120-129

56. Orrenius S, Gogvadze V, Zhivotovsky B: Calcium and mitochondria in the regulation of cell death. Biochem Biophys Res Commun 2015;460:72-81

57. Thornton C, Hagberg H: Role of mitochondria in apoptotic and necroptotic cell death in the developing brain. Clin Chim Acta 2015;

58. Inoue H, Tsukita K, Iwasato T, Suzuki Y, Tomioka M, Tateno M, Nagao M, Kawata A, Saido TC, Miura M, Misawa H, Itohara S, Takahashi R: The crucial role of caspase-9

in the disease progression of a transgenic ALS mouse model. EMBO J 2003;22:6665-6674

59. Pedrini S, Sau D, Guareschi S, Bogush M, Brown RH, Naniche N, Kia A, Trotti D, Pasinelli P: ALS-linked mutant SOD1 damages mitochondria by promoting conformational changes in Bcl-2. Hum Mol Genet 2010;19:2974-2986

60. Van Den Bosch L, Tilkin P, Lemmens G, Robberecht W: Minocycline delays disease onset and mortality in a transgenic model of ALS. Neuroreport 2002;13:1067-1070

61. Zhang W, Narayanan M, Friedlander RM: Additive neuroprotective effects of minocycline with creatine in a mouse model of ALS. Ann Neurol 2003;53:267-270

62. Carrì MT: Minocycline for patients with ALS. Lancet Neurol 2008;7:118-119; author reply 120-111

63. Locke M, Tanguay RM: Increased HSF activation in muscles with a high constitutive Hsp70 expression. Cell Stress Chaperones 1996;1:189-196

64. Barber SC, Mead RJ, Shaw PJ: Oxidative stress in ALS: a mechanism of neurodegeneration and a therapeutic target. Biochim Biophys Acta 2006;1762:1051-1067

65. Carlesi C, CaldarazzoIenco E, Mancuso M, Siciliano G: Amyotrophic Lateral Sclerosis: A Genetic Point Of View. Curr Mol Med 2014;

66. Beal MF: Mitochondria and the pathogenesis of ALS. Brain 2000;123 (Pt 7):1291-1292

67. Sanhueza M, Chai A, Smith C, McCray BA, Simpson TI, Taylor JP, Pennetta G: Network analyses reveal novel aspects of ALS pathogenesis. PLoS Genet 2015;11:e1005107

68. Carrì MT, Valle C, Bozzo F, Cozzolino M: Oxidative stress and mitochondrial damage: importance in non-SOD1 ALS. Front Cell Neurosci 2015;9:41

69. Bruijn LI, Beal MF, Becher MW, Schulz JB, Wong PC, Price DL, Cleveland DW: Elevated free nitrotyrosine levels, but not protein-bound nitrotyrosine or hydroxyl radicals, throughout amyotrophic lateral sclerosis (ALS)-like disease implicate tyrosine nitration as an aberrant in vivo property of one familial ALS-linked superoxide dismutase 1 mutant. Proc Natl Acad Sci U S A 1997;94:7606-7611

70. Kanno T, Tanaka K, Yanagisawa Y, Yasutake K, Hadano S, Yoshii F, Hirayama N, Ikeda JE: A novel small molecule, N-(4-(2-pyridyl)(1,3-thiazol-2-yl))-2-(2,4,6-trimethylphenoxy) acetamide, selectively protects against oxidative stress-induced cell death by activating the Nrf2-ARE pathway: therapeutic implications for ALS. Free Radic Biol Med 2012;53:2028-2042

71. Li R, Strykowski R, Meyer M, Mulcrone P, Krakora D, Suzuki M: Male-specific differences in proliferation, neurogenesis, and sensitivity to oxidative stress in neural progenitor cells derived from a rat model of ALS. PLoS One 2012;7:e48581

72. Anand A, Thakur K, Gupta PK: ALS and oxidative stress: the neurovascular scenario. Oxid Med Cell Longev 2013;2013:635831

73. Desnuelle C, Dib M, Garrel C, Favier A: A double-blind, placebo-controlled randomized clinical trial of alpha-tocopherol (vitamin E) in the treatment of amyotrophic lateral sclerosis. ALS riluzole-tocopherol Study Group. Amyotroph Lateral Scler Other Motor Neuron Disord 2001;2:9-18

74. Kwieciński H, Janik P, Jamrozik Z, Opuchlik A: [The effect of selegiline and vitamin E in the treatment of ALS: an open randomized clinical trials]. Neurol Neurochir Pol 2001;35:101-106

75. Dupuis L: Oxidative stress sensitivity in ALS muscle cells. Exp Neurol 2009;220:219-223

76. Chiò A: Role of mitochondria in ALS. Amyotroph Lateral Scler Other Motor Neuron Disord 2000;1:140

77. Dawson VL: Maiming mitochondria in familial ALS. Nat Med 2004;10:905-906

78. Genevini P, Papiani G, Ruggiano A, Cantoni L, Navone F, Borgese N: Amyotrophic lateral sclerosis-linked mutant VAPB inclusions do not interfere with protein degradation pathways or intracellular transport in a cultured cell model. PLoS One 2014;9:e113416

79. Martins D, English AM: SOD1 oxidation and formation of soluble aggregates in yeast: relevance to sporadic ALS development. Redox Biol 2014;2:632-639

80. May S, Hornburg D, Schludi MH, Arzberger T, Rentzsch K, Schwenk BM, Grässer FA, Mori K, Kremmer E, Banzhaf-Strathmann J, Mann M, Meissner F, Edbauer D: C9orf72 FTLD/ALS-associated Gly-Ala dipeptide repeat proteins cause neuronal toxicity and Unc119 sequestration. Acta Neuropathol 2014;128:485-503

81. Schwartz JC, Podell ER, Han SS, Berry JD, Eggan KC, Cech TR: FUS is sequestered in nuclear aggregates in ALS patient fibroblasts. Mol Biol Cell 2014;25:2571-2578

82. Stieber A, Gonatas JO, Gonatas NK: Aggregates of mutant protein appear progressively in dendrites, in periaxonal processes of oligodendrocytes, and in neuronal and astrocytic perikarya of mice expressing the SOD1(G93A) mutation of familial amyotrophic lateral sclerosis. J Neurol Sci 2000;177:114-123

83. Pasinelli P, Belford ME, Lennon N, Bacskai BJ, Hyman BT, Trotti D, Brown RH: Amyotrophic lateral sclerosis-associated SOD1 mutant proteins bind and aggregate with Bcl-2 in spinal cord mitochondria. Neuron 2004;43:19-30

84. Wang J, Slunt H, Gonzales V, Fromholt D, Coonfield M, Copeland NG, Jenkins NA, Borchelt DR: Copper-binding-site-null SOD1 causes ALS in transgenic mice: aggregates of non-native SOD1 delineate a common feature. Hum Mol Genet 2003;12:2753-2764

85. Ivanova MI, Sievers SA, Guenther EL, Johnson LM, Winkler DD, Galaleldeen A, Sawaya MR, Hart PJ, Eisenberg DS: Aggregation-triggering segments of SOD1 fibril formation support a common pathway for familial and sporadic ALS. Proc Natl Acad Sci U S A 2014;111:197-201

86. Pratt AJ, Shin DS, Merz GE, Rambo RP, Lancaster WA, Dyer KN, Borbat PP, Poole FL, Adams MW, Freed JH, Crane BR, Tainer JA, Getzoff ED: Aggregation propensities of superoxide dismutase G93 hotspot mutants mirror ALS clinical phenotypes. Proc Natl Acad Sci U S A 2014;111:E4568-4576

87. Lee S, Kim HJ: Prion-like Mechanism in Amyotrophic Lateral Sclerosis: are Protein Aggregates the Key? Exp Neurobiol 2015;24:1-7

88. Watanabe M, Dykes-Hoberg M, Culotta VC, Price DL, Wong PC, Rothstein JD: Histological evidence of protein aggregation in mutant SOD1 transgenic mice and in amyotrophic lateral sclerosis neural tissues. Neurobiol Dis 2001;8:933-941

89. Marino M, Papa S, Crippa V, Nardo G, Peviani M, Cheroni C, Trolese MC, Lauranzano E, Bonetto V, Poletti A, DeBiasi S, Ferraiuolo L, Shaw PJ, Bendotti C: Differences in protein quality control correlate with phenotype variability in 2 mouse models of familial amyotrophic lateral sclerosis. Neurobiol Aging 2015;36:492-504

90. Leinweber B, Barofsky E, Barofsky DF, Ermilov V, Nylin K, Beckman JS: Aggregation of ALS mutant superoxide dismutase expressed in Escherichia coli. Free Radic Biol Med 2004;36:911-918

91. Crippa V, Carra S, Rusmini P, Sau D, Bolzoni E, Bendotti C, De Biasi S, Poletti A: A role of small heat shock protein B8 (HspB8) in the autophagic removal of misfolded proteins responsible for neurodegenerative diseases. Autophagy 2010;6:958-960

92. Gehrig SM, van der Poel C, Sayer TA, Schertzer JD, Henstridge DC, Church JE, Lamon S, Russell AP, Davies KE, Febbraio MA, Lynch GS: Hsp72 preserves muscle function and slows progression of severe muscular dystrophy. Nature 2012;484:394-398

93. Niwa J, Yamada S, Ishigaki S, Sone J, Takahashi M, Katsuno M, Tanaka F, Doyu M, Sobue G: Disulfide bond mediates aggregation, toxicity, and ubiquitylation of familial amyotrophic lateral sclerosis-linked mutant SOD1. J Biol Chem 2007;282:28087-28095

94. Liu J, Shinobu LA, Ward CM, Young D, Cleveland DW: Elevation of the Hsp70 chaperone does not effect toxicity in mouse models of familial amyotrophic lateral sclerosis. J Neurochem 2005;93:875-882

95. Wang L, Popko B, Roos RP: The unfolded protein response in familial amyotrophic lateral sclerosis. Hum Mol Genet 2011;20:1008-1015

96. Harding HP, Zhang Y, Ron D: Protein translation and folding are coupled by an endoplasmic-reticulum-resident kinase. Nature 1999;397:271-274

97. Krebs J, Agellon LB, Michalak M: Ca(2+) homeostasis and endoplasmic reticulum (ER) stress: An integrated view of calcium signaling. Biochem Biophys Res Commun 2015;460:114-121

98. Schwenk BM, Edbauer D: The ER under rapid fire. EMBO J 2014;33:1195-1197

99. Viana RJ, Nunes AF, Rodrigues CM: Endoplasmic reticulum enrollment in Alzheimer's disease. Mol Neurobiol 2012;46:522-534

100. Wootz H, Hansson I, Korhonen L, Näpänkangas U, Lindholm D: Caspase-12 cleavage and increased oxidative stress during motoneuron degeneration in transgenic mouse model of ALS. Biochem Biophys Res Commun 2004;322:281-286

101. Groenendyk J, Agellon LB, Michalak M: Coping with endoplasmic reticulum stress in the cardiovascular system. Annu Rev Physiol 2013;75:49-67

102. Hassler J, Cao SS, Kaufman RJ: IRE1, a double-edged sword in pre-miRNA slicing and cell death. Dev Cell 2012;23:921-923

103. Maurel M, Chevet E, Tavernier J, Gerlo S: Getting RIDD of RNA: IRE1 in cell fate regulation. Trends Biochem Sci 2014;39:245-254

104. Bertolotti A, Zhang Y, Hendershot LM, Harding HP, Ron D: Dynamic interaction of BiP and ER stress transducers in the unfolded-protein response. Nat Cell Biol 2000;2:326-332

105. Mishiba K, Nagashima Y, Suzuki E, Hayashi N, Ogata Y, Shimada Y, Koizumi N: Defects in IRE1 enhance cell death and fail to degrade mRNAs encoding secretory pathway proteins in the Arabidopsis unfolded protein response. Proc Natl Acad Sci U S A 2013;110:5713-5718

106. Yoshida H, Matsui T, Yamamoto A, Okada T, Mori K: XBP1 mRNA is induced by ATF6 and spliced by IRE1 in response to ER stress to produce a highly active transcription factor. Cell 2001;107:881-891

107. Lee AH, Iwakoshi NN, Glimcher LH: XBP-1 regulates a subset of endoplasmic reticulum resident chaperone genes in the unfolded protein response. Mol Cell Biol 2003;23:7448-7459

108. Deldicque L, Cani PD, Philp A, Raymackers JM, Meakin PJ, Ashford ML, Delzenne NM, Francaux M, Baar K: The unfolded protein response is activated in skeletal muscle by high-fat feeding: potential role in the downregulation of protein synthesis. Am J Physiol Endocrinol Metab 2010;299:E695-705

109. Zhang L, Nosak C, Sollazzo P, Odisho T, Volchuk A: IRE1 inhibition perturbs the unfolded protein response in a pancreatic β-cell line expressing mutant proinsulin, but does not sensitize the cells to apoptosis. BMC Cell Biol 2014;15:29

110. Yang C, Diiorio P, Jurczyk A, O'Sullivan-Murphy B, Urano F, Bortell R: Pathological endoplasmic reticulum stress mediated by the IRE1 pathway contributes to pre-insulitic beta cell apoptosis in a virus-induced rat model of type 1 diabetes. Diabetologia 2013;56:2638-2646

111. Bruchmann A, Roller C, Walther TV, Schäfer G, Lehmusvaara S, Visakorpi T, Klocker H, Cato AC, Maddalo D: Bcl-2 associated athanogene 5 (Bag5) is overexpressed in prostate cancer and inhibits ER-stress induced apoptosis. BMC Cancer 2013;13:96

112. Yang X, Xiang X, Xia M, Su J, Wu Y, Shen L, Xu Y, Sun L: Inhibition of JNK3 promotes apoptosis induced by BH3 mimetic S1 in chemoresistant human ovarian cancer cells. Anat Rec (Hoboken) 2015;298:386-395

113. Chan JY, Luzuriaga J, Maxwell EL, West PK, Bensellam M, Laybutt DR: The balance between adaptive and apoptotic unfolded protein responses regulates β-cell death under ER stress conditions through XBP1, CHOP and JNK. Mol Cell Endocrinol 2015;

114. Nakagawa T, Zhu H, Morishima N, Li E, Xu J, Yankner BA, Yuan J: Caspase-12 mediates endoplasmic-reticulum-specific apoptosis and cytotoxicity by amyloid-beta. Nature 2000;403:98-103

115. Hitomi J, Katayama T, Eguchi Y, Kudo T, Taniguchi M, Koyama Y, Manabe T, Yamagishi S, Bando Y, Imaizumi K, Tsujimoto Y, Tohyama M: Involvement of caspase-4 in endoplasmic reticulum stress-induced apoptosis and Abeta-induced cell death. J Cell Biol 2004;165:347-356

116. Obeng EA, Boise LH: Caspase-12 and caspase-4 are not required for caspase-dependent endoplasmic reticulum stress-induced apoptosis. J Biol Chem 2005;280:29578-29587

117. Kim SJ, Zhang Z, Hitomi E, Lee YC, Mukherjee AB: Endoplasmic reticulum stress-induced caspase-4 activation mediates apoptosis and neurodegeneration in INCL. Hum Mol Genet 2006;15:1826-1834

118. Hiramatsu N, Chiang WC, Kurt TD, Sigurdson CJ, Lin JH: Multiple Mechanisms of Unfolded Protein Response-Induced Cell Death. Am J Pathol 2015;185:1800-1808

119. Gething MJ: Role and regulation of the ER chaperone BiP. Semin Cell Dev Biol 1999;10:465-472

120. Elanchezhian R, Palsamy P, Madson CJ, Lynch DW, Shinohara T: Age-related cataracts: homocysteine coupled endoplasmic reticulum stress and suppression of Nrf2-dependent antioxidant protection. Chem Biol Interact 2012;200:1-10

121. Petri S, Körner S, Kiaei M: Nrf2/ARE Signaling Pathway: Key Mediator in Oxidative Stress and Potential Therapeutic Target in ALS. Neurol Res Int 2012;2012:878030

122. Vattemi G, Engel WK, McFerrin J, Askanas V: Endoplasmic reticulum stress and unfolded protein response in inclusion body myositis muscle. Am J Pathol 2004;164:1-7

123. Nagaraju K, Casciola-Rosen L, Lundberg I, Rawat R, Cutting S, Thapliyal R, Chang J, Dwivedi S, Mitsak M, Chen YW, Plotz P, Rosen A, Hoffman E, Raben N: Activation of the endoplasmic reticulum stress response in autoimmune myositis: potential role in muscle fiber damage and dysfunction. Arthritis Rheum 2005;52:1824-1835

124. Ikezoe K, Nakamori M, Furuya H, Arahata H, Kanemoto S, Kimura T, Imaizumi K, Takahashi MP, Sakoda S, Fujii N, Kira J: Endoplasmic reticulum stress in myotonic dystrophy type 1 muscle. Acta Neuropathol 2007;114:527-535

125. Chen D, Mazala DAG, English SA, Chin ER: BiP deficiency and ER stress in skeletal muscle of a mouse model of amyotrophic lateral sclerosis. The FASEB Journal 2012;26:lb783

126. von Lewinski F, Keller BU: Ca2+, mitochondria and selective motoneuron vulnerability: implications for ALS. Trends Neurosci 2005;28:494-500

127. Jaiswal MK: Calcium, mitochondria, and the pathogenesis of ALS: the good, the bad, and the ugly. Front Cell Neurosci 2013;7:199

128. Chao CC, Yam WC, Lin-Chao S: Coordinated induction of two unrelated glucose-regulated protein genes by a calcium ionophore: human BiP/GRP78 and GAPDH. Biochem Biophys Res Commun 1990;171:431-438

129. Al-Hashimi AA, Caldwell J, Gonzalez-Gronow M, Pizzo SV, Aboumrad D, Pozza L, Al-Bayati H, Weitz JI, Stafford A, Chan H, Kapoor A, Jacobsen DW, Dickhout JG, Austin RC: Binding of anti-GRP78 autoantibodies to cell surface GRP78 increases tissue

factor procoagulant activity via the release of calcium from endoplasmic reticulum stores. J Biol Chem 2010;285:28912-28923

130. Chen M, Zhang Y, Yu VC, Chong YS, Yoshioka T, Ge R: Isthmin targets cell-surface GRP78 and triggers apoptosis via induction of mitochondrial dysfunction. Cell Death Differ 2014;21:797-810

131. Venugopal S, Chen M, Liao W, Er SY, Wong WS, Ge R: Isthmin is a novel vascular permeability inducer that functions through cell-surface GRP78-mediated Src activation. Cardiovasc Res 2015;107:131-142

132. Jin HR, Zhao J, Zhang Z, Liao Y, Wang CZ, Huang WH, Li SP, He TC, Yuan CS, Du W: The antitumor natural compound falcarindiol promotes cancer cell death by inducing endoplasmic reticulum stress. Cell Death Dis 2012;3:e376

133. Gaudette BT, Iwakoshi NN, Boise LH: Bcl-xL protein protects from C/EBP homologous protein (CHOP)-dependent apoptosis during plasma cell differentiation. J Biol Chem 2014;289:23629-23640

134. Hiramatsu N, Kasai A, Du S, Takeda M, Hayakawa K, Okamura M, Yao J, Kitamura M: Rapid, transient induction of ER stress in the liver and kidney after acute exposure to heavy metal: evidence from transgenic sensor mice. FEBS Lett 2007;581:2055-2059

135. Park GB, Hur DY, Kim D: Combining CAL-101 with Celecoxib Enhances Apoptosis of EBV-transformed B-Cells Through MAPK-induced ER Stress. Anticancer Res 2015;35:2699-2708

136. Verfaillie T, van Vliet A, Garg AD, Dewaele M, Rubio N, Gupta S, de Witte P, Samali A, Agostinis P: Pro-apoptotic signaling induced by photo-oxidative ER stress is amplified by Noxa, not Bim. Biochem Biophys Res Commun 2013;438:500-506

137. Bartolome A, Guillen C, Benito M: Autophagy plays a protective role in endoplasmic reticulum stress-mediated pancreatic β cell death. Autophagy 2012;8:1757-1768

138. Benbrook DM, Long A: Integration of autophagy, proteasomal degradation, unfolded protein response and apoptosis. Exp Oncol 2012;34:286-297

139. Ghavami S, Yeganeh B, Stelmack GL, Kashani HH, Sharma P, Cunnington R, Rattan S, Bathe K, Klonisch T, Dixon IM, Freed DH, Halayko AJ: Apoptosis, autophagy and ER stress in mevalonate cascade inhibition-induced cell death of human atrial fibroblasts. Cell Death Dis 2012;3:e330

140. Hetz C, Thielen P, Matus S, Nassif M, Court F, Kiffin R, Martinez G, Cuervo AM, Brown RH, Glimcher LH: XBP-1 deficiency in the nervous system protects against amyotrophic lateral sclerosis by increasing autophagy. Genes Dev 2009;23:2294-2306

141. Pehar M, Jonas MC, Hare TM, Puglielli L: SLC33A1/AT-1 protein regulates the induction of autophagy downstream of IRE1/XBP1 pathway. J Biol Chem 2012;287:29921-29930

142. Glembotski CC: Roles for the sarco-/endoplasmic reticulum in cardiac myocyte contraction, protein synthesis, and protein quality control. Physiology (Bethesda) 2012;27:343-350

143. Thévenod F, Lee WK: Cadmium and cellular signaling cascades: interactions between cell death and survival pathways. Arch Toxicol 2013;87:1743-1786

144. Kim HM, Lee ES, Lee BR, Yadav D, Kim YM, Ko HJ, Park KS, Lee EY, Chung CH: C-C chemokine receptor 2 inhibitor ameliorates hepatic steatosis by improving ER stress and inflammation in a type 2 diabetic mouse model. PLoS One 2015;10:e0120711

145. Nakanishi K, Sudo T, Morishima N: Endoplasmic reticulum stress signaling transmitted by ATF6 mediates apoptosis during muscle development. J Cell Biol 2005;169:555-560

146. Nakanishi K, Dohmae N, Morishima N: Endoplasmic reticulum stress increases myofiber formation in vitro. FASEB J 2007;21:2994-3003

147. Wu J, Ruas JL, Estall JL, Rasbach KA, Choi JH, Ye L, Boström P, Tyra HM, Crawford RW, Campbell KP, Rutkowski DT, Kaufman RJ, Spiegelman BM: The unfolded protein response mediates adaptation to exercise in skeletal muscle through a PGC-1α/ATF6α complex. Cell Metab 2011;13:160-169

148. Nogalska A, D'Agostino C, Engel WK, Cacciottolo M, Asada S, Mori K, Askanas V: Activation of the Unfolded Protein Response in Sporadic Inclusion-Body Myositis but Not in Hereditary GNE Inclusion-Body Myopathy. J Neuropathol Exp Neurol 2015;74:538-546

149. Moorwood C, Barton ER: Caspase-12 ablation preserves muscle function in the mdx mouse. Hum Mol Genet 2014;23:5325-5341

150. Atkin JD, Farg MA, Turner BJ, Tomas D, Lysaght JA, Nunan J, Rembach A, Nagley P, Beart PM, Cheema SS, Horne MK: Induction of the unfolded protein response in familial amyotrophic lateral sclerosis and association of protein-disulfide isomerase with superoxide dismutase 1. J Biol Chem 2006;281:30152-30165

151. Kikuchi H, Almer G, Yamashita S, Guégan C, Nagai M, Xu Z, Sosunov AA, McKhann GM, Przedborski S: Spinal cord endoplasmic reticulum stress associated with a microsomal accumulation of mutant superoxide dismutase-1 in an ALS model. Proc Natl Acad Sci U S A 2006;103:6025-6030

152. Kieran D, Woods I, Villunger A, Strasser A, Prehn JH: Deletion of the BH3-only protein puma protects motoneurons from ER stress-induced apoptosis and delays motoneuron loss in ALS mice. Proc Natl Acad Sci U S A 2007;104:20606-20611

153. Atkin JD, Farg MA, Walker AK, McLean C, Tomas D, Horne MK: Endoplasmic reticulum stress and induction of the unfolded protein response in human sporadic amyotrophic lateral sclerosis. Neurobiol Dis 2008;30:400-407

154. Nishitoh H, Kadowaki H, Nagai A, Maruyama T, Yokota T, Fukutomi H, Noguchi T, Matsuzawa A, Takeda K, Ichijo H: ALS-linked mutant SOD1 induces ER stress- and ASK1-dependent motor neuron death by targeting Derlin-1. Genes Dev 2008;22:1451-1464

155. Saxena S, Cabuy E, Caroni P: A role for motoneuron subtype-selective ER stress in disease manifestations of FALS mice. Nat Neurosci 2009;12:627-636

156. Jaronen M, Goldsteins G, Koistinaho J: ER stress and unfolded protein response in amyotrophic lateral sclerosis-a controversial role of protein disulphide isomerase. Front Cell Neurosci 2014;8:402

157. Dobrowolny G, Aucello M, Rizzuto E, Beccafico S, Mammucari C, Boncompagni S, Bonconpagni S, Belia S, Wannenes F, Nicoletti C, Del Prete Z, Rosenthal N, Molinaro M, Protasi F, Fanò G, Sandri M, Musarò A: Skeletal muscle is a primary target of SOD1G93A-mediated toxicity. Cell Metab 2008;8:425-436

158. Appel SH: Is ALS a systemic disorder? Evidence from muscle mitochondria. Exp Neurol 2006;198:1-3

159. Shaw BF, Lelie HL, Durazo A, Nersissian AM, Xu G, Chan PK, Gralla EB, Tiwari A, Hayward LJ, Borchelt DR, Valentine JS, Whitelegge JP: Detergent-insoluble aggregates associated with amyotrophic lateral sclerosis in transgenic mice contain primarily full-length, unmodified superoxide dismutase-1. J Biol Chem 2008;283:8340-8350

160. Higgins CM, Jung C, Xu Z: ALS-associated mutant SOD1G93A causes mitochondrial vacuolation by expansion of the intermembrane space and by involvement of SOD1 aggregation and peroxisomes. BMC Neurosci 2003;4:16

161. Antel JP, Chelmicka-Schorr E, Sportiello M, Stefansson K, Wollmann RL, Arnason BG: Muscle acid protease activity in amyotrophic lateral sclerosis: correlation with clinical and pathologic features. Neurology 1982;32:901-903

162. Lilo E, Wald-Altman S, Solmesky LJ, Ben Yaakov K, Gershoni-Emek N, Bulvik S, Kassis I, Karussis D, Perlson E, Weil M: Characterization of human sporadic ALS biomarkers in the familial ALS transgenic mSOD1(G93A) mouse model. Hum Mol Genet 2013;22:4720-4725

163. Robberecht W, Philips T: The changing scene of amyotrophic lateral sclerosis. Nat Rev Neurosci 2013;14:248-264

164. Kaufman RJ: Stress signaling from the lumen of the endoplasmic reticulum: coordination of gene transcriptional and translational controls. Genes Dev 1999;13:1211-1233

165. Kaufman RJ: Orchestrating the unfolded protein response in health and disease. J Clin Invest 2002;110:1389-1398

166. Cleveland DW, Rothstein JD: From Charcot to Lou Gehrig: deciphering selective motor neuron death in ALS. Nat Rev Neurosci 2001;2:806-819

167. Capitanio D, Vasso M, Ratti A, Grignaschi G, Volta M, Moriggi M, Daleno C, Bendotti C, Silani V, Gelfi C: Molecular Signatures of Amyotrophic Lateral Sclerosis Disease Progression in Hind and Forelimb Muscles of an SOD1(G93A) Mouse Model. Antioxid Redox Signal 2012;

168. Zhou J, Yi J, Fu R, Liu E, Siddique T, Rios E, Deng HX: Hyperactive intracellular calcium signaling associated with localized mitochondrial defects in skeletal muscle of an animal model of amyotrophic lateral sclerosis. J Biol Chem 2010;285:705-712

169. Deforges S, Branchu J, Biondi O, Grondard C, Pariset C, Lecolle S, Lopes P, Vidal PP, Chanoine C, Charbonnier F: Motoneuron survival is promoted by specific exercise in a mouse model of amyotrophic lateral sclerosis. In *J Physiol* England, 2009, p. 3561-3572

170. Bloemberg D, Quadrilatero J: Rapid determination of myosin heavy chain expression in rat, mouse, and human skeletal muscle using multicolor immunofluorescence analysis. PLoS One 2012;7:e35273

171. Guido AN, Campos GE, Neto HS, Marques MJ, Minatel E: Fiber type composition of the sternomastoid and diaphragm muscles of dystrophin-deficient mdx mice. Anat Rec (Hoboken) 2010;293:1722-1728

172. Ohoka N, Hattori T, Kitagawa M, Onozaki K, Hayashi H: Critical and functional regulation of CHOP (C/EBP homologous protein) through the N-terminal portion. J Biol Chem 2007;282:35687-35694

173. Tankersley CG, Haenggeli C, Rothstein JD: Respiratory impairment in a mouse model of amyotrophic lateral sclerosis. J Appl Physiol 2007;102:926-932

174. Hegedus J, Putman CT, Gordon T: Progressive motor unit loss in the G93A mouse model of amyotrophic lateral sclerosis is unaffected by gender. Muscle Nerve 2009;39:318-327

175. Mead RJ, Bennett EJ, Kennerley AJ, Sharp P, Sunyach C, Kasher P, Berwick J, Pettmann B, Battaglia G, Azzouz M, Grierson A, Shaw PJ: Optimised and rapid pre-clinical screening in the SOD1(G93A) transgenic mouse model of amyotrophic lateral sclerosis (ALS). PLoS One 2011;6:e23244

176. Marcuzzo S, Zucca I, Mastropietro A, de Rosbo NK, Cavalcante P, Tartari S, Bonanno S, Preite L, Mantegazza R, Bernasconi P: Hind limb muscle atrophy precedes cerebral neuronal degeneration in G93A-SOD1 mouse model of amyotrophic lateral sclerosis: a longitudinal MRI study. Exp Neurol 2011;231:30-37

177. Ozawa K, Miyazaki M, Matsuhisa M, Takano K, Nakatani Y, Hatazaki M, Tamatani T, Yamagata K, Miyagawa J, Kitao Y, Hori O, Yamasaki Y, Ogawa S: The endoplasmic reticulum chaperone improves insulin resistance in type 2 diabetes. In *Diabetes* United States, 2005, p. 657-663

178. Chambers JE, Marciniak SJ: Cellular mechanisms of endoplasmic reticulum stress signaling in health and disease. 2. Protein misfolding and ER stress. In *Am J Physiol Cell Physiol* United States, 2014 the American Physiological Society., 2014, p. C657-670

179. Scheuner D, Song B, McEwen E, Liu C, Laybutt R, Gillespie P, Saunders T, Bonner-Weir S, Kaufman RJ: Translational control is required for the unfolded protein response and in vivo glucose homeostasis. In *Mol Cell* United States, 2001, p. 1165-1176

180. Periasamy M, Kalyanasundaram A: SERCA pump isoforms: their role in calcium transport and disease. Muscle Nerve 2007;35:430-442

181. Hegedus J, Putman CT, Tyreman N, Gordon T: Preferential motor unit loss in the SOD1 G93A transgenic mouse model of amyotrophic lateral sclerosis. J Physiol 2008;586:3337-3351

182. Nogalska A, Engel WK, McFerrin J, Kokame K, Komano H, Askanas V: Homocysteine-induced endoplasmic reticulum protein (Herp) is up-regulated in sporadic inclusion-body myositis and in endoplasmic reticulum stress-induced cultured human muscle fibers. J Neurochem 2006;96:1491-1499

183. Vitadello M, Doria A, Tarricone E, Ghirardello A, Gorza L: Myofiber stress-response in myositis: parallel investigations on patients and experimental animal models of muscle regeneration and systemic inflammation. Arthritis Res Ther 2010;12:R52

184. Kim HJ, Jamart C, Deldicque L, An GL, Lee YH, Kim CK, Raymackers JM, Francaux M: Endoplasmic reticulum stress markers and ubiquitin–proteasome pathway activity in response to a 200-km run. Med Sci Sports Exerc 2011;43:18-25

185. de Theije CC, Langen RC, Lamers WH, Gosker HR, Schols AM, Köhler SE: Differential sensitivity of oxidative and glycolytic muscles to hypoxia-induced muscle atrophy. J Appl Physiol (1985) 1985;118:200-211

186. Baltgalvis KA, Berger FG, Pena MM, Davis JM, White JP, Carson JA: Muscle wasting and interleukin-6-induced atrogin-I expression in the cachectic Apc (Min/+) mouse. Pflugers Arch 2009;457:989-1001

187. Yu Z, Li P, Zhang M, Hannink M, Stamler JS, Yan Z: Fiber type-specific nitric oxide protects oxidative myofibers against cachectic stimuli. PLoS One 2008;3:e2086

188. Li P, Waters RE, Redfern SI, Zhang M, Mao L, Annex BH, Yan Z: Oxidative phenotype protects myofibers from pathological insults induced by chronic heart failure in mice. Am J Pathol 2007;170:599-608

189. Tarricone E, Scapin C, Vitadello M, Esposito F, Margonato V, Milano G, Samaja M, Gorza L: Cellular distribution of Hsp70 expression in rat skeletal muscles. Effects of moderate exercise training and chronic hypoxia. Cell Stress Chaperones 2008;13:483-495

190. Sotelo-Silveira JR, Lepanto P, Elizondo V, Horjales S, Palacios F, Martinez-Palma L, Marin M, Beckman JS, Barbeito L: Axonal Mitochondrial Clusters Containing Mutant SOD1 in Transgenic Models of ALS. Antioxidants & Redox Signaling 2009;11:1535-1546

191. Wong M, Martin LJ: Skeletal muscle-restricted expression of human SOD1 causes motor neuron degeneration in transgenic mice. Human Molecular Genetics 2010;19:2284-2302

192. Jaiswal MK, Keller BU: Cu/Zn Superoxide Dismutase Typical for Familial Amyotrophic Lateral Sclerosis Increases the Vulnerability of Mitochondria and Perturbs Ca2+ Homeostasis in SOD1(G93A) Mice. Molecular Pharmacology 2009;75:478-489

193. Jaiswal MK, Zech WD, Goos M, Leutbecher C, Ferri A, Zippelius A, Carri MT, Nau R, Keller BU: Impairment of mitochondrial calcium handling in a mtSOD1 cell culture model of motoneuron disease. Bmc Neuroscience 2009;10

194. Prell T, Lautenschlager J, Grosskreutz J: Calcium-dependent protein folding in amyotrophic lateral sclerosis. Cell Calcium 2013;54:132-143

195. Chin ER, Allen DG: The role of elevations in intracellular [Ca2+] in the development of low frequency fatigue in mouse single muscle fibres. J Physiol 1996;491 (Pt 3):813-824

196. Chin ER, Grange RW, Viau F, Simard AR, Humphries C, Shelton J, Bassel-Duby R, Williams RS, Michel RN: Alterations in slow-twitch muscle phenotype in transgenic mice overexpressing the Ca2+ buffering protein parvalbumin. J Physiol 2003;547:649-663

197. Goonasekera SA, Lam CK, Millay DP, Sargent MA, Hajjar RJ, Kranias EG, Molkentin JD: Mitigation of muscular dystrophy in mice by SERCA overexpression in skeletal muscle. Journal of Clinical Investigation 2011;121:1044-1052

198. Parsons SA, Millay DP, Sargent MA, McNally EM, Molkentin JD: Age-dependent effect of myostatin blockade on disease severity in a murine model of limb-girdle muscular dystrophy. American Journal of Pathology 2006;168:1975-1985

199. Millay DP, Goonasekera SA, Sargent MA, Maillet M, Aronow BJ, Molkentin JD: Calcium influx is sufficient to induce muscular dystrophy through a TRPC-dependent mechanism. Proceedings of the National Academy of Sciences of the United States of America 2009;106:19023-19028

200. Goonasekera SA, Davis J, Kwong JQ, Accornero F, Wei-Lapierre L, Sargent MA, Dirksen RT, Molkentin JD: Enhanced Ca2+ influx from STIM1-Orai1 induces muscle pathology in mouse models of muscular dystrophy. Hum Mol Genet 2014;

201. Goonasekera SA, Lam CK, Millay DP, Sargent MA, Hajjar RJ, Kranias EG, Molkentin JD: Mitigation of muscular dystrophy in mice by SERCA overexpression in skeletal muscle. J Clin Invest 2011;121:1044-1052

202. Mázala DA, Grange RW, Chin ER: The role of proteases in excitation-contraction coupling failure in muscular dystrophy. Am J Physiol Cell Physiol 2014:ajpcell.00267.02013

203. Chin ER, Allen DG: The contribution of pH-dependent mechanisms to fatigue at different intensities in mammalian single muscle fibres. J Physiol 1998;512 (Pt 3):831-840

204. Chin ER, Green HJ, Grange F, Mercer JD, Obrien PJ: TECHNICAL CONSIDERATIONS FOR ASSESSING ALTERATIONS IN SKELETAL-MUSCLE SARCOPLASMIC-RETICULUM CA++-SEQUESTRATION FUNCTION IN-VITRO. Molecular and Cellular Biochemistry 1994;139:41-52

205. Mead RJ, Bennett EJ, Kennerley AJ, Sharp P, Sunyach C, Kasher P, Berwick J, Pettmann B, Battaglia G, Azzouz M, Grierson A, Shaw PJ: Optimised and Rapid Pre-clinical Screening in the SOD1(G93A) Transgenic Mouse Model of Amyotrophic Lateral Sclerosis (ALS). Plos One 2011;6

206. Turner BJ, Talbot K: Transgenics, toxicity and therapeutics in rodent models of mutant SOD1-mediated familial ALS. Progress in Neurobiology 2008;85:94-134

207. Chin ER, Olson EN, Richardson JA, Yang Q, Humphries C, Shelton JM, Wu H, Zhu W, Bassel-Duby R, Williams RS: A calcineurin-dependent transcriptional pathway controls skeletal muscle fiber type. Genes Dev 1998;12:2499-2509

208. Marcuzzo S, Zucca I, Mastropietro A, de Rosbo NK, Cavalcante P, Tartari S, Bonanno S, Preite L, Mantegazza R, Bernasconi P: Hind limb muscle atrophy precedes cerebral neuronal degeneration in G93A-SOD1 mouse model of amyotrophic lateral sclerosis: A longitudinal MRI study. Experimental Neurology 2011;231:30-37

209. Dvořáková P, Hernychova L, Vojtěšek B: [Analysis of protein using mass spectrometry]. Klin Onkol 2014;27 Suppl 1:S104-109

210. Hentze N, Mayer MP: Analyzing protein dynamics using hydrogen exchange mass spectrometry. J Vis Exp 2013;

211. Chen L, Wang N, Sun D, Li L: Microwave-assisted acid hydrolysis of proteins combined with peptide fractionation and mass spectrometry analysis for characterizing protein terminal sequences. J Proteomics 2014;100:68-78

212. Zhang Y, Liu R, Ni M, Gill P, Lee AS: Cell surface relocalization of the endoplasmic reticulum chaperone and unfolded protein response regulator GRP78/BiP. J Biol Chem 2010;285:15065-15075

213. Ferreiro E, Baldeiras I, Ferreira IL, Costa RO, Rego AC, Pereira CF, Oliveira CR: Mitochondrial- and endoplasmic reticulum-associated oxidative stress in Alzheimer's disease: from pathogenesis to biomarkers. Int J Cell Biol 2012;2012:735206

214. Senft D, Ronai ZA: UPR, autophagy, and mitochondria crosstalk underlies the ER stress response. Trends Biochem Sci 2015;40:141-148

215. Leustek T, Toledo H, Brot N, Weissbach H: Calcium-dependent autophosphorylation of the glucose-regulated protein, Grp78. Arch Biochem Biophys 1991;289:256-261

216. Mázala DA, Pratt SJ, Chen D, Molkentin JD, Lovering RM, Chin ER: SERCA1 overexpression minimizes skeletal muscle damage in dystrophic mouse models. Am J Physiol Cell Physiol 2015;308:C699-709

217. Valle-Rios R, Maravillas-Montero JL, Burkhardt AM, Martinez C, Buhren BA, Homey B, Gerber PA, Robinson O, Hevezi P, Zlotnik A: Isthmin 1 is a secreted protein expressed in skin, mucosal tissues, and NK, NKT, and th17 cells. J Interferon Cytokine Res 2014;34:795-801

218. Yuan B, Xian R, Ma J, Chen Y, Lin C, Song Y: Isthmin inhibits glioma growth through antiangiogenesis in vivo. J Neurooncol 2012;109:245-252

219. Xiang W, Ke Z, Zhang Y, Cheng GH, Irwan ID, Sulochana KN, Potturi P, Wang Z, Yang H, Wang J, Zhuo L, Kini RM, Ge R: Isthmin is a novel secreted angiogenesis inhibitor that inhibits tumour growth in mice. J Cell Mol Med 2011;15:359-374

220. Rao J, Zhang C, Wang P, Lu L, Qian X, Qin J, Pan X, Li G, Wang X, Zhang F: C/EBP homologous protein (CHOP) contributes to hepatocyte death via the promotion of ERO1α signalling in acute liver failure. Biochem J 2015;466:369-378

Appendices

UNIVERSITY OF MARYLAND
INSTITUTIONAL ANIMAL CARE AND USE COMMITTEE

1204 Marie Mount Hall
College Park, MD 20742-5125
TEL 301.405.4212
FAX 301.314.1475
iacuc-office@umd.edu
www.umresearch.umd.edu/IACUC

DATE:	May 29, 2012
TO:	Eva Chin, PhD
FROM:	University of Maryland College Park (UMCP) IACUC
PROJECT TITLE:	[327057-2] Analysis of skeletal muscle function in mouse models of neuromuscular diseases
IACUC REFERENCE #:	R-12-30
SUBMISSION TYPE:	Revision
ACTION:	APPROVED
APPROVAL DATE:	May 29, 2012
EXPIRATION DATE:	May 29, 2015

Thank you for your submission of the Animal Study Protocol [R-12-30] Analysis of skeletal muscle function in mouse models of neuromuscular diseases. The University of Maryland College Park (UMCP) IACUC has APPROVED your submission. This approval is based on the committee's review of the appropriate use and care of animals within your research goals.

Research must be conducted in accordance with this approved submission. All changes must be submitted to the University of Maryland College Park (UMCP) IACUC as a revision. Conducting research outside the scope of your approved submission is reportable to federal entities and will be investigated by the University of Maryland College Park (UMCP) IACUC and may require interruptions to the research project.

Any revision to previously approved materials must be approved by this committee prior to initiation. Please use the appropriate revision forms for this procedure which are found on the IRBNet Forms and Templates Page.

All UNANTICIPATED PROBLEMS involving UNEXPECTED MORBIDITY or MORTALITY to animals or study personnel must be reported promptly to this office.

This protocol requires continuing review by this committee on an annual basis. Please use the appropriate forms for this procedure. Your documentation for continuing review must be received with sufficient time for review and continued approval before the expiration date of May 29, 2015.

Please note that all research records must be retained for a minimum of three years after the completion of the project.

If you have any questions, please contact Amanda Underwood at 301-405-5037 or graebel@umd.edu. Please include your project title and reference number in all correspondence with this committee.

W. Ray Stricklin, IACUC Chair

This letter has been electronically signed in accordance with all applicable regulations, and a copy is retained within University of Maryland College Park (UMCP) IACUC's records.

UNIVERSITY OF MARYLAND
DIVISION OF RESEARCH
Laboratory Animal Resources

Central Animal Resources Facility
College Park, Maryland 20742
TEL 301.405.4921

September 9, 2014

Dapeng Chen
SPH – Kinesiology

Dear Dapeng;

This letter is to acknowledge your attendance at the **September 9, 2014** UMD Principal Investigator and Animal User refresher class. You are now in compliance with current Campus regulations that require attendance at an animal-use training program.

The Campus is committed to the humane and appropriate use of animals in research and teaching. We hope that the training session provided you with some insight into the current rules and regulations governing animal care and use. We also hope that it will enable you to work more efficiently and effectively within the UMD Animal Care Program.

The Institutional Animal Care and Use Committee (IACUC) welcomes suggestions on how the campus program can be improved. Any comments or questions concerning the animal care program and/or animal care and use should be directed to me.

Thank you for your participation. Please keep this letter for your records.

Sincerely,

Douglas A. Powell

Douglas Powell, DVM, DCLAM
University Attending Veterinarian